Huebnerite Veins near Round Mountain, Nye County, Nevada

GEOLOGICAL SURVEY PROFESSIONAL PAPER 1287

Huebnerite Veins near Round Mountain, Nye County, Nevada

By DANIEL R. SHAWE, EUGENE E. FOORD, *and* NANCY M. CONKLIN

GEOLOGICAL SURVEY PROFESSIONAL PAPER 1287

A study of the geology, mineralogy, and chemistry of huebnerite-bearing veins suggests their formation during two major episodes of mineralization

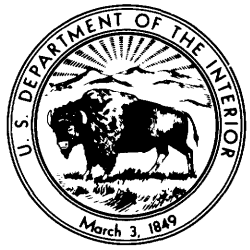

UNITED STATES GOVERNMENT PRINTING OFFICE, WASHINGTON : 1984

UNITED STATES DEPARTMENT OF THE INTERIOR

WILLIAM P. CLARK, ***Secretary***

GEOLOGICAL SURVEY

Dallas L. Peck, ***Director***

Library of Congress Cataloging in Publication Data
Shawe, Daniel R., 1925–
Huebnerite veins near Round Mountain, Nye County, Nevada.
(Geological Survey Professional Paper ; 1287)
Bibliography: 40 p.
Supt. of Docs. No.: I 19.16:1287
1. Huebnerite. 2. Mineralogy—Nevada—Nye County.
I. Foord, Eugene E. II. Conklin, Nancy M. III. Title. IV. Series
QE391.H84S53 1984 549'.74 82-600307

For sale by the Branch of Distribution
U.S. Geological Survey
604 South Pickett Street
Alexandria, VA 22304

CONTENTS

ILLUSTRATIONS

TABLES

HUEBNERITE VEINS NEAR ROUND MOUNTAIN, NYE COUNTY, NEVADA

By DANIEL R. SHAWE, EUGENE E. FOORD, and NANCY M. CONKLIN

ABSTRACT

Small huebnerite-bearing quartz veins occur in and near Cretaceous (about 95 m.y. old) granite east and south of Round Mountain. The veins are short, lenticular, and strike mostly northeast and northwest in several narrow east-trending belts. The quartz veins were formed about 80 m.y. ago near the end of an episode of doming and metamorphism of the granite and emplacement of aplite and pegmatite dikes in and near the granite. An initial hydrothermal stage involved deposition of muscovite, quartz, huebnerite, fluorite, and barite in the veins. Veins were then sheared, broken, and recrystallized. A second hydrothermal stage, possibly associated with emplacement of a rhyolite dike swarm and granodiorite stock about 35 m.y. ago, saw deposition of more muscovite, quartz, fluorite, and barite, and addition of scheelite, tetrahedrite-tennantite, several sulfide minerals, and chalcedony. Finally, as a result of near-surface weathering, secondary sulfide and numerous oxide, tungstate, carbonate, sulfate, phosphate, and silicate minerals formed in the veins.

Depth of burial at the time of formation of the veins, based on geologic reconstruction, was about 3–3.5 km. The initial hydrothermal stage ended with deposition of quartz at a temperature of about 210°C and pressures of about 240–280 bars (hydrostatic conditions) from fluids with salinity of about 5 weight percent sodium chloride. Fluorite then was deposited at about 250°–280°C from solutions of similar salinity and containing a small amount of carbon dioxide. During shearing that followed initial mineralization, quartz was recrystallized at a temperature of 270°–290°C and in association with fluids of about 5 weight percent sodium chloride equivalent and containing carbon dioxide. Late-stage fluorite was deposited from fluids with similar salinity but devoid of carbon dioxide at a temperature of about 210°C.

Huebnerite in the veins is of nearly end-member composition in the huebnerite-wolframite-ferberite series; iron content increases with altitude in the system. The present veins are interpreted to be near the bottom of the original system. A postulated upper part, now removed by erosion, may have formed in granite cupolas where deposits were richer and the tungstate much more iron rich.

INTRODUCTION AND ACKNOWLEDGMENTS

Small huebnerite-bearing quartz veins in granite just east of Round Mountain, Nye County, Nev., have been known since 1907 (Ferguson, 1921, p. 388–390). The veins have produced only a small quantity of tungsten since their discovery, and residual surface material near the veins also has produced a little tungsten, in 1915. According to Schilling (1963), the total production of tungsten from the Round Mountain district is between 1,000 and 10,000 units of WO_3 (1 unit equals 20 lbs). H. K. Stager (oral commun., Sept. 1983) indicated that recorded production is 500–1,000 units, mostly from residual surface material. Some of the tungsten veins have been prospected for uranium (Kral, 1951, p. 154).

The Round Mountain district is better known as a gold district, having produced a little more than 0.5 million oz of gold through 1959 (Koschmann and Bergendahl, 1968, p. 194), both from placer deposits and from lode deposits in Tertiary rhyolite. A stockwork gold deposit in Tertiary rhyolite was reactivated in 1976, and during the first 2 years of renewed mining more than 50,000 oz of gold was produced (R. J. Leone, written commun., 1978). About 50,000 oz of gold per year has been produced since then (Russell Wood, oral commun., Dec. 1980) for a total production of about 200,000 oz during the present phase of mining. Production of the deposit and development of new reserves are continuing. Newly discovered reserves in a nearby ore body of 8.4 million oz gold and 15.7 million oz silver were announced recently (Wall Street Journal, Jan. 5, 1982).

Despite the apparent economic insignificance of the huebnerite veins, their study is important for several reasons. First, the huebnerite is of nearly end-member composition, a rarity worldwide. Second, the veins appear to have been formed many millions of years following emplacement (in Cretaceous time) of a granite pluton with which they are associated. Commonly, such tungsten-bearing veins are interpreted to have formed as a final event related to magmatic emplacement of granite. Third, tourmaline in the granite pluton is not related genetically to the tungsten-bearing veins as is common the world over, but instead it is related to an Oligocene granodiorite stock that invades the granite and is substantially younger than the huebnerite veins. Finally, the huebnerite veins present evidence of two major episodes of mineralization. The first episode saw deposition of huebnerite along with quartz, muscovite, and fluorite closely following invasion in Late Cretaceous time of the granite by aplite and pegmatite dikes. The second episode of mineralization was introduction into the huebnerite veins of several sulfide minerals,

tetrahedrite-tennantite, barite, and chalcedony, and formation of scheelite, in a zone spatially associated with the Oligocene granodiorite stock, and at a time probably shortly following emplacement of the stock.

This study is part of a broad investigation by the U.S. Geological Survey of the geology and mineral deposits of the Round Mountain and Manhattan 7½-minute quadrangles, Nye County, Nev.

We wish to thank Charles M. Taylor of C. M. Taylor Microprobe Co. for examining one of the huebnerite specimens (DRS–79–68) by electron microprobe to measure iron content of color-zoned crystals. The late Graham R. Hunt of the U.S. Geological Survey performed optical-spectral studies of several huebnerite specimens. Discussions with C. G. Cunningham and J. T. Nash of the Geological Survey proved helpful in our interpretation of the fluid inclusion data, and discussions with G. A. Desborough and B. F. Leonard, III, of the Geological Survey aided our microprobe and other mineralogic studies. Comments on the manuscript by G. P. Landis and W. H. Raymond improved our interpretations of some of the data.

GEOLOGIC SETTING OF THE VEINS

The huebnerite veins near Round Mountain occur in and near Cretaceous granite that forms a large pluton extending 23 km southeast across the Toquima Range from Round Mountain to a long-inactive silver camp at Belmont (fig. 1). The granite is emplaced in Paleozoic sedimentary and metamorphic rocks. A swarm of Oligocene rhyolite and andesite dikes and a granodiorite stock intrude granite about 3 km east and southeast of Round Mountain. Miocene silicic volcanic rocks overlie both granite and sedimentary rocks locally in the area, and Quaternary alluvium fills the intermontane valleys that flank the Toquima Range (Ferguson, 1921; Shawe, 1977a).

The Paleozoic rocks are marine sedimentary rocks: quartzite, silty argillite, and limestone of Cambrian (possibly in part latest Precambrian) age, and argillite, limestone, dolomite, chert, and quartzite of Ordovician age. Aggregate thickness of the Paleozoic rocks, in part probably the result of repetition by thrust faulting, is at least 1.5 km. Locally the argillite has been metamorphosed to phyllitic shale, and near the contact with granite it consists of knotted (chloritoid) schist and muscovite-biotite schist. In places the limestone is tremolitized strongly, although not necessarily in proximity to the granite contact. In only a few places does limestone contain epidote and garnet, possibly as a result of contact metamorphism adjacent to granite.

"The granite typically is a coarse-grained, granular-textured, light-gray rock that contains quartz, microcline, orthoclase, sodic plagioclase, biotite, and muscovite. Accessory minerals are monazite, apatite, [zircon,] and iron-titanium oxide minerals. Fluorite and tourmaline are present locally. Some rocks of the pluton are quartz monzonite and granodiorite rather than granite" (Shawe, 1977a). An apparently early phase of the granite pluton present 8 km south-southeast of Round Mountain and extending to Belmont is porphyritic and contains large microcline crystals mostly 2–8 cm long.

Much of the granite is foliated, especially near the border of the pluton. Foliation that is manifested chiefly by alined biotite and muscovite flakes, and locally by lensoid quartz and feldspar grains, is conformable with the contact. The moderately outward dipping contacts of the granite pluton and the conformable foliation in the granite impart a domelike form to the pluton. The pluton is cut by numerous aplite and pegmatite dikes and by quartz veins. Aplite and pegmatite commonly occur together in individual dikes, and thus are coeval, although some dikes locally are cut by younger dikes of the same composition. Some foliated dikes are cut by unfoliated dikes. Quartz veins everywhere cut the aplite and pegmatite dikes. The veins include many that are barren and some that are sulfide-bearing in addition to those with huebnerite. In places iron-oxide stain in granite is intense; numerous limonite pseudomorphs after cubic pyrite suggest that most of the iron-stained rock is hydrothermally altered granite that has been weathered.

The date of emplacement of the granite was 90–100 m.y. ago (Shawe, 1977a). Several potassium-argon ages on muscovite and biotite from foliated granite, pegmatite dikes, and quartz veins are about 80 m.y., indicating that doming and metamorphism of the granite, and emplacement of pegmatite and aplite dikes and quartz veins, took place in a single episode many millions of years after emplacement of the pluton.

The Oligocene dike swarm east and south of Round Mountain trends northeast and is about 1.5 km wide and 11 km long. The Oligocene stock intrudes the swarm near its northeast end. The intrusives are dated as about 35 m.y. old (Shawe, 1977a). Mineralization that formed tourmaline along with andalusite and dumortierite in granite and tourmaline in rhyolite dikes, is spatially associated with, and apparently genetically related to, the granodiorite stock. Surprisingly the tourmaline mineralization is in no way related to the much earlier episode of huebnerite mineralization, but as described later, did involve a small degree of tungsten mineralization.

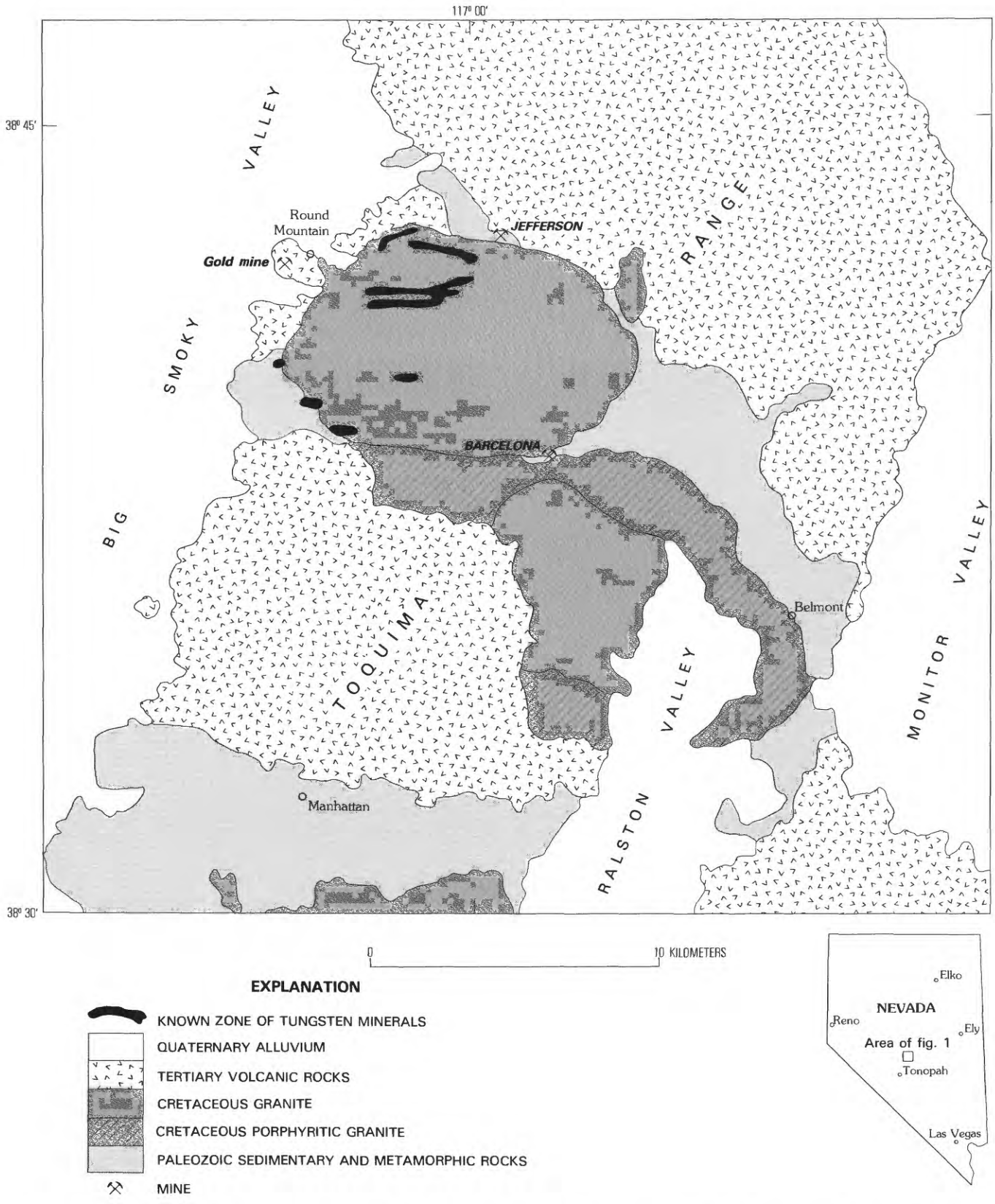

FIGURE 1.—Geologic map of the area near Round Mountain, showing zones of tungsten minerals east and south of Round Mountain.

DISTRIBUTION AND FORM OF THE VEINS

The huebnerite veins east of Round Mountain are found in an area that covers about 25–35 km^2 (fig. 2). Despite this broad distribution, the veins occur in only a few clusters that are narrow east-trending zones no more than 200 m wide and 4 km long (fig. 2). The huebnerite veins have been found in a vertical interval of about 500 m, between altitudes of about 2,125 m and 2,625 m (6,800 ft and 8,400 ft). Geologic reconstruction of the granite pluton prior to erosion suggests that veins in the core of the pluton were 1.5–2 km below its apex. There is no evidence that individual veins extend for more than about a hundred meters vertically and most probably are much less than that. Veins within the east-trending clusters are narrow (mostly no more than 30 cm wide) and short (generally less than 30 m long). According to Brown (1911), numerous quartz stringers and veins that ranged in thickness from 2.5 cm to 1 m extended across the principal east-trending belt. Mostly tabular, the veins pinch and swell locally and may vary greatly in thickness in a short distance. They occur singly in most places within the east-trending clusters, although in a few places they appear to occur as very short, en echelon segments. Ferguson (1921, p. 389) stated that the veins locally "are close enough together to give a banded appearance to the granite." Some of the thicker veins split along strike into several thin, nearly parallel veinlets. Most of the veins are in granite where they tend to strike northeast and dip moderately to steeply southeast (table 1). A few veins 5 km south of Round Mountain occur in muscovite-biotite schist close to the granite contact. These veins lie in the schist foliation and dip away (southwestward) from the granite contact at low to moderate angles. One vein is known in quartzite north of the granite contact and east of Round Mountain.

At the time of tungsten mining in 1911, as reported by Brown (1911), workings consisted of three tunnels in granite. Tunnel No. 1 followed veins and stringers for 60 m across the belt, with a crosscut extending 60 m west that exposed "a large body of milling ore, varying in width from three to ten feet [1–3 m]." Tunnel No. 2 was "a drift on the strike of the belt for a distance of 400 feet [120 m], exposing large bodies of good milling ore, varying in width from four to twelve feet [1.2 to 3.7 m]." Tunnel No. 3 was also "a drift on the belt for a distance of 390 feet [120 m], cross-cutting many veins and stringers," with two drifts from it following separate veins 30 m in length. These workings exposed "very good ore bodies***having a width of from five to fourteen feet [1.5 to 4.3 m]." The locations of these tunnels are not certain now, but probably they are the same as the workings known near the bottom of Shoshone Canyon at and near the Darrough prospect (fig. 2).

ALTERATION RELATED TO THE VEINS

The huebnerite-bearing quartz veins are bounded by a selvage of hydrothermally altered rock. This selvage is most evident in granite and is inconspicuous in schist. Granite adjacent to veins has been strongly altered so that virtually all feldspar crystals have been replaced by sericite. Biotite commonly has been converted to muscovite, and coarse muscovite crystals have developed locally in masses of sericite within replaced feldspar crystals. Quartz, pyrite, chalcopyrite, fluorite, and huebnerite have been added to wall rocks locally. According to Brown (1911) huebnerite crystals occurred in bunches in clay selvages adjacent to the larger veins and in the enclosing granite walls. Our studies were not adequate to determine the thickness of the altered granite selvage adjacent to huebnerite veins. The granite in some places has been widely altered—mainly sericitized and pyritized—probably by mineralizing events other than the tungsten episode, and this fact has prevented our distinguishing the altered rocks related only to tungsten mineralization. Schist wall rocks adjacent to huebnerite veins contain finely crystallized muscovite and biotite, but so does all the schist in the vicinity of the granite contact. Some of the schist wall rocks contain tiny cubes of pyrite (weathered to limonite) and minor huebnerite. We were unable to determine alteration products related solely to the emplacement of the huebnerite veins.

Locally, within the area of huebnerite veins, the granite has been strongly greisenized with development of much muscovite and some fluorite. Greisen is here defined as altered granite consisting of dominant muscovite and containing significant fluorite; quartz, feldspar, and other minerals may be present. In places the greisen bounds quartz veins not known to contain huebnerite but probably of the same mineralizing episode, and in other places greisen forms small pipes not closely associated with quartz veins.

DESCRIPTION OF THE VEIN MINERALS

Minerals of the huebnerite veins comprise three groups: primary (hydrothermal) gangue minerals, primary (hydrothermal) ore minerals, and secondary (alteration) minerals formed as a result of weathering of the veins. Primary gangue minerals are quartz, muscovite, allanite, fluorite, barite, calcite, and chalcedony. Monazite may be a gangue mineral, but we have no direct evidence that it is. Primary ore minerals are huebnerite, scheelite, tetrahedrite-tennantite, pyrite,

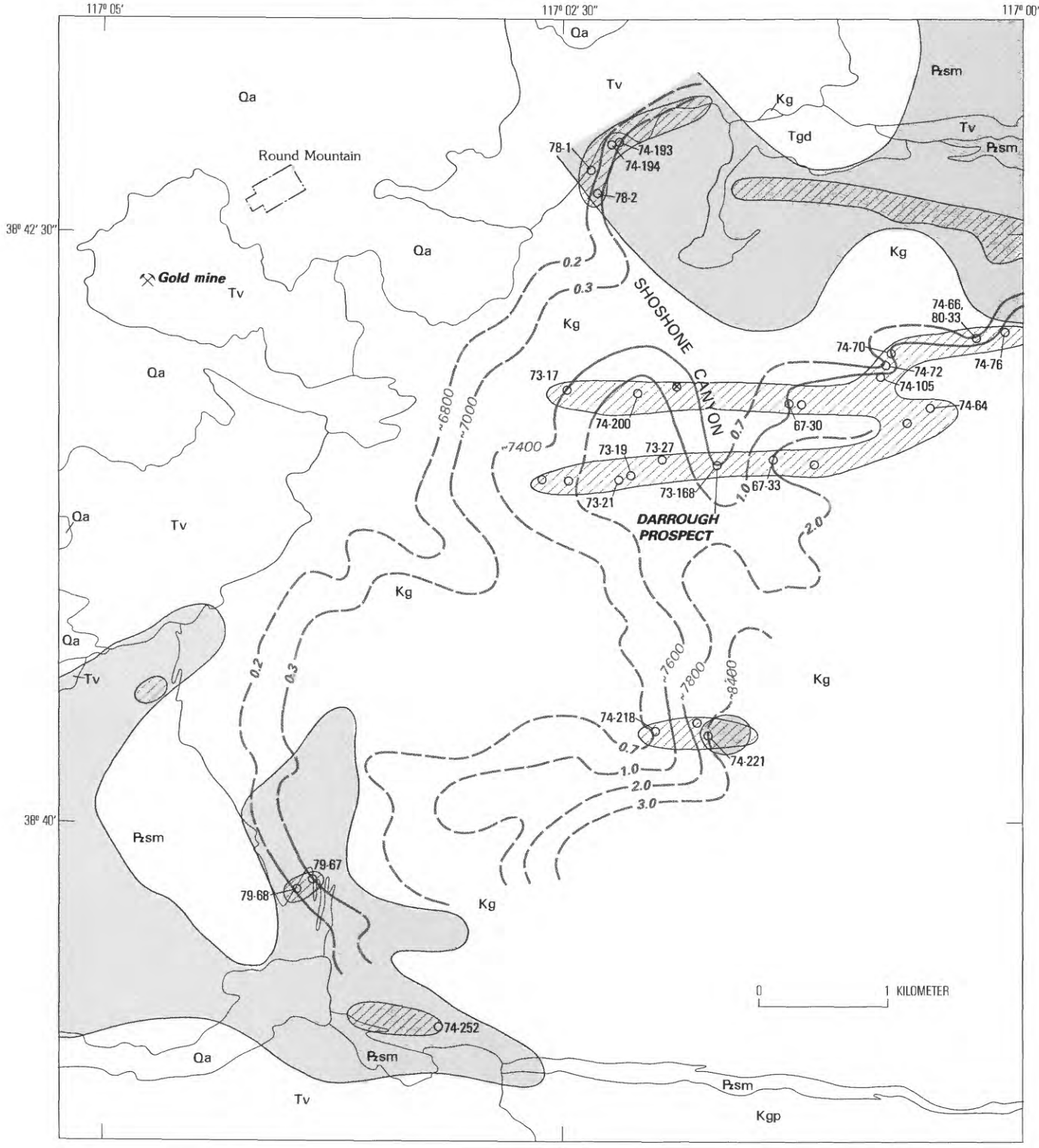

FIGURE 2.—Generalized geologic map of the tungsten area near Round Mountain, showing localities of samples described in this report. Open circle is locality where huebnerite was identified in vein material; only collected samples are labeled with sample numbers. Open circle with X is locality referred to in text. Thin solid line, contact. Pzsm, Paleozoic sedimentary and metamorphic rocks; Kgp, Cretaceous porphyritic granite; Kg, Cretaceous granite; Tgd, Tertiary granodiorite stock; Tv, Tertiary volcanic rocks; Qa, Quaternary alluvium. Cross-lined areas, tungsten-mineralized zones (0.005–1.0 percent W or visible huebnerite); shaded areas, base- and precious-metal-mineralized zones (as much as 3.0 percent Cu, 10.0 percent Pb, 5.0 percent Zn, 0.00036 percent Au, and 0.15 percent Ag). Dashed lines are generalized topographic contours, in feet, labeled with iron content (in percent, determined by spectrographic analysis) in huebnerite at sample localities (see table 6): 0.2 percent Fe approximates 6,800 ft, 0.3 approximates 7,000, 0.7 approximates 7,400, 1.0 approximates 7,600, 2.0 approximates 7,800, 3.0 approximates 8,400 (see fig. 36). (1 ft=0.3 m.)

TABLE 1.—*Description of huebnerite-bearing quartz-vein samples collected east and south of Round Mountain*

[Localities shown on figure 2; leader (–), not determined]

Sample No. DRS–	Strike and dip of vein	Host rock	Scheelite	Sulfide or sulfosalt	Barite
67-30	N. 15° W. 35° E.	Granite	no	no	no
67-33	N. 60° E. 55° SE.	--do---	sparse	no	yes
73-17	N. 15° E. 70° E.	--do---	no	no	no
73-19	N. 30° E. 50° SE.	--do---	no	no	no
73-21	N. 40° E. 60° SE.	--do---	no	no	no
73-27	-- --	--do---	no	no	no
73-168	-- --	--do---	no	no	no
74-64	N. 40° W. 30° NE.	--do---	--	--	no
74-66	N. 18° E. 61° E.	--do---	abundant	yes	no
74-70	N. 42° E. 51° SE.	--do---	no	no	yes
74-72	-- --	--do---	no	no	no
74-76	N. 35° E. 16° SE.	--do---	sparse	no	no
74-105	N. 19° E. 39° E.	--do---	no	no	no
74-193	N. 30° E. 85° SE.	--do---	sparse	yes	no
74-194	N. 10° E. 80° E.	--do---	--	yes	no
74-200	-- --	--do---	no	no	no
74-218	-- --	--do---	no	no	no
74-221	N. 45° E. 65° SE.	--do---	abundant	yes	yes
74-252A,B	N. 15° E. 79° W.	--do---	sparse	yes	no
78-1	-- --	Quartzite	no	yes	no
78-2	N. 35° E. 67° SE.	Granite	abundant	yes	yes
79-67A,B	-- --	Schist	sparse	no	no
79-68	N. 15° W. 40° W.	--do---	abundant	yes	no

galena, sphalerite, chalcopyrite, pyrrhotite, covellite, and blaubleibender covellite (a variety of covellite that remains blue in polarized light under the reflecting microscope). Secondary minerals are covellite, blaubleibender covellite, chalcocite, stromeyerite, acanthite, stibiconite, azurite, malachite, chrysocolla, cerussite, anglesite, brochantite, limonite, jarosite, plumbojarosite, autunite, pyrolusite, psilomelane, other manganese oxides, tungstite(?), ferritungstite, jixianite(?), stolzite, calcite, and opaline silica (chalcedony).

PRIMARY GANGUE MINERALS

QUARTZ

Alpha quartz is the principal component of the veins. It tends to fill the vein space as a solid mass of intergrown crystals that individually are as much as 10 cm long and 2 cm wide. In places vugs remain, and a few veins have much open space in their cores into which euhedral, commonly slightly tapered quartz crystals penetrate (fig. 3). Crystals here tend to grow perpendicular to the vein walls and may develop forms resembling cockscomb structure. However, many quartz crystals are randomly oriented, and large open spaces within veins may be lined with doubly terminated quartz prisms that have grown transversely on crystals that penetrate the vugs (fig. 3). Most of the quartz is milky white but tends to be only slightly milky or clear and colorless where crystals penetrate vugs. Locally clear quartz crystals that penetrate vugs are smoky gray.

Shears parallel to the walls of the veins are common, and shear surfaces generally are slickensided. Only rarely has quartz in parts of the veins been strongly broken and sheared, and then refilled with younger quartz. For example, in one place (sample DRS–74–193) vein quartz has been brecciated, the breccia filled with chalcedony, and the chalcedony-filled breccia veined with clear mosaic quartz (grains less than 1 mm in size) that shows mild strain but is virtually free of fluid inclusions. However, some veins are composite, such that part of the vein consists of quartz that filled an initial open-space fracture that was again opened and filled with quartz. The reopened fracture in some places is one wall of the original vein and in other places it is within the original vein. Massive quartz of the older and younger parts of a vein generally seems to merge owing to recrystallization, as described below.

Massive, milky-white vein quartz may be extensively recrystallized, and virtually all of it is strained. As seen in thin sections, this material appears as dominantly anhedral intergrown crystals (mosaic structure; locally,

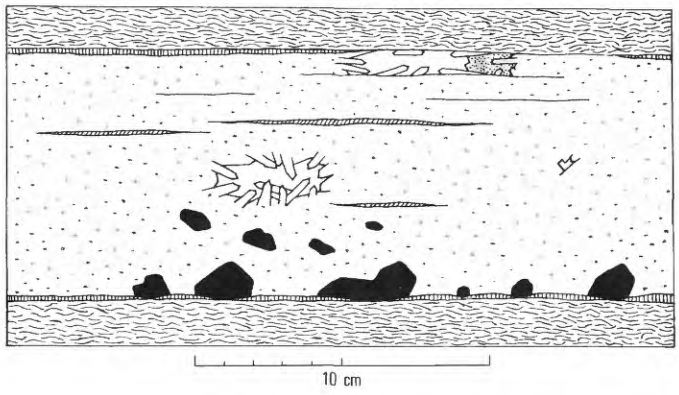

FIGURE 3.—Diagrammatic sketch of huebnerite-bearing quartz vein (sample DRS–79–68) in quartz-mica schist. Sample is from prospect dump; attitude of schist foliation at prospect is N. 15° W., 40° W. Wavy dash pattern, schist wall rock; sparse stipple, massive milky quartz; clear colorless quartz crystals project into vugs (solid white); cross lining, muscovite selvages and seams; solid black, huebnerite; close stipple, fluorite.

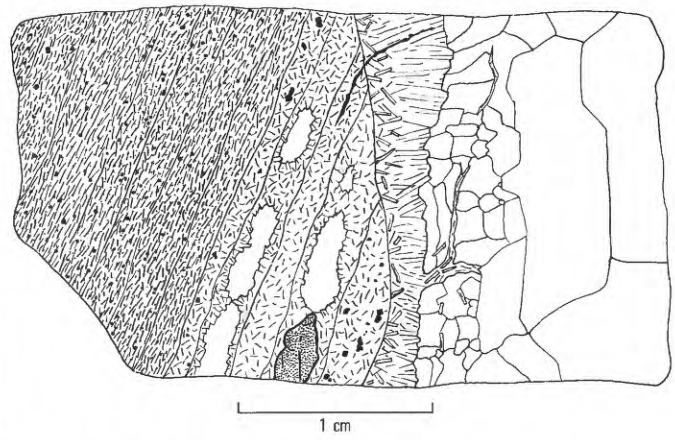

FIGURE 4.—Sketch of thin section of sample DRS–79–68B showing locally transgressing contact between huebnerite-bearing quartz vein (right) and quartz-mica schist wall rock (left). Wall rock schist (subparallel dashes) contains abundant tiny pyrite cubes weathered to limonite (black specks); some schist septa are almost wholly muscovite (unoriented dashes) locally with some pyrite (black blebs); other septa contain clear unstrained quartz (solid white) and minor huebnerite (high relief, close-stippled mineral) in muscovite. Quartz vein (no huebnerite present in this thin section) has muscovite (bladed) selvage and contains wisps and flakes of muscovite. Quartz (solid white) is strained, and near vein selvage shows well-developed mosaic structure. A thin, limonite-filled fracture (near top of thin section) extends from a schist septum across vein wall and into muscovite selvage of the vein.

almost mortar structure) with uneven extinction, mostly 1–5 mm across (fig. 4), but locally also as strung-out aggregates of tiny crystals that average about 0.1 mm in size (fig. 5). Leonard, Mead, and Conklin (1968, p. 56) described similar quartz in a tungsten lode at the New Snowbird deposit, Idaho. In places the finer grained aggregates occur in zones that parallel vein walls, and they probably resulted from shearing. The recrystallized quartz in places contains very abundant, minute, somewhat cymoidal fractures 0.03–0.15 mm long that are arranged in narrow elongate zones parallel to the vein walls. The zones of minute fractures vary according to the crystallographic orientation of the quartz crystals. Where the *c* axis is parallel to the vein walls, the fractures are nearly parallel and on end. Where the *c* axis is oblique or normal to the vein walls, the fractures are arranged en echelon in the elongate zones, which themselves are parallel to the vein walls. Commonly, alternating zones of fractures have alternating orientations of the contained fractures, such that the direction of zone elongation bisects the acute angle formed by the alternating fracture orientations, producing a crude herringbone effect.

Fluid inclusions are present in much of the quartz. As seen in thin sections, most of the inclusions occur in strings or trains that commonly transgress grain boundaries (fig. 6). Most sets of subparallel fluid inclusion trains are alined with vein walls, but other orientations are common (fig. 5). In places, sets of subparallel fluid inclusion trains seem restricted to small fields or cells that show an orientation different from those of adjacent fields, as though the fields became rotated unevenly following formation of the trains of inclusions. Fluid inclusions tend to be absent from quartz near free crystal faces that border vugs in the massive vein quartz (figs. 6, 19, 20). Quartz prisms that penetrate voids and are almost wholly surrounded by space appear to be almost totally devoid of fluid inclusions (figs. 18, 21). Thus, as seen in hand specimens, quartz crystals that penetrate vugs appear to be clear and colorless, whereas massive quartz is opaque and white as the result of diffusion of light caused by millions of microscopic fluid inclusions.

The fluid inclusions vary in shape and size. Extremely small (<0.01 mm) inclusions tend to be equidimensional and to show negative quartz crystal forms. Medium-size (0.02–0.05 mm) inclusions are somewhat oblong and slightly irregular, with stubby spurs extending from some corners. Large (as much as 0.1 mm) inclusions tend to be quite ragged and irregular, some being weblike in form. All three forms of inclusions occur mostly in trains, although all also may occur randomly scattered. There seem to be no criteria evident by which any of the fluid inclusions could be identified as primary; virtually all may be secondary. However, J. T. Nash of the U.S. Geological Survey (written communs., January 1969 and March 1980) reported sparse primary fluid inclusions in clear, colorless quartz. Most of the fluid inclusions contain a single gas bubble whose diameter is about half the diameter of the inclusion, but sizes of bubbles relative to apparent volume of the fluid in the inclusions vary. Some inclu-

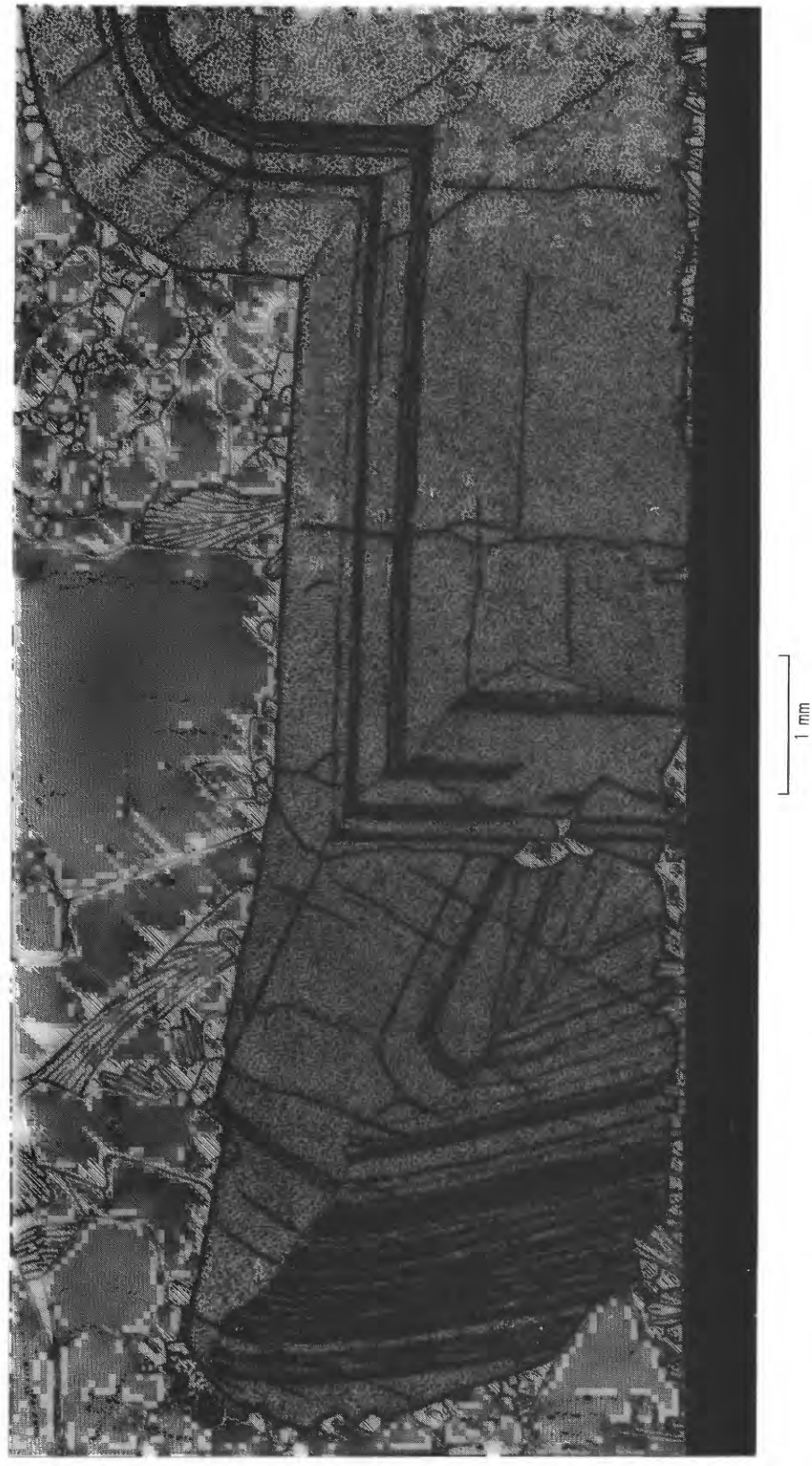
1 mm

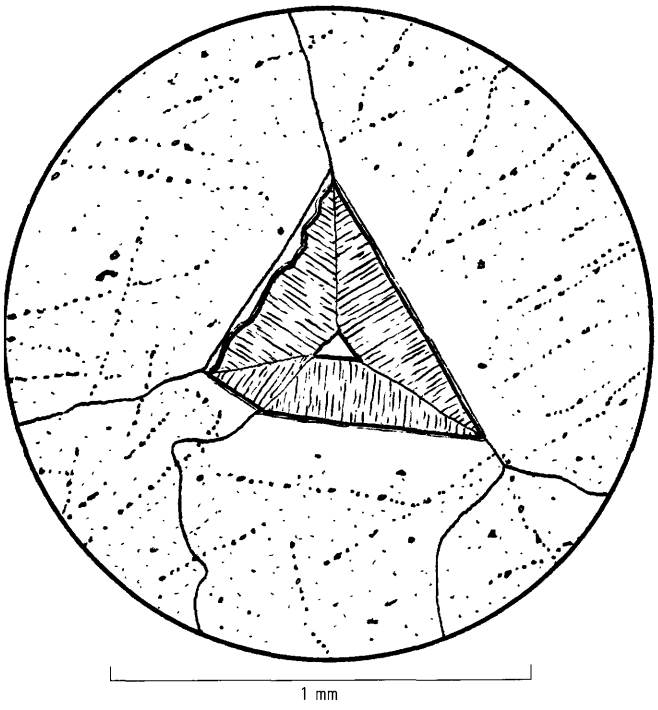

FIGURE 6.—Quartz charged with fluid inclusions (black specks), thin section of sample DRS–78–2A. Small vug (center) is partly lined with botryoidal chalcedony (on upper left quartz prism face) and filled with fibrous chalcedony; core of vug is granular chalcedony. Note the dominant subparallel orientation of trains of fluid inclusions, some of which transgress boundaries of quartz crystals, and the lack of fluid inclusions near the vug.

sions contain a second bubble, consisting of liquid carbon dioxide, within which the gas bubble is suspended. The diameter of this carbon dioxide bubble varies substantially among different inclusions, from slightly longer to perhaps twice as long as the diameter of the enclosed gas bubble.

Fluid inclusions that contain only a single bubble are much more abundant than those that also contain liquid carbon dioxide. The carbon dioxide-bearing inclusions are irregularly distributed; most thin sections examined in this study contain very few. Locally, however, the carbon dioxide-bearing inclusions are quite abundant, but still unevenly distributed. One thin section of quartz vein material from sample DRS–67–30 shows abundant carbon dioxide-bearing fluid inclusions in one large area that is defined by a set of subparallel trains of fluid inclusions, whereas another part of the thin section that is defined by another set of trains of fluid inclusions is almost devoid of carbon dioxide-bearing inclusions.

According to J. T. Nash (written communs., January 1969 and March 1980), massive milky quartz of the veins contains small fluid inclusions that have filling temperatures of 250°–270°C. Liquid carbon dioxide is present in many of these fluid inclusions. Nash estimated that original fluids contained about 2–10 mol percent (5–20 weight percent) carbon dioxide. Freezing temperatures of fluid inclusions in this quartz indicate a salinity of 5.2 weight percent sodium chloride equivalent. Fluid inclusions in clear quartz crystals that penetrate vugs give filling temperatures of about 190°C. The fluid inclusions in clear quartz contain no liquid carbon dioxide. Freezing temperatures of fluid inclusions in clear quartz indicate a salinity of 5.7 weight percent sodium chloride equivalent.

MUSCOVITE

Muscovite is a common component of the huebnerite veins, and although it makes up perhaps only 1–5 percent of the vein material, it is everywhere present (figs. 3, 4, 5). The muscovite is colorless, very pale silvery gray, or very pale yellowish green. It almost universally forms a thin selvage 1–5 mm thick on the vein walls. Muscovite flakes tend to grow perpendicular to the vein margins (figs. 4, 5). Although the *c* axes of the crystals commonly are nearly parallel to the margin, their orientation otherwise appears to be random so that the muscovite forms a feltlike layer viewed normal to the vein wall. In places the muscovite in the vein

FIGURE 5 (facing page).—Zoned huebnerite crystals (dense stipple)grown on vein wall (black), thin section of sample DRS–79–68A. Compound (twinned?) crystal at right displays simple growth zone pattern. Note that crystal touches the vein wall locally, and otherwise has grown upon quartz (solid white) or muscovite (bladed) selvage. Complexly zoned huebnerite crystal at left commenced growth at the left end of the compound crystal, near the vein wall. Note that growth zones are grossly different above and below a growth boundary that extends diagonally toward the upper left of the crystal; uniform extinction under the microscope indicates crystallographic continuity across the growth boundary of the two differently zoned segments. The complex growth zonation of the huebnerite suggests a possibly complex history of crystal growth, partial dissolution, and regrowth of a differently zoned segment. Fluorite (high-relief, patterned, labeled F) forms two small crystals, one between quartz and huebnerite crystals near the initiation point of the complexly zoned huebnerite crystal, and one near the middle of the upper edge of that crystal. Barite (high-relief, patterned, labeled B) forms an irregular patch on the upper right point of the complexly zoned huebnerite crystal. Muscovite (plumose and bladed) has grown on huebnerite crystals and in a vug (upper left). Quartz (solid white, and marked with numerous strings of fluid inclusions) is strained; at the left, shapes of original growth prisms remain; at the right, quartz has recrystallized and displays mosaic and mortar structure.

selvage shows a slightly plumose habit (figs. 4, 5). Thin lensoid layers of muscovite 1–2 mm thick are found locally within quartz veins, oriented parallel to the vein walls (fig. 3). Originally these may have been selvages on veins that were reopened and again filled with quartz so that the selvage that clung to the original vein quartz then formed a layer enclosed within vein quartz. Muscovite flakes in some of these internal lenses have a pronounced "rake" (fig. 3) as though the flakes were dragged out of their normal perpendicular alinement by shearing within the vein. Irregular small patches and clusters of muscovite flakes are found intergrown with quartz and huebnerite throughout the veins.

As seen in thin sections, muscovite also occurs as crystals 0.1–1 mm long that fill thin shears in quartz that parallel the vein walls (fig. 4). Unlike the muscovite crystals in thicker lensoid layers that are oriented normal to the muscovite layers, the muscovite crystals in the thinner shears are parallel to the vein walls. These thin, muscovite-filled shears are closely associated with parallel streaks of finely crystallized quartz.

A purified portion[1] of muscovite selvage from sample DRS–79–68 was analyzed by J. E. Taggart of the U.S. Geological Survey using X-ray fluorescence techniques. Results of the analysis, in weight percent, are given in table 2. Muscovite separated from samples DRS–79–67 and DRS–79–68 was analyzed spectrographically; results are given in table 3[2]. These samples were handpicked but not carefully purified mechanically, and the analytical results show evidence of minor impurities.

The unusually high magnesium content of the muscovites shown by both X-ray fluorescence and spectrographic analyses, and the abnormally high silica and abnormally low alumina shown by the X-ray fluorescence analysis, indicate that the muscovites are phengitic. In phengite the octahedral Al is replaced by Mg and (or) Fe^{+2} and the tetrahedral Al is replaced by Si. Data for a phengite of similar composition from a pegmatite at Amelia, Va. (Glass, 1935), are given for comparison in table 2.

Substantial amounts of silver, copper, molybdenum, lead, and zinc in sample DRS–79–68 (table 3) are likely present in sulfide impurities, and abnormally high amounts of tungsten in samples DRS–79–67 and DRS–79–68 (table 3) are probably present in huebnerite or scheelite. Most of the other minor elements shown in the spectrographic analyses could be present in the muscovite structure. Amounts of lithium and barium in muscovite from sample DRS–79–68 are sufficiently high that, if added to the components analyzed by X-ray fluorescence, they would raise the total to nearly 100 percent.

TABLE 2.—*Chemical analysis of muscovite from Round Mountain huebnerite vein compared with chemical analysis of phengite from Amelia, Va., pegmatite (Glass, 1935)*

[Leaders (---), not looked for]

	Muscovite from Round Mountain huebnerite vein	Phengite from Amelia, Va., pegmatite
SiO_2	49.5	49.16
Al_2O_3	30.0	30.81
Fe (as Fe_2O_3)	.17	---
FeO	---	1.43
MgO	2.94	2.22
CaO	.05	---
Na_2O	<.2	.48
K_2O	11.10	10.90
TiO_2	.09	---
P_2O_5	<.05	---
MnO	.60	---
S	<.02	---
Loss on ignition[1]	3.91	---
H_2O+	---	4.73
H_2O-	---	.15
Other	---	.19
Totals	98.36	100.07

[1]30 minutes at 900°C.

Muscovite collected from vein material at the Darrough tungsten prospect (sample DRS–67–122, same location as DRS–73–168) has a potassium-argon age of 79.2 ± 2.2 m.y. (Marvin and Dobson, 1979, p. 23).

ALLANITE

A few small elongate prisms of a brown, pleochroic mineral showing inclined extinction, high relief, and moderate birefringence were identified optically as allanite in sample DRS–78–2B. The allanite crystals are enclosed in vein quartz (fig. 21) and are inferred to have been deposited during the initial main phase of vein formation.

FLUORITE

Fluorite is widely but irregularly distributed through the huebnerite veins. Where present it is generally sparse and may make up less than 1 percent of a vein;

[1]Purification of the muscovite entailed trimming of the selvage with adiamond saw, crushing, grinding, and sieving. A 35–60 mesh fraction was treated with magnetic separation and heavy liquids; bromoform (D 2.85) floated quartz, and methylene iodide-bromoform mixture (D 3.10) sank heavy minerals. The sample was finally hand picked to assure a virtually pure concentrate (0.80 g).

[2]Approximate lower limits of determination for elements analyzed by the six-step spectrographic method, data for which are presented in tables 3, 6, and 7, are given in table 4.

TABLE 3.—*Semiquantitative spectrographic analyses, in weight percent, of some minerals from huebnerite-bearing quartz veins (sample localities shown on fig. 2)*

[Analyses by Nancy M. Conklin. N, not detected at limit of detection or at value shown (see table 4). L, detected, but below limit of determination or below value shown. Also looked for but not found: Au, Co, La, Pd, Pt, Te, U, Zr, Ce, Ge, Hf, In, Re, Ta, Th, Tl]

Mineral-----	Muscovite	Muscovite	Fluorite	Barite	Tetrahedrite-tennantite	Tetrahedrite-tennantite	Galena
Sample No.--	DRS-79-67	DRS-79-68	DRS-79-67	DRS-74-221	DRS-78-1	DRS-78-2	DRS-74-221
Si	>10	>10	0.03	0.07	1	3	0.3
Al	>10	>10	.07	L .001	.015	.015	.015
Fe	.7	1.5	.1	.07	.7	1	.003
Mg	3	3	.005	L .001	.001	.007	L .001
Ca	1.5	.05	>10	.007	1.5	3	.003
Na	.3	.3	N .05	N	.2	.1	N .05
K	7	10	N	N	N	N	N
Ti	.07	.07	N	N	N	N	N
Mn	.3	.3	.15	.003	.02	.005	.0007
Ag	N	.01	N	.002	>2	>2	.3
As	N	N	N	N	>10	>10	N
B	.003	.003	N	N	N	.015	N
Ba	.07	.7	.0015	>10	.05	.7	.007
Be	.007	.007	N	.0003	N	N	N
Bi	N	.0015	N	N	.15	.7	.3
Cd	N	N	N	N	.15	.07	N
Cr	.0002	.0003	N	L	N	N	N
Cu	.0015	.07	N	.0015	>10	>10	I
Ga	.003	.007	N	N	N	N	N
Li	.07	.15	N	N	N	N	N
Mo	N	.07	N	N	N	N	N
Nb	.0015	.0015	.005	N	N	N	N
Ni	.0015	N	N	N	N	N	N
Pb	.003	.7	N	.01	.1	.15	>10
Sb	N	N	N	N	>10	>10	.07
Sc	.0007	.001	N	N	N	N	N
Sn	N	.001	N	N	N	N	N
Sr	.03	.003	.7	.5	.007	.07	.0015
V	.007	.007	N	N	.0015	.0015	N
W	.3	.02	.3	N	.03	N	N
Y	N	N	.015	N	N	N	N
Yb	N	N	.0015	N	N	N	N
Zn	N	.03	N	N	7	5	N

TABLE 4.—*Approximate lower limits of determination for elements analyzed by the 6-step spectrographic method (in percent)*

Si	0.002	Ga	0.0005	Sr	0.0005
Al	.001	Gd	.005	Sm	.01
Fe	.001	Ge	.001	Ta	.02
Mg	.002	Hf	.01	Tb	.03
Ca	.002	Ho	.002	Te	.2
Na	.05	In	.001	Th	.02
K	.7	Ir	.005	Tl	.005
Ti	.0002	La	.003	Tm	.002
P	.2	Li	.005	U	.05
Mn	.0001	Lu	.003	V	.0007
Ag	.00005	Mo	.0003	W	.01
As	.1	Nb	.001	Y	.001
Au	.002	Nd	.007	Yb	.0001
B	.002	Ni	.0005	Zn	.02
Ba	.00015	Os	.005	Zr	.001
Be	.0001	Pb	.001		
Bi	.001	Pd	.0001		
Cd	.002	Pr	.01		
Ce	.015	Pt	.003		
Co	.0003	Re	.003		
Cr	.0001	Rh	.0002		
Cu	.0001	Ru	.001		
Dy	.005	Sb	.015		
Er	.005	Sc	.0005		
Eu	.01	Sn	.001		

locally, however, such as where wall rocks are schist, it may constitute as much as 25 percent of short segments of a vein. It is mostly white but also pale green and pale to deep purple; Ferguson (1921, p. 389) described "complex delicate pink crystals" in many veins; color varieties occur both separately and together. Typically, fluorite is a late vein mineral, filling vugs. Locally, the tabular interior parts of veins that were open space following quartz deposition are lined or filled with fluorite (fig. 3). Crystals that line vugs commonly have cubic form. Also, fluorite occurs in minor amounts associated with both early and late vein minerals. Tiny crystals are seen under the microscope in or adjacent to huebnerite (fig. 5), and fluorite is found enclosed in some growth layers in zoned huebnerite (fig. 7). Locally it is found intergrown with muscovite in vein selvages (fig. 8), where it apparently formed during initial stages of vein formation. Where quartz has been recrystallized, traces of fluorite may occur together with muscovite and pyrite in small patches interstitial to quartz

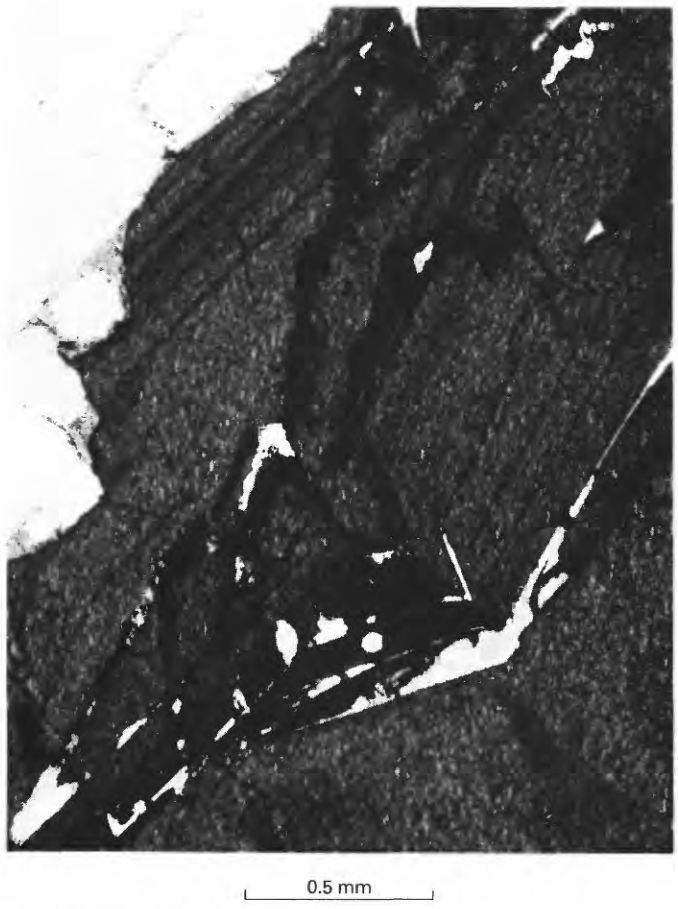

FIGURE 7.—Part of a zoned huebnerite crystal, plane-polarized light, thin section of sample DRS–79–68A. Crystal faces on the inner part of the huebnerite crystal (lower right) are coated with a thin, uneven layer of fluorite. Zoned and partly broken layers of huebnerite that contain blebs of quartz and fluorite overlie the inner fluorite layer. Quartz is molded against the corroded exterior of the huebnerite crystal (upper left).

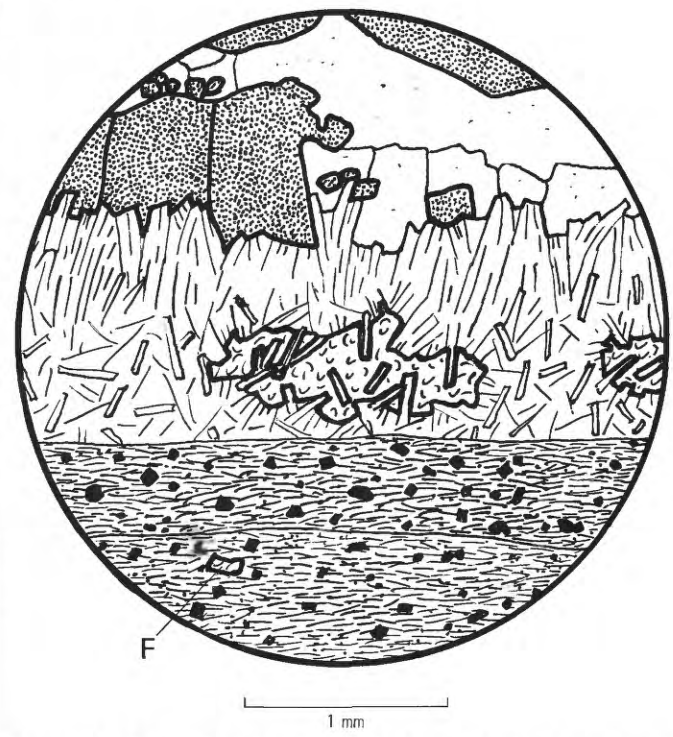

FIGURE 8.—Edge of huebnerite-bearing quartz vein (above) and sheared wall rock (below), thin section of sample DRS–79–68C. Sheared wall rock consists of muscovite (subparallel dashes), pyrite weathered to limonite (black cubes and blebs), and a trace of fluorite (high relief, patterned, labeled F); the sheared zone (2–5 mm thick) laterally (beyond the field of view) transgresses the margin of the vein and may be enclosed wholly in vein material or wholly in wall rock. Tetrahedrite-tennantite and its oxidation products occur in the sheared zone elsewhere. Vein selvage is muscovite (bladed and plumose), randomly oriented against the vein wall, and inward tending to be plumose, locally intergrown with fluorite that constitutes about 20 percent of the selvage. Huebnerite (high relief, dense stipple) and strained quartz (solid white, marked by fluid inclusions) fill the interior of the vein.

grains (fig. 9). Fluorite occurs also in trace amounts as a postvein mineral, within parts of veins that were strongly sheared following vein formation (fig. 8).

Examination of sample DRS–79–67 with an ultraviolet lamp indicated the presence of both phosphorescent and nonphosphorescent fluorite, suggesting the possibility of two separate episodes of fluorite deposition that resulted in fluorites of slightly different trace-element composition. Also, some fluorite in the huebnerite veins shows bluish-white fluorescence under short-wave ultraviolet radiation, and some does not.

A six-step semiquantitative emission spectrographic analysis of the pale fluorite in DRS–79–67 is presented in table 3. Minor impurities suggested by the data are pyrite (iron), muscovite (silicon and aluminum), and huebnerite (manganese and tungsten). Strontium, yttrium, and ytterbium likely are present in the fluorite structure.

Fluid inclusions are present in fluorite. According to J. T. Nash (written communs., January 1969 and March 1980), fluorite that fills vugs in quartz vein material contains fluid inclusions that have filling temperatures of 230°–260°C. Freezing temperatures of fluid inclusions in this fluorite indicate a salinity of 5.8–6.0 weight percent sodium chloride equivalent. Some of the fluorite that has fluid inclusions with a filling temperature of 260°C contains no visible carbon dioxide but decrepitates on heating, suggesting the presence of some carbon dioxide dissolved in the aqueous phase of the inclusions. Freezing temperatures of fluid inclusions in this fluorite indicate a salinity of 4.5 weight percent sodium chloride. Late-stage fluorite, also occurring as vug fillings, gives filling temperatures of about 190°C. No liquid carbon dioxide is evident in fluid inclusions in the late-stage fluorite.

FIGURE 9.—Transitional vein margin, plane-polarized light, thin section of sample DRS–67–33D. Field of view includes quartz (upper right) that contains fluid inclusions and is similar in appearance to vein quartz, plagioclase (upper left) that shows limonite-filled cleavages, and randomly oriented bladed muscovite (lower left); all three minerals are intergrown in lower right. Pyrite cube (center) that is oxidized to limonite and contains small blebs of quartz is abutted by an elongate grain of fluorite on its upper left face. Massive vein quartz lies just below the field of view.

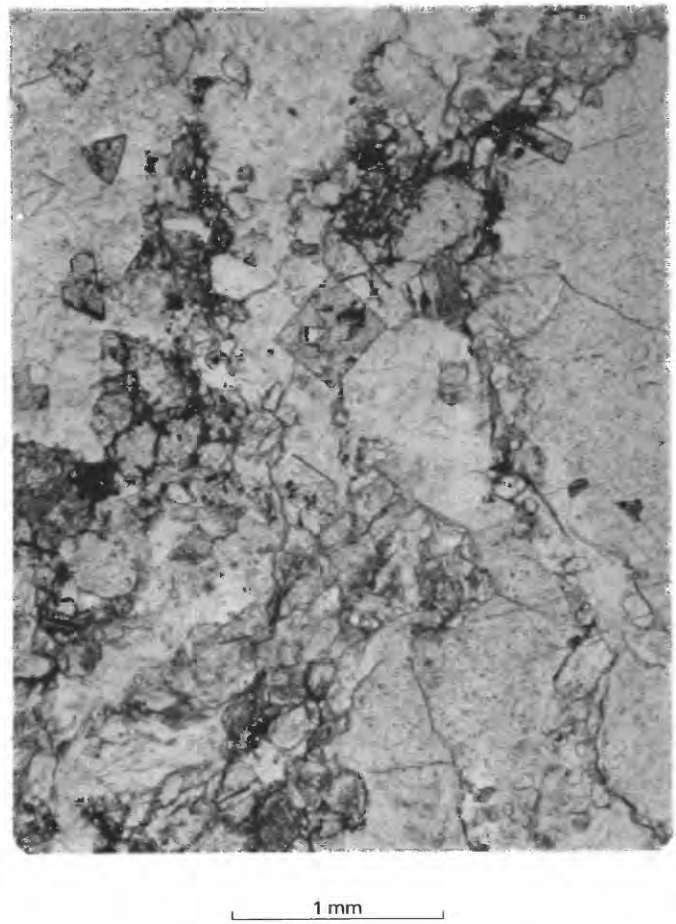

FIGURE 10.—Late-stage veinlet in huebnerite-bearing quartz vein, plane-polarized light, thin section of sample DRS–74–70. Quartz (right, and upper left) is strained, and is crowded with fluid inclusions, some of which contain liquid carbon dioxide; note subparallel trains of abundant fluid inclusions. Irregular late-stage veinlet (lower left to upper right) is chalcedony that contains barite pseudomorphs after cubic pyrite (light-gray, squarish crystals), muscovite (randomly oriented, bladed crystals), and scattered dustlike limonite (black). Note that some barite pseudomorphs and muscovite crystals occur in vein quartz outside the chalcedony veinlet. Beyond the field of view, clear quartz veinlets that contain barite cut chalcedony veinlets.

BARITE

Barite is present only locally and in very small amounts in the huebnerite veins. Rare, small, irregular patches that are aggregates of tabular crystals have grown on huebnerite (fig. 5), where barite probably was an early vein mineral. Barite occurs also as white crystals less than 1 mm across in places intergrown with quartz and elsewhere penetrating vugs where free surfaces show characteristic tabular orthorhombic form. Locally, tabular barite crystals as large as 3 cm across and 0.5 cm thick occur in vugs in vein quartz. A thin section of sample DRS–74–70 as seen under the microscope contains late-stage barite (fig. 10). In this sample "milled" granite lies in a matrix of vein quartz that contains huebnerite and is itself veined by thin (about 1 mm or less), irregular veinlets of chalcedony that contain muscovite and barite. The barite appears to have replaced pyrite inasmuch as it occurs as aggregates of barite crystals pseudomorphous after a cubic mineral (fig. 10). The cores of some such pseudomorphs contain limonite, probably oxidized from original pyrite (fig. 11).

Barite separated from sample DRS–74–221, collected from a huebnerite- and sulfide-bearing quartz vein (fig. 2), was analyzed spectrographically (table 3). Of the elements detected, barium, and probably calcium, lead, and strontium, are present in the barite structure; other elements may be present in mineral impurities within the analyzed barite.

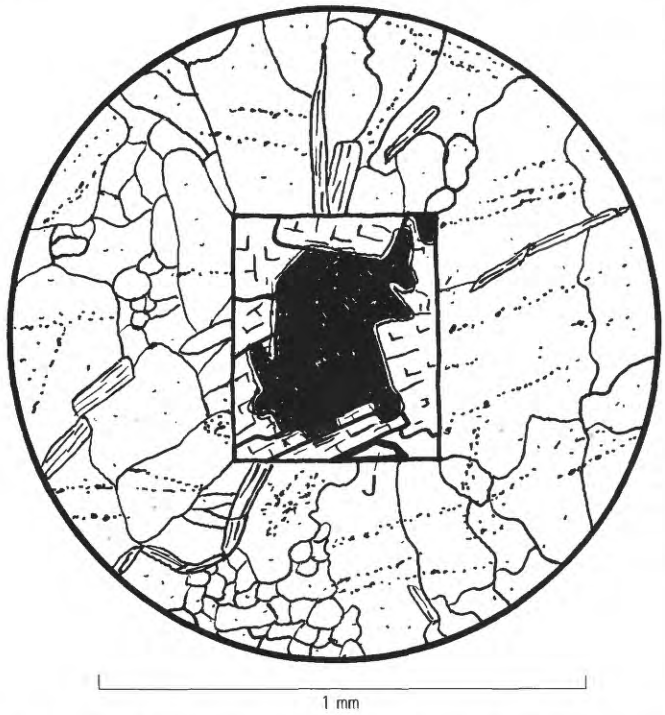

FIGURE 11.—Barite pseudomorphous after pyrite in quartz vein, thin section of sample DRS–74–70. Variously oriented barite crystals (white, patterned) replace periphery of pyrite cube (center), core remnant of which has been oxidized to limonite (black). Unidentified high-relief, moderately birefringent, pale-yellow (color not shown) mineral (labeled J) at lower edge of pseudomorph may be jarosite. Pseudomorph lies in strained vein quartz (white) that shows mosaic and mortar structure and contains abundant trains of fluid inclusions (dark specks, mostly alined subparallel). Muscovite (bladed) forms individual crystals and short stringers scattered in quartz.

CALCITE

Calcite occurs in minor amount and only locally as tiny (0.03 mm and less) crystals associated with scheelite, pyrite (oxidized), and muscovite, and it is considered to be hydrothermal in origin in those places.

CHALCEDONY

Chalcedony is found in late-stage veinlets in the huebnerite-bearing quartz veins; because it contains minerals such as muscovite, barite, and pyrite (weathered to limonite), it is interpreted to be a hydrothermal mineral in these occurrences.

MONAZITE

We have no direct evidence of the occurrence of monazite in the quartz veins, although Ferguson (1921, p. 389) reported recovery of monazite along with huebnerite from residual surface material near a vein 3 km southeast of Round Mountain. Ferguson (1921, p. 389–390) inferred that the monazite and huebnerite were derived from a pegmatitic quartz vein. Monazite is an accessory mineral of the granite locally, for example in Shoshone Canyon along the vein where sample DRS–73–168 was collected.

PRIMARY ORE MINERALS

HUEBNERITE

Huebnerite is the principal primary ore mineral of the tungsten-bearing quartz veins. Small local concentrations may exceed 10 percent of the vein material (these parts have been prospected or mined), but the huebnerite content of much of the veins ranges from but a few percent down to substantially less than 1 percent. Huebnerite content varies as much within a vein as from vein to vein. The huebnerite is dark brownish black on fresh cleavage surfaces, showing deep-blood-red internal reflection in bright light. Cleavage is well developed on {010}, and cleavage (parting) less developed on {100}. Huebnerite occurs as stubby, tabular to prismatic crystals, generally subhedral to euhedral, either singly or as composite clusters. Single crystals are as much as 5 cm long, although commonly 1 cm or less in size. In granite huebnerite tends to occur in the cores of quartz veins where it is intergrown with quartz as subhedral crystals and as aggregates of crystals. In this environment tabular, somewhat tapered crystals are common. In schist huebnerite tends to occur as stubby, euhedral crystals growing from one wall of flat veins (fig. 3). Vein material with huebnerite growing from one wall was not observed in place in schist, but was noted in material from prospect dumps. Presumably the huebnerite is on the footwall of these flat veins, analogous to the example from Panasqueira, Portugal, illustrated by Kelly and Rye (1979, fig. 9). A thin (3 cm), northeast-striking, nearly vertical quartz vein in granite at the locality marked with an open circle and X on figure 2 displays prismatic crystals that grow perpendicularly into the vein from its northwest wall.

Where huebnerite has grown from vein walls, crystals commonly fan or flare outward from their base in the direction of growth (fig. 3). The center of the base of such a crystal is in direct contact with the wall, and outward the crystal rests on a progressively thicker selvage of muscovite, which shows thickest development on the walls between separate huebnerite crystals (fig. 3). This relationship indicates simultaneous deposition of huebnerite and muscovite beginning with the onset of vein mineralization. Inclusion of flakes of muscovite within huebnerite also indicates synchronous crystallization of huebnerite and muscovite.

Many of the subhedral to euhedral crystals of huebnerite show growth zones that, as seen in thin sections

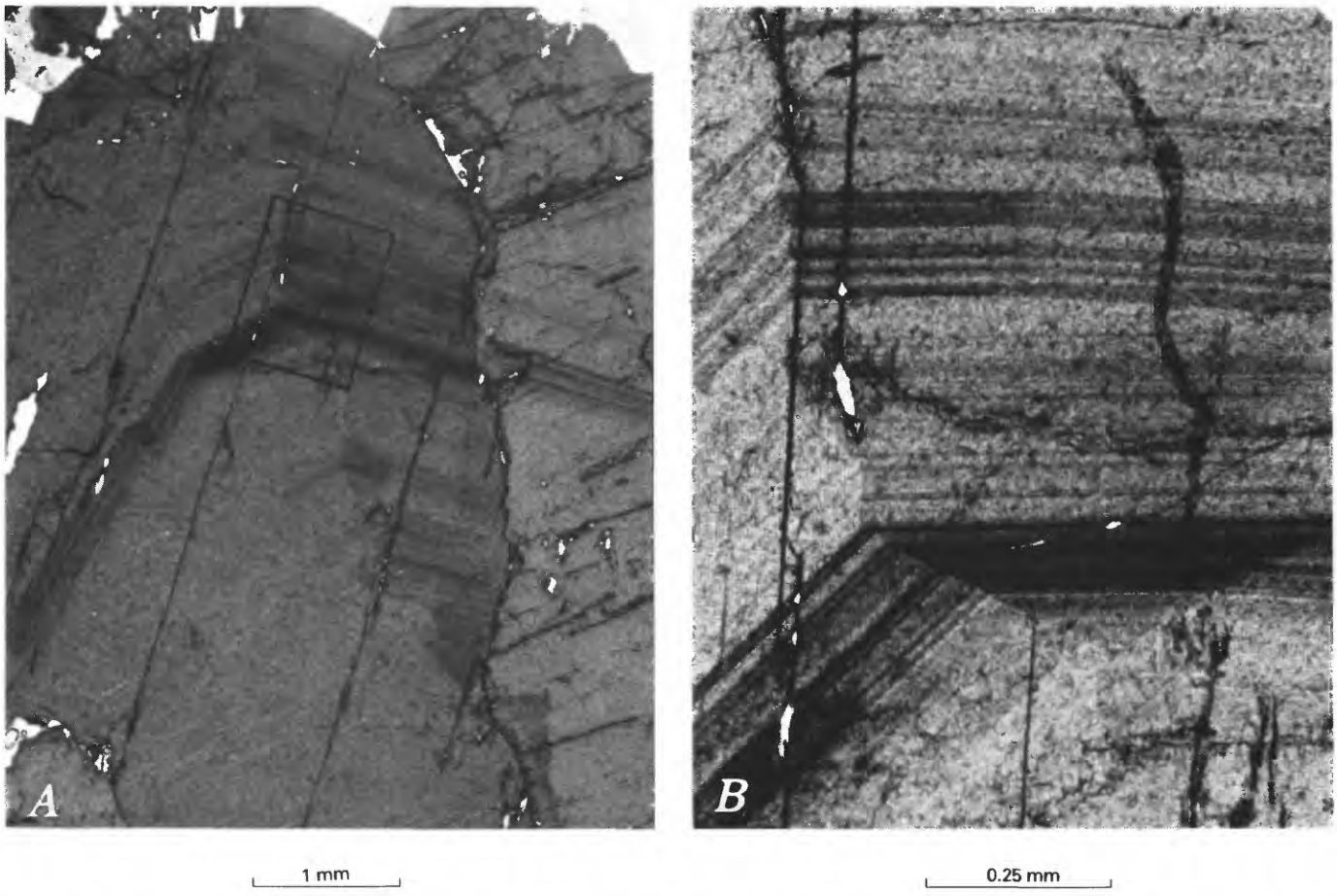

FIGURE 12.—Zoned huebnerite crystal, plane-polarized light, thin section of sample DRS–79–68. Rectangular outline in *A* shows area of *B*.

and less plainly in polished sections, are alternating lighter and darker brown zones that reflect the crystallographic form of the growing crystals (figs. 12–14). Some euhedral huebnerite crystals have been fractured, dismembered, or otherwise deformed during growth (fig. 14). Growth zones may be truncated or separated, and the resulting fracture space filled by later stage huebnerite or by quartz (figs. 13, 14). This dismemberment resulted from brecciation rather than replacement, as can be shown locally by the fact that segments of huebnerite can be fitted together if interstitial later huebnerite and quartz are removed. The "milling" of some huebnerite crystals as a result of excessive deformation of the vein material was accompanied by recrystallization of quartz, as evidenced by the fact that the dispersed "milled" fragments of huebnerite are embedded in fine-grained mosaic quartz (figs. 15, 16).

In places where quartz shows pronounced mosaic structure and is sheared (for example, samples DRS–67–33 and DRS–74–221), huebnerite may appear "worm eaten" and is intergrown with granular quartz crystals. Locally this huebnerite may have lighter colored, mottled patches against quartz. Some huebnerite crystals show evidence of solution etching where they are adjacent to voids in the vein material, as well as where they are embedded in recrystallized quartz. Beddoe-Stephens and Fortey (1981) reported that, in the Carrock Fell tungsten deposit in the English Lake district, wolframite that occurs in quartz veins near vugs tends to be veined and replaced by scheelite, arsenopyrite, pyrite, carbonate minerals, and less commonly by quartz.

The density measured by Berman balance of three samples of huebnerite from Round Mountain quartz veins ranges from 7.24 to 7.26. Calculated density of pure $MnWO_4$ is 7.234.

Chemical data for Round Mountain huebnerites are presented in a later section of this report.

SCHEELITE

Scheelite is a widespread but sparse component of the huebnerite veins. It is restricted, however, to a specific environment and is therefore present in some veins and virtually absent from others (table 1). It is associated with sulfides and sulfosalts within the areas

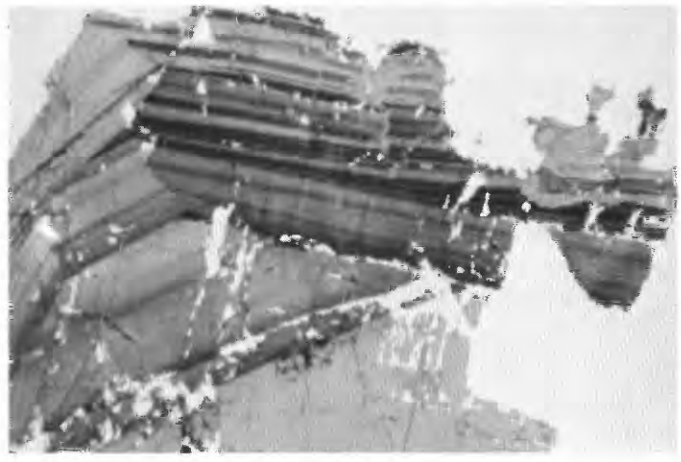

FIGURE 13.—Zoned and fractured huebnerite crystal, plane-polarized light, thin section of sample DRS–79–67. White patches in lower half of view are areas plucked during grinding of thin section. Upper part of crystal lies along an irregular boundary against strained quartz (also white). Irregular corrosion of the outer part of the huebnerite crystal before crystallization of quartz is implied. Note converging growth zones in huebnerite crystal that suggest diminished and arrested growth of the crystal periodically along some faces, and that imply a directional influx of material that formed the growing crystal. Some growth zones have been truncated (upper left), but the mechanism of truncation is not evident. Note also fractured growth zones at top center where fractures are filled by light-colored huebnerite, and corroded huebnerite growth zones at right center filled by light-colored huebnerite. Scale is approximate.

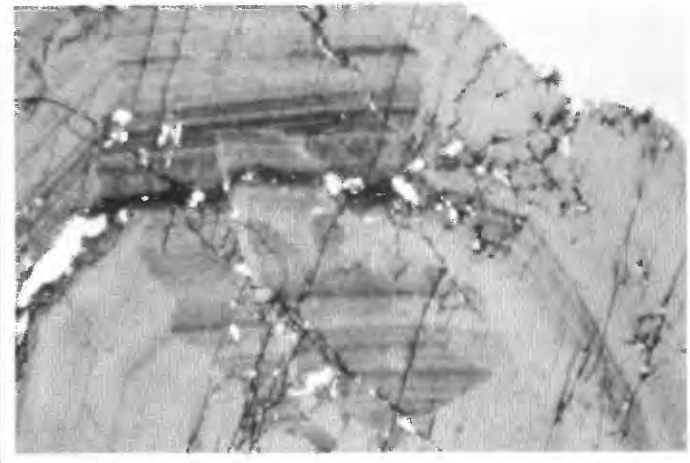

FIGURE 14.—Zoned and fractured huebnerite crystal, plane-polarized light, thin section of sample DRS–79–68. White patches within crystal are areas plucked during grinding of thin section. Quartz (white, upper right) has grown on huebnerite. Note segment of zoned huebnerite (center) that was fractured and displaced upward (so that growth zones are offset) and then overgrown with continuous layers of huebnerite. Bleaching or filling of huebnerite has occurred along the margins of the fractured and displaced segment. Scale is approximate.

of base- and precious-metal mineralization of the tungsten-bearing veins, and it occurs in some veins devoid of sulfides and sulfosalts but close to the areas of base- and precious-metal mineralization. With one known exception, scheelite is absent from veins more distant from these zones of mineralization (compare table 1 and fig. 2). Within scheelite-bearing veins the mineral occurs in sparse to trace amounts. On a microscopic scale it is seen to occur closely associated with huebnerite, and there it ranges from a few percent to perhaps 50 percent of the tungsten-bearing mineral present in a thin section (sparse to abundant in table 1).

White to very pale yellowish green scheelite occurs as irregular patches and blebs on the margins of and within huebnerite crystals, and as small veinlets or fracture fillings a fraction of a millimeter wide in huebnerite (figs. 17, 18). Locally, veinlets of scheelite as much as 1 mm wide fill fractures that extend through huebnerite and into adjacent vein quartz. Small specks, patches, and veinlets of scheelite occur in quartz near concentrations of huebnerite. The veinlets, some of which are aggregates of scheelite and muscovite (fig. 17), appear to fill late shears; the patches commonly are fillings of vugs in quartz (fig. 19). These relations of scheelite to other minerals are similar to those described for scheelite in a tungsten-bearing quartz lode at the New Snowbird deposit, Idaho, by Leonard, Mead, and Conklin (1968, p. C6).

Microprobe examination of scheelite associated with huebnerite in sample DRS–74–193 revealed the presence of about 0.045 percent MnO, 0.35 percent FeO, 81.64 percent WO_3, 18.80 percent CaO, and 0.00 percent MoO_3 (total, 100.83 percent; average of two analyses). Examination of the scheelite under ultraviolet light using a scheelite fluorescence analyzer manufactured by Ultra-violet Products, Inc., Los Angeles, Calif.[1], showed that the scheelite fluoresces bright blue and contains virtually no molybdenum.

TETRAHEDRITE-TENNANTITE

Tetrahedrite-tennantite (referred to as tetrahedrite by Ferguson, 1921, p. 389–390) is present in some of the huebnerite veins where it is generally sparse but may locally make up a few percent of the vein material. These veins are found in zones of base- and precious-metal mineralization indicated on figure 2. Tetrahedrite-tennantite forms small grains as much as 5 mm across in milky white quartz. Under the microscope the grains are seen to fill vugs in quartz (figs. 20–22).

[1]Brand or manufacturers' names used in this report are for descriptive purposes only and do not constitute endorsement by the U.S. Geological Survey.

FIGURE 15.—"Milled" huebnerite crystal, plane-polarized light, thin section of sample DRS–79–68C. Original huebnerite crystal (dark gray) has been broken and is dispersed in strained and recrystallized quartz (white) that contains large numbers of fluid inclusions (tiny dark specks). Irregular patches of muscovite and fluorite (light gray) are intermingled with very fine grained mosaic quartz and fragments of huebnerite to the right of the large crystal of huebnerite.

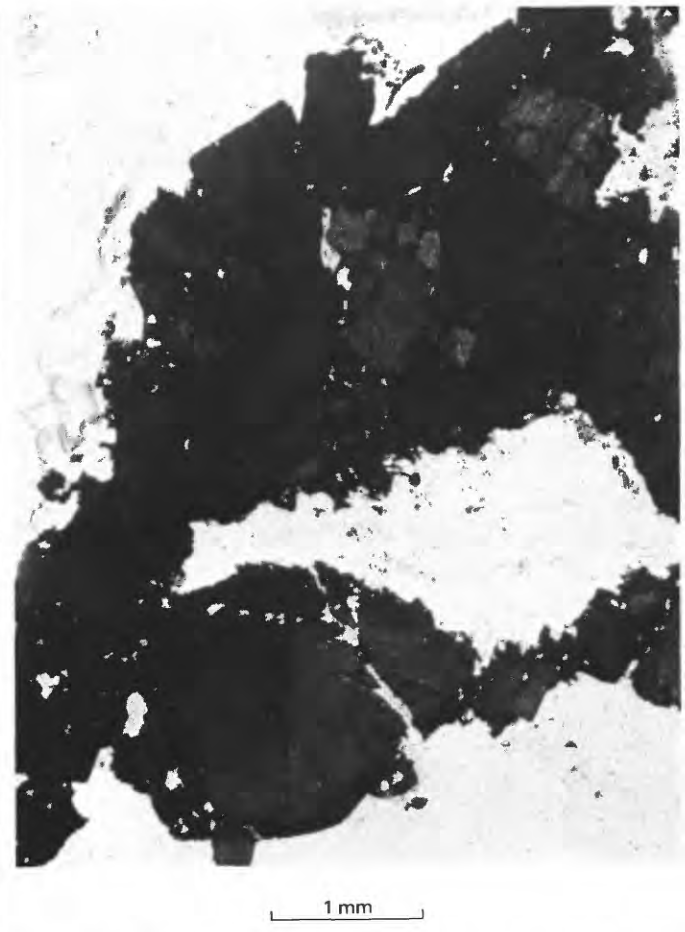

FIGURE 16.—"Milled" and "mixed" huebnerite fragments, plane-polarized light, thin section of sample DRS–79–68E. Extremely disrupted huebnerite (dark gray) consists of a large number of disoriented fragments of different sizes, color shades, and degrees of zoning, embedded in strained mosaic quartz (white) that contains large numbers of fluid inclusions (dark specks).

Tetrahedrite-tennantite separated from samples DRS–78–1 and DRS–78–2, collected from huebnerite-bearing veins (fig. 2), was identified optically in polished sections and by X-ray diffraction, and analyzed spectrographically. The spectrographic analyses are given in table 3. The substantial amounts of copper, antimony, arsenic, zinc, and silver indicated in the analyses show that the sulfosalt is zincian tetrahedrite-tennantite. Also, appreciable amounts of silicon, calcium, barium, and tungsten given in the analyses suggest the presence of some impurities in the analyzed sulfosalts such as quartz, calcite, barite, and a tungsten mineral. The small amounts of aluminum given rule out the presence of much feldspar. Also, the low aluminum contents rule out a large number of sodium-bearing minerals to account for the sodium that is present; possibly a secondary iron-sodium sulfate such as natrojarosite or copper-sodium sulfate such as krohnkite or natrochalcite could account for the presence of sodium. Elements such as iron, bismuth, cadmium, and lead may be present mostly in the sulfosalt structure, or otherwise in minor amounts of sulfide impurities.

Minor amounts of tetrahedrite-tennantite are found along with pyrite, chalcopyrite, and fluorite dispersed as small crystals (less than 1 mm) in wall rock near huebnerite veins at the Darrough prospect (fig. 2).

SULFIDES

Sulfides are found in only trace to minor amounts (probably less than 1 percent) in most of the vein material from the tungsten-bearing veins. Local concentrations in vein material of hand-specimen size may reach several percent. Like tetrahedrite-tennantite, sulfides occur in the tungsten-bearing veins within the zones of base- and precious-metal mineralization shown on figure 2.

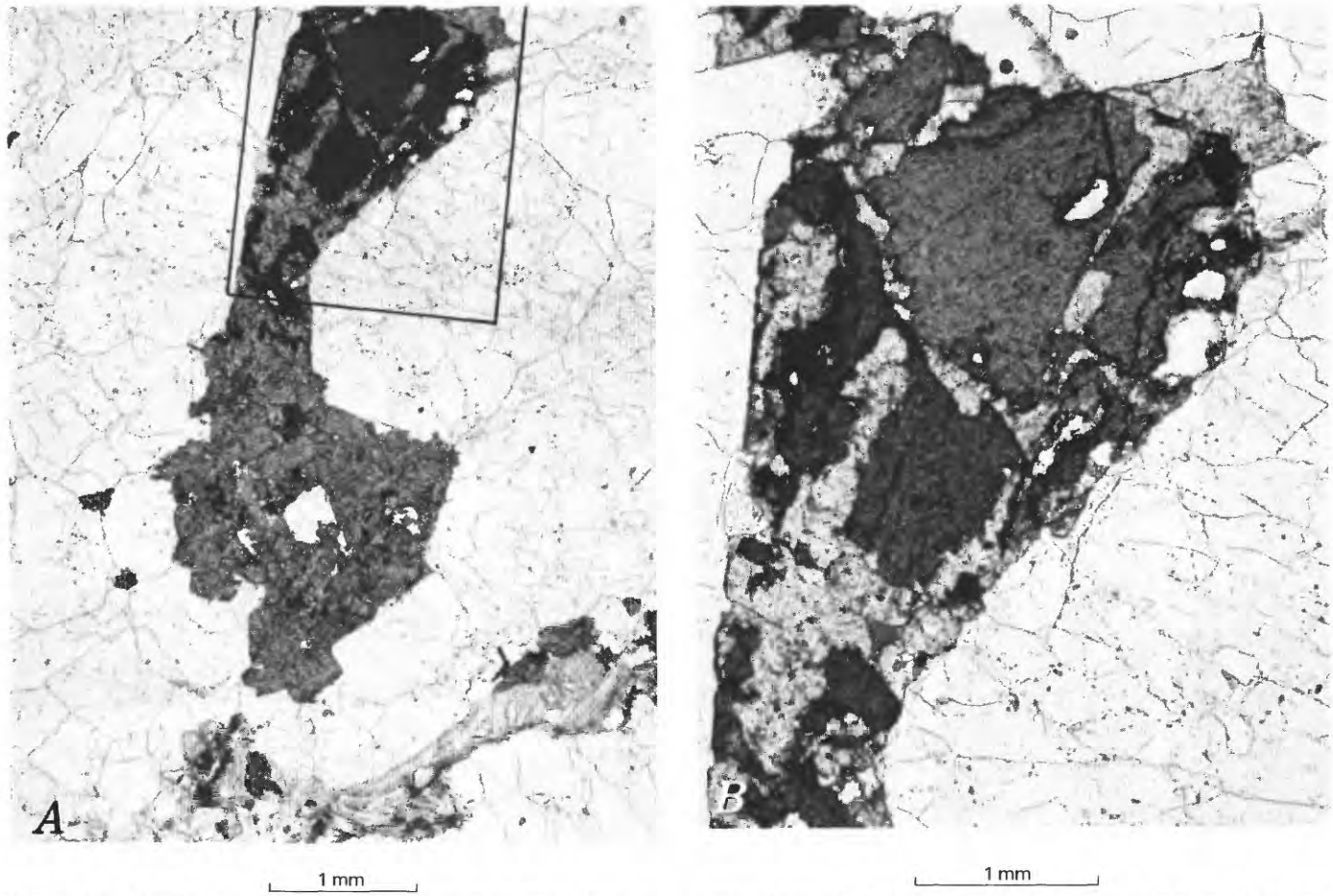

FIGURE 17.—Huebnerite, veined and partly replaced by scheelite, plane-polarized light, thin section of sample DRS–78–2B. Rectangular outline in *A* shows area of *B*. *A*, Quartz (white) that is locally sheared, strained, and universally crowded with fluid inclusions (dark specks) in variously oriented trains. Mosaic structure is developed only locally in quartz, and apparent original prismatic form of much of the quartz is still evident. Enclosed in quartz is a central patch of huebnerite (dark gray), irregularly veined and largely replaced by scheelite (medium gray). Quartz prism faces surround some of the patch and suggest that the scheelite may be in part a vug filling. Veinlet in quartz (lower part of view) contains scheelite and muscovite (bladed, light gray). *B*, Scheelite (light gray) appears to replace huebnerite (medium gray) irregularly; also it fills cracks where huebnerite has been fractured and separated, as for example in the upper right where a Z-shaped fracture separated slightly and slipped in a left-lateral sense to provide an opening that was filled with scheelite.

Pyrite is by far the most abundant and widespread sulfide. It and other sulfides such as sphalerite, galena, covellite (CuS), chalcopyrite, and pyrrhotite characteristically are late-stage minerals in the veins. Both covellite and blaubleibender covellite are present in the veins, but not everywhere together. The sulfides occur in shears in quartz, filling vugs in quartz in the fashion of tetrahedrite-tennantite (figs. 20–22), and in late-stage veinlets of chalcedony (fig. 10). Figure 23 shows pyrite (altered to limonite) filling vugs in quartz and partly replacing quartz prisms that penetrate vugs. Pyrite also forms crystals about 1 mm in diameter that, along with quartz prisms, line vug walls, and that appear to have grown contemporaneously with the late quartz (fig. 24). Pyrite occurs also as cubes disseminated locally in vein quartz (fig. 9) and widely in wall rocks (figs. 4, 8). Sulfides also occur as irregular grains enclosed in mosaic quartz where they may have crystallized simultaneously with mosaic quartz but are probably younger than the initial stage of quartz mineralization. Sphalerite that is enclosed in mosaic vein quartz near vugs has been fractured, "milled," and dispersed apparently simultaneously with recrystallization of quartz (fig. 25). Figure 26 shows examples of covellite that apparently replaced galena, and figure 27 shows chalcopyrite exsolved from sphalerite. Molybdenite has not been recognized within huebnerite veins, although spectrographic analyses of a few samples (DRS–79–68, table 3; DRS–67–33, table 6; DRS–74–194, DRS–74–221, DRS–74–252A, table 7) show minor amounts of molybdenum.

Some late shearing in the veins postdated deposition of sulfide and sulfosalt minerals.

FIGURE 18.—Huebnerite veined with scheelite, plane-polarized light, thin section of sample DRS–79–68A. Fractured and somewhat granulated huebnerite (dark gray) has been veined and otherwise filled with late-stage scheelite (medium gray). Huebnerite and scheelite are veined and surrounded by strained quartz (white) that displays mosaic structure. Quartz is crowded with fluid inclusions (dark specks).

FIGURE 19.—Vug in quartz (white) filled with scheelite (medium gray), plane-polarized light, thin section of sample DRS–79–68A. Quartz that bounds the vug consists of well-formed prisms, is only slightly strained, and contains few fluid inclusions. Elsewhere the quartz has well-developed mosaic structure, is strongly strained, and contains numerous fluid inclusions (dark specks). Huebnerite (dark gray, at top) is part of a grain that has been partly broken and filled with quartz locally. Muscovite (bladed, light gray) is randomly oriented in a clot in quartz 1 mm above the scheelite-filled vug, and elsewhere forms plumose bunches in and near huebnerite and in the vug. Some of the larger black blebs in quartz are limonite probably oxidized from pyrite.

A spectrographic analysis of galena from DRS–74–221 is given in table 3. Silver, bismuth, and antimony probably are held in the galena structure, copper is present mostly in covellite, and silicon, aluminum, barium, and strontium are present in minor mineral impurities.

SECONDARY MINERALS

Secondary minerals in the huebnerite veins near Round Mountain are mostly oxidation products that resulted from near-surface weathering. They occur as alteration halos around primary vein minerals, particularly the ore minerals, and in fractures and vugs near the primary vein minerals. A few secondary minerals appear to be low-temperature precipitates that resulted from solution and redeposition of vein or wall rock components by near-surface ground waters.

SULFIDES

Sulfides have formed commonly as initial breakdown products of weathering of primary sulfide and sulfosalt minerals. As shown on figure 28, chalcocite (Cu_2S), acanthite (Ag_2S), and stromeyerite ($(AgCu)_2S$), identified by optical properties, X-ray diffraction, and the scanning electron microscope, have formed as an initial breakdown of tetrahedrite-tennantite. In places covellite and blaubleibender covellite appear to be alteration products of primary copper-bearing sulfide minerals, and in addition appear to be alteration products of the initial alteration minerals chalcocite and stromeyerite (fig. 28).

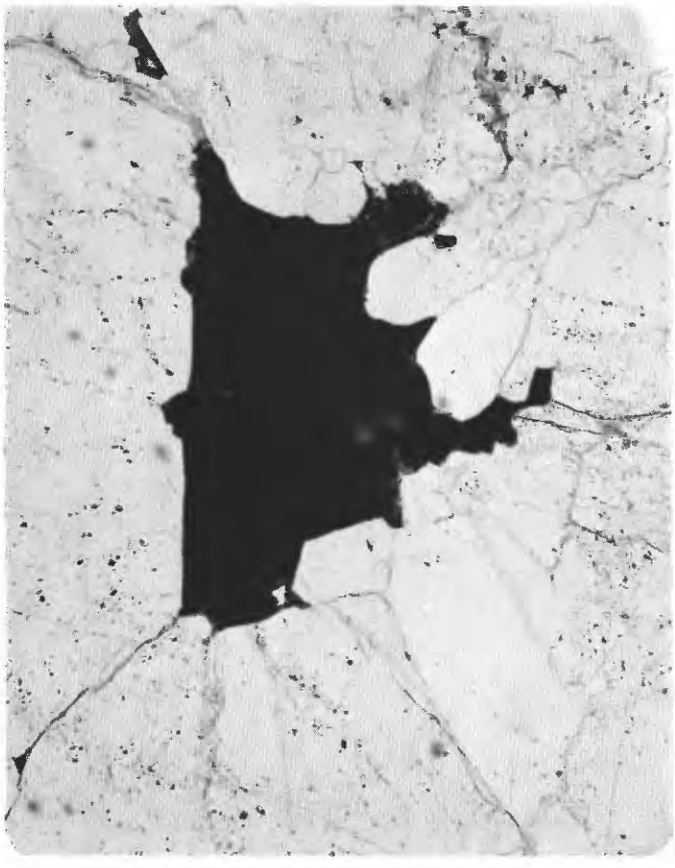

FIGURE 20.—Tetrahedrite-tennantite (black) filling vug in quartz (white), plane-polarized light, thin section of sample DRS–78–2A. Quartz contains abundant fluid inclusions (dark specks); inclusions tend to be least abundant where quartz prisms penetrate the vug. Irregular, light-gray veinlets near top of view are muscovite. Chrysocolla fills a minute vug at upper left.

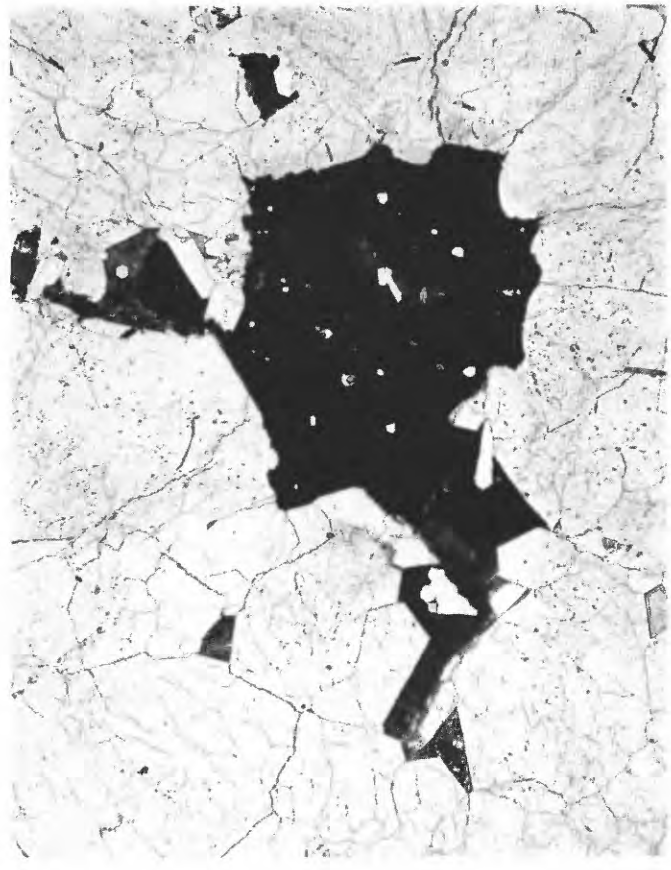

FIGURE 21.—Tetrahedrite-tennantite (black) filling vug in quartz (white), plane-polarized light, polished thin section of sample DRS–78–2B. White blebs within tetrahedrite-tennantite, some of which contain bubbles, are areas plucked during grinding of the thin section. Dark-gray areas within the large vug and in smaller nearby vugs are weathering products, mostly malachite. Quartz contains abundant fluid inclusions (dark specks) that are sparse or absent in small quartz prisms that penetrate the vug. Small, dark-gray, needlelike prisms at center right and above tetrahedrite-tennantite-filled vug are allanite. Light-gray vug filling at lower right edge of view is chalcedony.

OXIDES, TUNGSTATES, CARBONATES, SULFATES, PHOSPHATES, AND SILICATES

Oxide minerals have formed directly from weathering of some ore minerals such as huebnerite, or are further breakdown products of weathered sulfide and sulfosalt minerals. Manganese oxides, including pyrolusite (MnO_2), psilomelane (colloidal MnO_2), and probably other manganese oxides, are common alteration products of huebnerite (fig. 29). Some of the manganese oxide minerals contain significant barium, as indicated by scanning electron microscope studies. Weathered huebnerite has a dull-black appearance as a result of the presence of manganese oxide minerals. Black and dark-brown manganese oxide and manganese-iron oxide mixtures commonly line vugs or coat fractures in the quartz veins near the sites of primary ore minerals. Manganese oxide dendrites coat fracture surfaces in many places in and near the veins.

Stibiconite ($Sb_3O_6(OH)$) has formed both as an early (fig. 30) or late (fig. 28) weathering product of tetrahedrite-tennantite.

Limonite is almost ubiquitous in and near the huebnerite veins. It has been derived mostly from the oxidation of pyrite, and it occurs commonly as pseudomorphs after pyrite (figs. 4, 8, 9, 10, 11, and 19), fracture fillings (figs. 4 and 33), and as a wash or in dustlike form permeating vein material and wall rocks. Tungstite, a hydrous oxide, occurs as a minor buff-yellow alteration product on the surfaces of and in fractures in huebnerite crystals. It is generally associated with other secondary tungsten minerals and (or) stibiconite.

Chrysocolla is the only silicate weathering product identified in the huebnerite veins. It may have formed

FIGURE 22.—Copper minerals (shades of gray) filling vug in quartz (white), plane-polarized light, polished thin section of sample DRS–78–2B. Island remnants of original vug filling are irregular blebs of tetrahedrite-tennantite; these are surrounded by secondary copper and antimony oxides (in the photomicrograph these minerals are indistinguishable and together appear as nearly black patches); surrounding the tetrahedrite-tennantite and associated oxides and filling the arm of the vug in the lower three-fourths of the view are green secondary copper minerals (mostly malachite?) and minor brown secondary antimony(?) and arsenic(?) minerals (dark gray); the other arms of the vug (upper left and upper right) contain azurite (medium gray) that shows concentric growth layers. Beyond the area of the view, azurite is bounded by crystal faces in open space of the vug. Note that the quartz prisms that penetrate the vug are nearly devoid of fluid inclusions (dark specks) that abound in the remaining quartz. Small vug in lower right is lined with chalcedony.

early in the weathering of copper-bearing sulfides inasmuch as it lines vugs that were later filled with malachite (fig. 31). Chrysocolla also was deposited before or contemporaneously with the precipitation of chalcedony that fills vugs (fig. 32). It fills late fractures, and itself is veined by very late chalcedony (fig. 33).

The tungstates, ferritungstite ($(W,Fe^{+3})_2O_4(OH)_2 \cdot \frac{1}{2}H_2O$—Machin and Susse, 1975—yellow tungstic ochre, sample DRS–74–221), jixianite(?) ($Pb(W,Fe^{+3})_2(O,OH)_7$, brownish-red tungstic ochre), and stolzite ($PbWO_4$, orange-yellow tungstic ochre), are minor alteration products found associated with the primary tungsten minerals. Because ferritungstite, jixianite, and stibiconite are all reported to have pyrochlore-type structure, conventional X-ray diffraction techniques cannot readily distinguish them with certainty, particularly when they are known to occur as mixtures. Jixianite is still an incompletely described mineral and discrepancies exist in the published descriptions (Jianchang, 1979; Hogarth and Chao, 1979, p. 1330).

Several carbonates—azurite, malachite, cerussite, and calcite—and sulfates—anglesite, brochantite, and jarosite-plumbojarosite—are common alteration products in the vicinity of primary vein sulfides. According to Kral (1951, p. 154), the phosphate autunite occurs in trace to small amounts in the tungsten veins east of Round Mountain; the mineral presumably is a weathering product of an unidentified primary uranium mineral.

REMOBILIZED MINERALS

Two minerals appear to have been in part simply remobilized from earlier vein minerals and deposited in very late stages. The silica of chalcedony probably was derived mainly from preexisting vein quartz; it appears to have been deposited in several late stages of mineralization (see fig. 34), the earlier ones probably low-temperature hydrothermal and the later ones possibly during weathering by cold ground waters. Opaline silica that fluoresces bright yellowish green under both shortwave and longwave ultraviolet radiation, probably owing to the presence of the uranyl ion, commonly coats fracture surfaces. Calcite that fluoresces pale salmon to orange pink and that may be slightly phosphorescent sparsely coats fractures in the veins along with other secondary minerals, particularly chalcedony. The calcite may have been reworked from earlier primary vein calcite or from calcium-bearing wall rocks.

SUMMARY OF TEXTURES AND PARAGENESIS

The huebnerite-bearing quartz veins near Round Mountain were filled with gangue and ore minerals to form nearly solid lenticular-tabular masses that locally contain vugs. Most vein walls are sharp and bounded by muscovite selvages, but in places veins merge with country rocks as if formed in part by replacement, and locally near veins some vein minerals impregnate the country rocks.

Figure 34 shows the interpreted paragenesis of mineral deposition, and events of deformation and recrystallization. The paragenesis is based on the previously described detailed interrelations of minerals—local sequences of mineral deposition, and correlations of specific mineral deposition from place to place.

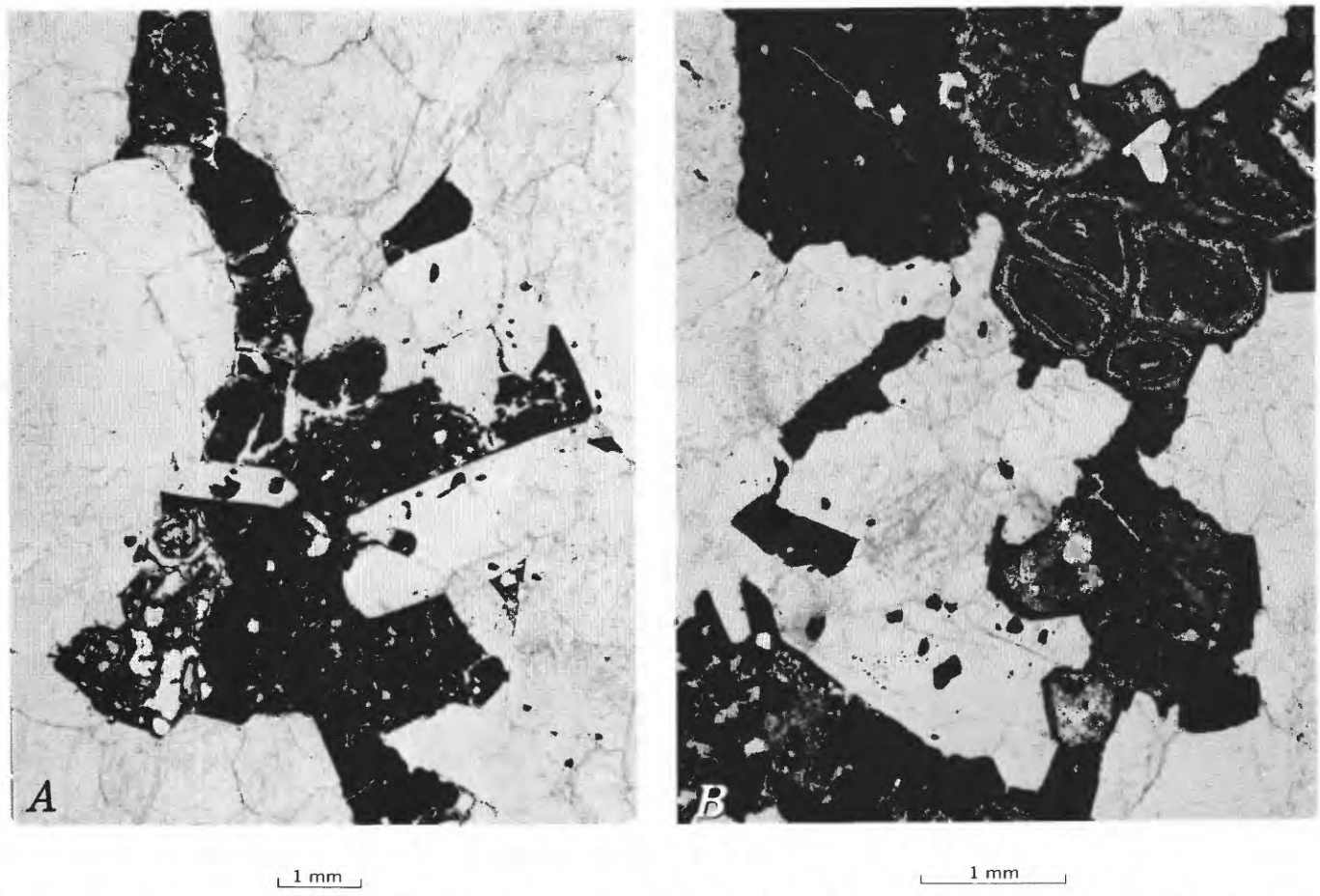

FIGURE 23.—Pyrite (altered to limonite) filling vugs in quartz and partly replacing quartz prisms that penetrate vugs, plane-polarized light, thin sections of samples DRS–74–252A$_1$ (*A*) and DRS–74–252A$_2$ (*B*). *A*, Quartz prisms (white) that penetrate vugs contain bleblike grains of limonite after pyrite (black). *B*, Granular pyrite in upper right (orbicular forms) has altered to concentric layers of limonite, jarosite, and chalcedony.

The paragenetic diagram (fig. 34) shows that an initial hydrothermal phase witnessed deposition of major amounts of quartz and lesser amounts of muscovite, huebnerite, fluorite, barite, and pyrite. A period of shearing and recrystallization followed in which much quartz was reconstituted; some new muscovite, huebnerite, fluorite, and pyrite were added at this stage, and muscovite and huebnerite were in part mechanically redistributed. Some scheelite and tetrahedrite-tennantite may have formed in the later part of this stage. A second hydrothermal stage saw deposition along shears and in the earlier vugs of small additional amounts of muscovite, quartz, fluorite, and barite; formation of minor calcite, scheelite, tetrahedrite-tennantite, and several sulfides; and finally precipitation of chalcedony. In places more than one younger episode of hydrothermal remineralization is evident. Near-surface weathering of the veins resulted in formation of small amounts of calcite, covellite, chalcedony, chalcocite, stibiconite, chrysocolla, malachite, azurite, manganese oxide, and jarosite.

Some uncertainty exists regarding part of the relations shown on figure 34. Muscovite is associated with chalcedony in some late veinlets that cut earlier vein minerals; the muscovite appears to have grown in place although it is possible that the muscovite crystals were mechanically emplaced in the chalcedony veinlets. More than one major episode of shearing may have affected the veins: an earlier episode that took place when quartz was recrystallized at the time carbon dioxide-bearing solutions moved through the veins, and a later (perhaps much later) episode that preceded and (or) accompanied scheelite, tetrahedrite-tennantite, and sulfide mineralization.

The paragenetic diagram (fig. 34) has been simplified inasmuch as several minerals of the veins are not shown. The positions of some minerals in the paragenetic sequence are uncertain, although most of the deleted minerals can be placed in their appropriate positions. Allanite probably was contemporaneous with early vein quartz. Chalcopyrite probably belongs with sphalerite; blaubleibender covellite with covellite; acanthite and

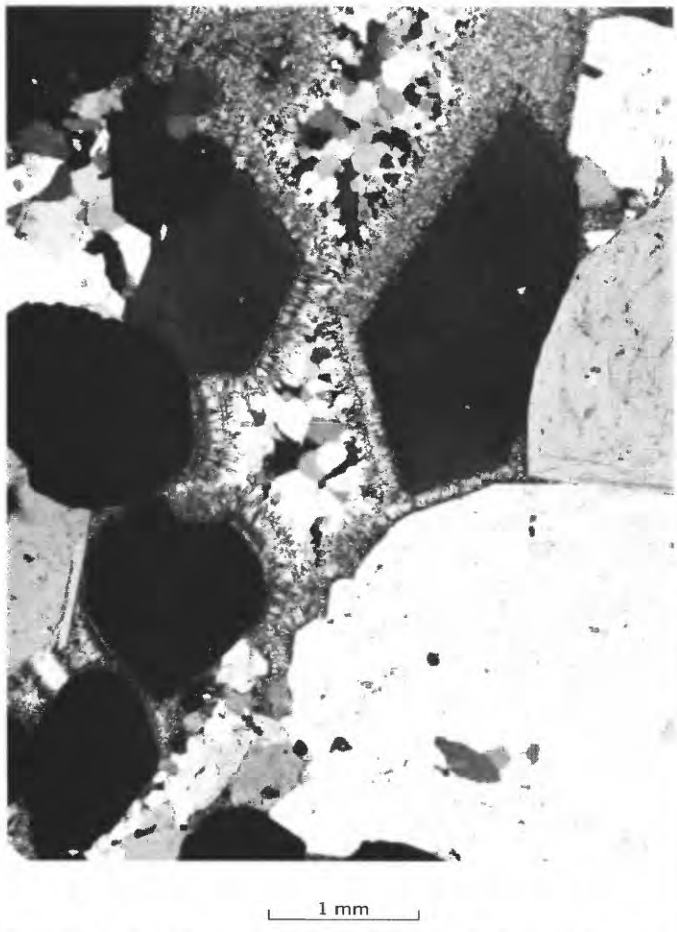

FIGURE 24.—Vug in quartz vein, under crossed nicols, thin section of sample DRS–74–252B_2. Pyrite crystals (black) and quartz prisms (white and shades of gray) line vug and are coated with chalcedony (fine grained, mottled gray). The core of the vug is filled with granular quartz (white, black, and shades of gray).

stromeyerite with chalcocite; and cerussite, anglesite, brochantite, limonite, jarosite-plumbojarosite, autunite, tungstite, ferritungstite, jixianite(?), and stolzite with stibiconite, chrysocolla, malachite, azurite, manganese oxide minerals, or jarosite.

CHEMICAL COMPOSITION OF THE HUEBNERITE

Chemical data were acquired to establish the iron-manganese compositions, the compositional variations, if any, in visible growth zones, and the trace-element compositions of the huebnerites, for the purpose of better defining the environment of their deposition.

Samples of huebnerite from 20 localities (shown on fig. 2) were analyzed using electron microprobe and emission spectrographic techniques. Synthetic huebnerite standards were made for use in the electron microprobe determinations. Stoichiometric proportions of MnO_2, WO_2, and Fe metal were fused to a melt and allowed to crystallize. The resulting material was entirely crystalline, and only slight iron-manganese variation was found in the 95 mol percent $MnWO_4$ standard. Natural huebnerite was prepared for analysis by hand picking crushed material selected from the vein samples. Examination of cleavage fragments under the microscope revealed no other mineral phases nor fluid inclusions, although it was evident that oxidation and replacement by iron-manganese oxides along cleavage planes, fractures, and other irregular surfaces have occurred in various degrees.

Conditions for microprobe analysis were 15 kilovolts operating voltage, 30 nanoamperes sample current, 10 micrometer beam diameter, and counting times of about 10 seconds on samples and standards using integrated beam current. Data were reduced by a computer program utilizing a linear least-squares best-fit line. No elements other than iron, manganese, and tungsten were detected above background. Results of the microprobe analyses of 19 samples are given in table 5.

Polished thin sections of four huebnerite-bearing samples (DRS–73–17, DRS–74–221, DRS–79–67, and DRS–79–68) were prepared for microprobe study of growth zones. The polished thin sections of huebnerite were examined under the microscope, in both transmitted and reflected light, and under the SEM, and no other mineral phases that might define the growth zones were detected.

Six-step semiquantitative emission spectrographic analyses of 23 samples of huebnerite are presented in table 6. Details of the six-step method, its precision, and comparison with other analytical methods were discussed by Myers, Havens, and Dunton (1961). In spite of the fact that the crushed huebnerite samples were carefully hand picked to remove other visible mineral phases before analysis, it is believed from the analytical data, as discussed later, that minor impurities were contained in some of the analyzed huebnerites.

IRON-MANGANESE COMPOSITION

The analytical data (tables 5 and 6) show that the mean iron contents of the huebnerites range from about 0.1 to 3.0 weight percent (recorded as Fe for spectrographic analyses and as FeO for microprobe analyses; the high value of 7.0 percent Fe (spectrographic) in sample DRS–74–221A is discounted, being attributed provisionally to pyrite). A comparison of the analytical data for iron (fig. 35) shows that iron values determined spectrographically are somewhat higher on average than those determined by microprobe.

Variations in the iron content of the Round Mountain huebnerites suggest the possibility of compositional zoning in the vein system. Indeed, the iron content (deter-

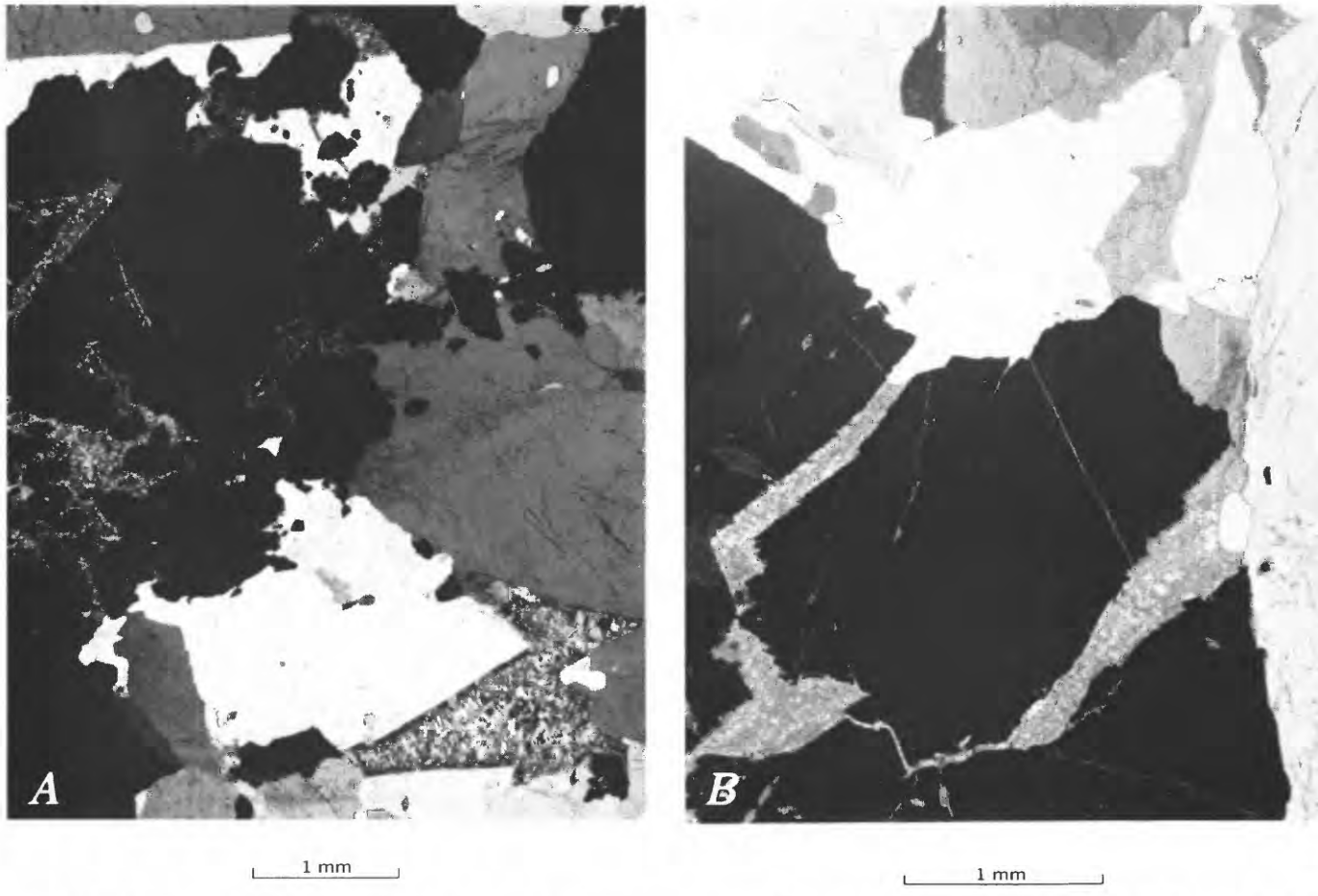

FIGURE 25.—Sphalerite that has been fractured, "milled," and dispersed in recrystallized mosaic quartz, under crossed nicols, thin section of sample DRS–74–252B_2. *A*, Strongly broken and dispersed sphalerite (black) in mosaic quartz (white and shades of gray). Broken sphalerite at left center has been filled with chalcedony (fine grained, mottled gray). Note vug at lower right filled with chalcedony (fine grained to fibrous, mottled gray). *B*, Fractured sphalerite (black) filled with chalcedony (fine grained, mottled gray). Note that quartz (white and shades of gray) penetrates fractures a short distance, suggesting that quartz recrystallized and molded itself against sphalerite as the fractures in sphalerite opened. Chalcedony deposition likely was the latest event.

mined by spectrographic analyses, which we believe to be more representative of the bulk compositions than are the microprobe analyses) appears to be a sensitive indicator of altitude within the vein system, increasing from values of about 0.2 percent Fe at an altitude of 2,125 m (6,800 ft) to about 3.0 percent Fe at an altitude of 2,625 m (8,400 ft) (figs. 2 and 36). It should be noted, however, that although the altitude correlation of microprobe-determined FeO is similar to that of spectrographically determined Fe (recalculated to FeO), sample DRS–74–221B is anomalous in its FeO (recalculated)-FeO ratios (see fig. 35). As discussed later, the vertical compositional zoning of the vein huebnerites is thought to reflect change in the pressure-temperature-composition conditions upward through the vein system.

A comparison of the FeO and MnO contents of the huebnerites as determined by microprobe analysis (fig. 37) reveals two fields of composition. A field of huebnerites with highest MnO to FeO ratios includes only huebnerites with which sulfides are associated in the veins. A field of huebnerites with lowest MnO to FeO ratios includes only huebnerites with which no sulfides are associated in the veins. In this comparison, sample DRS–74–221B does not appear anomalous. Assuming that the huebnerites and sulfides were deposited simultaneously in the vein system, we could explain the low content of iron in the sulfide-associated huebnerites by its preferential deposition in pyrite. Assuming that the sulfides were deposited in the veins later than the huebnerites, as the geological and mineralogical evidence indicates, we could explain the low content of iron in the sulfide-associated huebnerites by movement of iron out of huebnerite to be deposited as pyrite at the time of sulfide mineralization. We note the "reworked" character of the huebnerites that developed following their initial deposition but that predated (or accompanied?) deposition of sulfides.

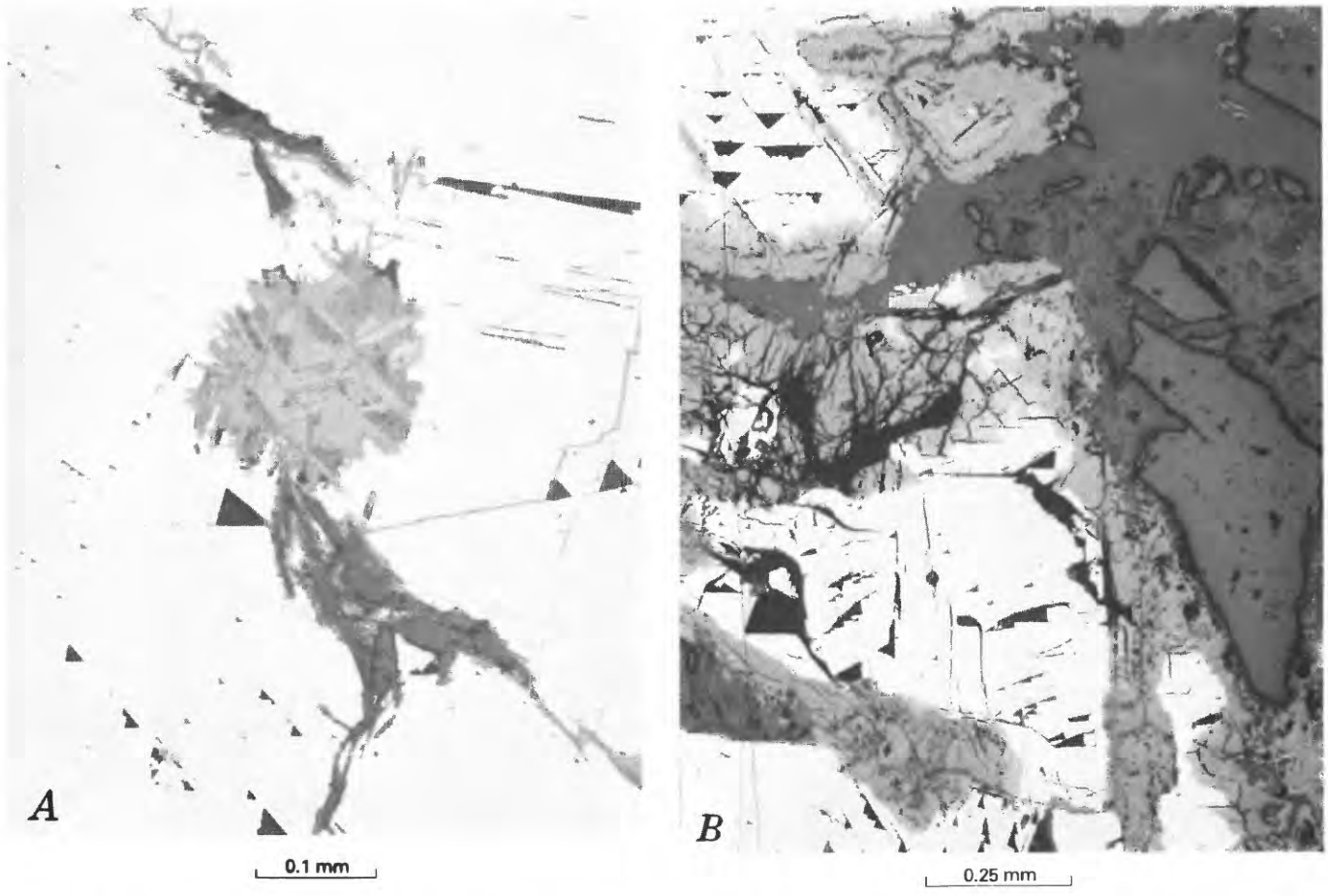

FIGURE 26.—Galena partly replaced by covellite, reflected light, polished sections of sample DRS–74–221. *A*, Galena (white) partly replaced by covellite (shades of gray) in irregular patches and along crystallographic planes. *B*, Galena (white) intergrown with or partly replaced by covellite (gray). Dark-gray areas near top and at right are quartz (high-relief fragments) and mounting medium.

TUNGSTEN-MANGANESE COMPOSITION

The variations in tungsten contents of 75.9 to 78.9 percent WO_3, as determined by microprobe analysis (table 5), compared to an ideal composition for huebnerite of 76.6 percent WO_3, led to the calculation of the molecular proportions of the components based on the microprobe data (structural formulas given in table 5). The results indicate compositions near stoichiometry and suggest that the compositional variations resulted largely from an instrumental factor, most likely variation in sample current, and are not real variations in tungsten composition.

We also plotted the MnO versus WO_3 compositions of the analyzed huebnerites (fig. 38) to evaluate further the compositional variations. Here again two distinct fields are shown, one of huebnerites with associated sulfides in the veins and one of huebnerites without associated sulfides in the veins. An exception is sample DRS–73–17 (queried on fig. 38), a huebnerite without associated sulfides that falls in the field of huebnerites with associated sulfides. The tendency for positive correlation of MnO and WO_3 within the separate fields suggests instrumental variation, probably in sample current during the time the analyses were made.

GROWTH ZONES

Because of the extremely low total iron contents, microprobe analyses of visible growth zones in huebnerite were inconclusive. Sample DRS–79–68 was examined by Dr. Charles M. Taylor (oral commun., 1979) and darker colored zones were found to contain very slightly more iron than lighter colored zones (0.2 versus 0.15 weight percent Fe). However, our studies failed to show convincing variations in iron content between darker and lighter parts of the huebnerite crystals, possibly because of the very thin character of the dark growth layers compared to the microprobe beam diameter employed. Nevertheless, local variation in the iron contents of the huebnerites (table 5) is evident despite our inability to correlate such with color variation.

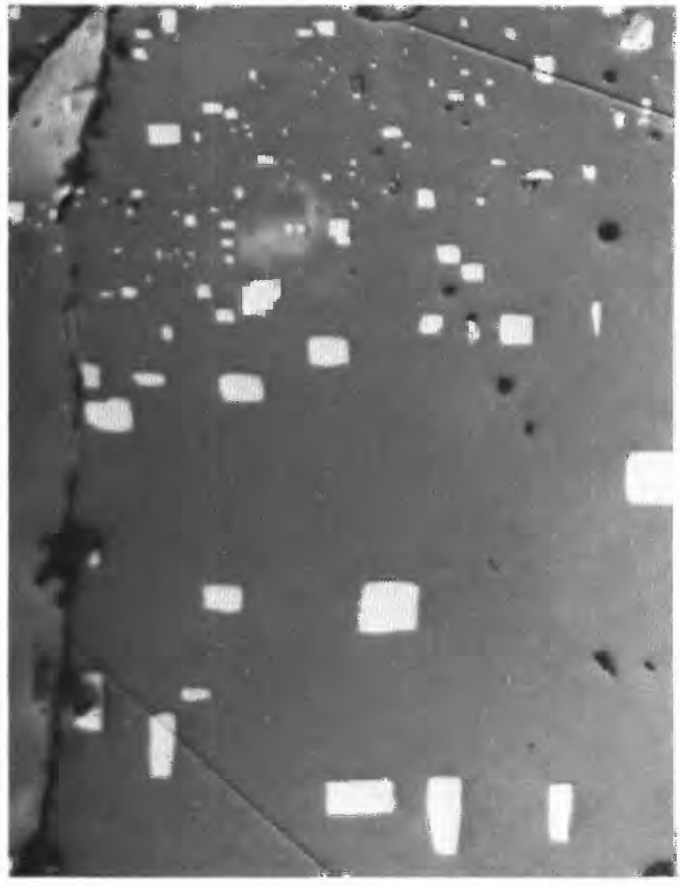

FIGURE 27.—Sphalerite (medium gray) that contains exsolved blebs of chalcopyrite (light gray), reflected light, polished section of sample DRS–74–252B.

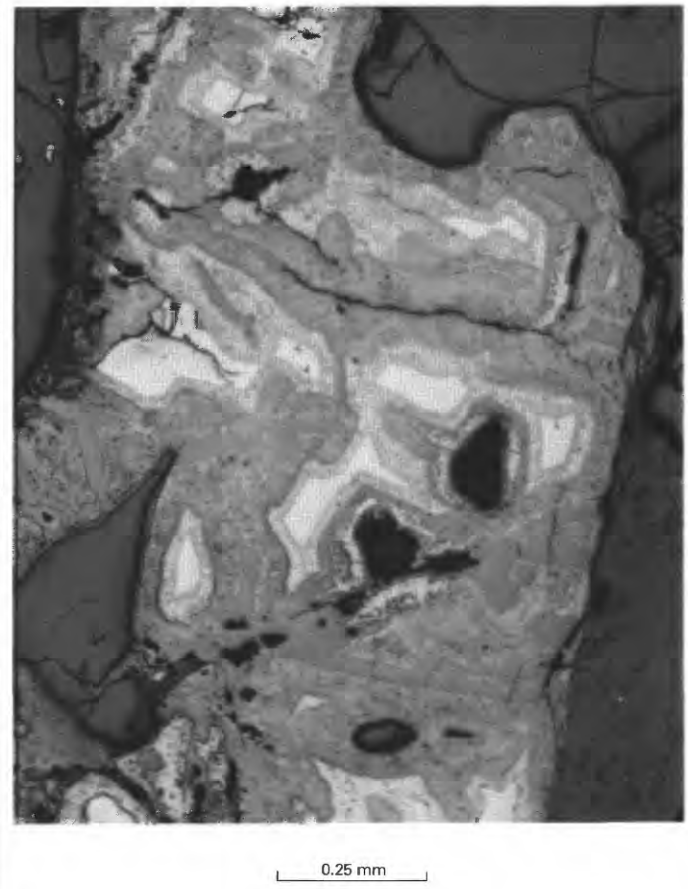

FIGURE 28.—Tetrahedrite-tennantite (light gray to white) partly replaced by a narrow halo of chalcocite, acanthite, and stromeyerite (mottled light to medium gray) and by intervening patches of gray isotropic mineral (stibiconite?) and covellite (mottled medium gray), reflected light, polished section of sample DRS–74–252A. Dark-gray areas are quartz (except mounting medium at lower right).

Iron-manganese zonation within huebnerite single crystals has been described by a number of authors (for example, Takla, 1976; Bird and Gair, 1976). The growth layers described by Bird and Gair (1976) for Hamme, N.C., huebnerites are similar in appearance to those observed in Round Mountain huebnerites, except that in the Round Mountain examples, growth layers appear to be much thinner. Patchy and random iron-manganese distribution in wolframite was reported by Moore and Howie (1978). Clark (1970) pointed out that many wolframites contain small but significant amounts of ferric iron and that this feature has received little attention in most recent studies. In crystals where the total iron is only 1.0 weight percent or less, small variations in amounts of ferrous (Fe^{+2}) and ferric (Fe^{+3}) iron might produce color zonation (Fe^{+2} producing lighter colored zones and Fe^{+3} producing darker colored zones). Moore and Howie (1978) reported appreciable excess ferrous oxide in some analyzed Cornish wolframites. Study of the stability relations of the wolframite series by Hsu (1976) has shown that wolframite of any composition can remain stable under the oxidation states prevailing in hydrothermal environments. The stability of ferberite and huebnerite does not differ appreciably in the presence of both oxygen and sulfur. Apparently neither fO_2 nor fS_2 exerts any noticeable influence on the composition of wolframite. Optical spectral studies (Graham R. Hunt, oral commun., 1980) were not able to distinguish Fe^{+2} from Fe^{+3} in several Round Mountain heubnerites (DRS–73–17, DRS–74–66, DRS–79–68) because of very low total iron content.

Moore and Howie (1979) in a study of cassiterite from Cornwall suggested that alternating color zones in that mineral resulted from other than chemical variation. They found that small variations in iron content did not correlate with color zones. Banerjee (1969) and Banerjee, Johnson, and Krs (1970) could not show conclusively by Mossbauer spectral studies of the cassiterite that color variation was related to differences in the Fe^{+2}:Fe^{+3} ratio. We note, however, that the extremely

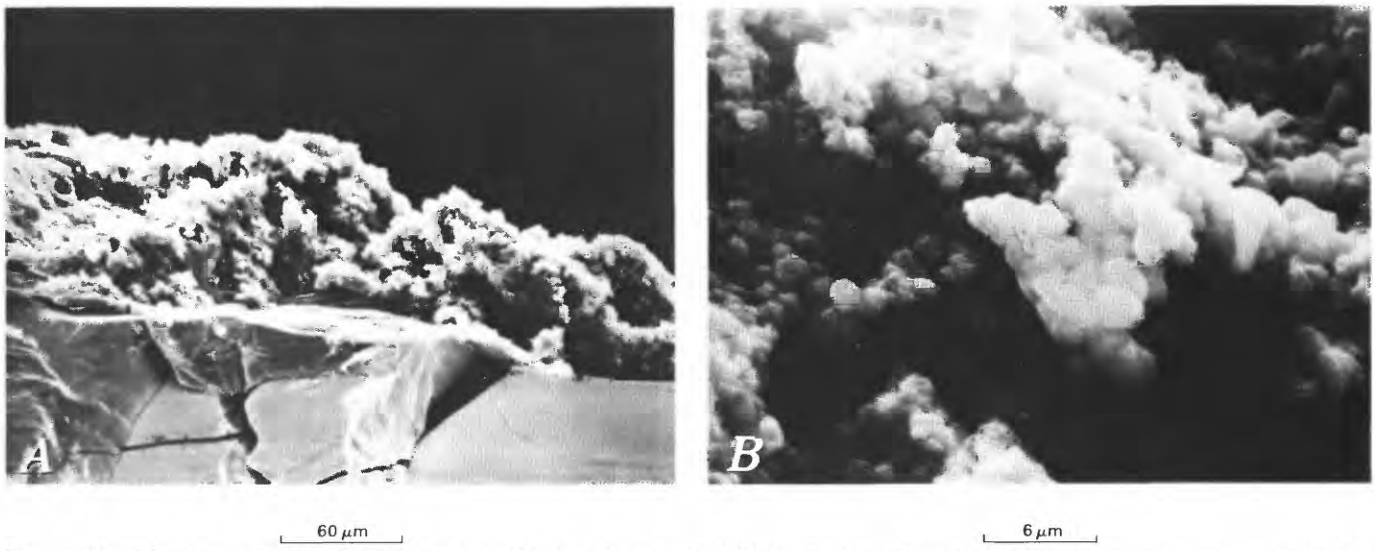

FIGURE 29.—Manganese oxide weathering product of huebnerite, sample DRS–79–68. *A*, oxide (pyrolusite?) coating a substrate of huebnerite; *B*, closer view of the manganese oxide mineral. Scales are 60 and 6 μm (micrometers), respectively.

low concentration of iron in the cassiterite would make detection of variation in the Fe^{+2}:Fe^{+3} ratio difficult.

TRACE-ELEMENT COMPOSITION

In light of the fact that the Round Mountain huebnerites were cleaned by hand picking, rather than by thorough mechanical and chemical means, the mineral residence of many of the minor elements detected is uncertain. Spectrographic analyses of huebnerite from Japan that was carefully purified by electromagnetic and heavy liquid separations and by acid treatment (Lee, 1955, p. 2, 49) revealed traces of titanium, magnesium, silicon, calcium, aluminum, zinc, copper, and silver. These trace elements may have been present in the huebnerite structure, in consideration of Lee's careful and effective methods of removing mineral impurities from the material that was analyzed. The minor amounts of elements detected by spectrographic analyses of the Round Mountain huebnerites thus may be held, in part, in the huebnerite structure rather than in mineral impurities. The character of our data, however, suggests that much of the minor elements detected are present as "impurities," that is, separate mineral phases; possibly some extraneous minor elements reside in fluid inclusions.

Spectrographic data given in table 6 suggest the identity of some "impurities" present in the analyzed huebnerites. Four samples contained greater than 0.5 percent Si, probably as quartz. Unusually high amounts (0.03–0.07 percent) of calcium and magnesium were detected in some huebnerites, and these elements in part may be present in carbonate minerals; some calcium may be present in scheelite (see, for example, Grubb, 1967). Certain elements, such as lead, zinc, copper, bismuth, silver, molybdenum, and cadmium, occur in amounts perhaps sufficient to indicate the presence of sulfides and sulfosalts, or weathering (secondary) products derived from them. The huebnerites that presumably contain sulfides or sulfosalts are widely and apparently randomly scattered throughout the tungsten-mineralized area. However, those with the highest amounts of sulfide- or sulfosalt-related metals were collected within the zones of base- and precious-metal mineralization (for example, samples DRS–74–221 and DRS–78–2; compare table 6 and fig. 2), although some huebnerite samples collected within the base- and precious-metal mineralization zones (for example, samples DRS–79–67 and DRS–79–68) contain no unusually high amounts of metals that could be attributed to sulfides or sulfosalts. Nickel and cobalt were detected and chromium was found in amounts perhaps anomalously high in a few huebnerite samples. The mineral residence of these elements is uncertain. Barium is present in significant quantities (0.03–0.1 percent) in some samples, probably reflecting admixed barite or barium-manganese oxides. Small amounts of strontium are present in the samples that contain unusually high amounts of barium. Small amounts of the yttrium-group rare-earth elements along with lanthanum, cerium, neodymium (in one sample), beryllium, niobium, scandium, and titanium were found in a few huebnerites; the mineral residence of these elements also is uncertain. Because of interference between the spectra of tungsten and niobium, niobium was determined on an emission line with a sensitivity less than that of the line normally used.

Judged from the total of elements present other than the major elements comprising huebnerite (see table 6), most of the huebnerite samples analyzed were reasonably free of "impurities."

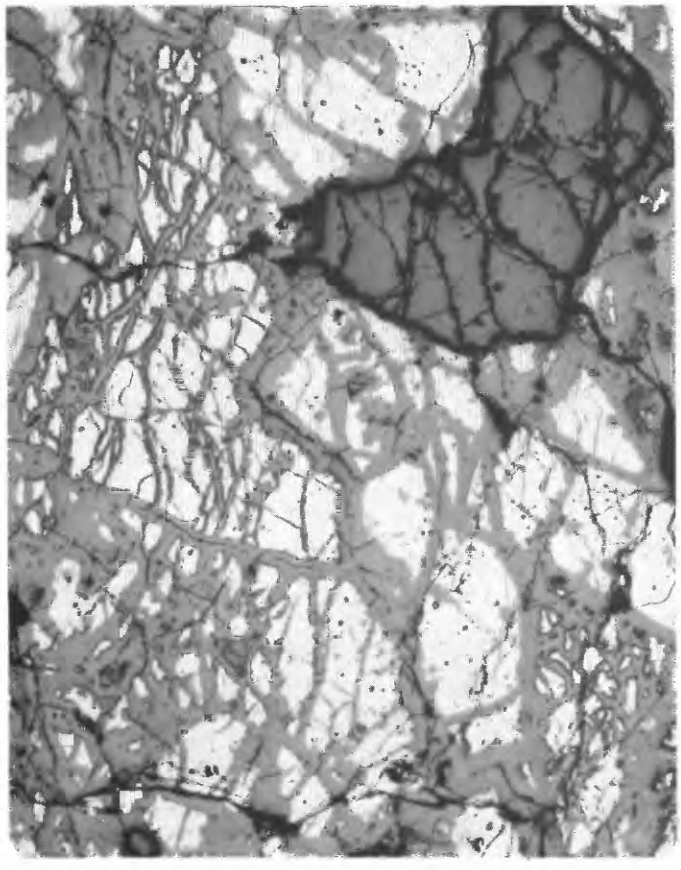

FIGURE 30.—Tetrahedrite-tennantite (light gray) partly replaced by stibiconite (medium gray) along irregular fractures, reflected light, polished section of sample DRS–78–2. Dark-gray grain in upper right is quartz.

FIGURE 31.—Secondary minerals in vein quartz (white), plane-polarized light, thin section of sample DRS–78–2A. Irregular veinlets are filled with growth layers of chrysocolla (medium gray). Vug bounded by sharp quartz prism faces (left center) is lined with layers of chrysocolla (medium gray), in part colloform, and filled with malachite (black). Small, sharp-cornered vug below (lower left) is lined with colloform chalcedony (nearly white) and filled with chrysocolla. Fluid inclusions (dark specks) form variously oriented trains in vein quartz.

VARIATIONS IN TUNGSTEN MINERALIZATION

One east-trending zone of tungsten mineralization that extends 2.5 km eastward from a point 3 km due east of Round Mountain (fig. 2) appears to be virtually devoid of well-defined huebnerite-bearing quartz veins. Instead, the zone contains local areas of tungsten-mineralized rock that are tourmalinized granite, iron- and quartz-mineralized fractures in granite, sheared and iron-mineralized argillite, or iron- and quartz-mineralized fractures in Oligocene rhyolite. The tungsten content of mineralized samples collected at these occurrences is low and ranges from 0.005 to 0.01 percent; identity of the tungsten mineral or minerals here is not known. Despite their low tungsten content, the occurrences contain substantially more tungsten than other nearby mineralized rocks. The tungsten-bearing deposits in this east-trending zone contain, in weight percent, as much as 0.02 Ag, 0.3 As, 0.007 Bi, 3.0 Cu, 0.002 Mo, 0.2 Pb, 0.5 Sb, and 1.0 Zn. Because some of these mineral occurrences are in Oligocene rhyolite or tourmaline-mineralized granite near the Oligocene stock east of Round Mountain, it is clear that there was a Tertiary tungsten-mineralizing event substantially younger than the emplacement of the huebnerite veins in Late Cretaceous time. In view of the small amount of tungsten involved in the younger (Tertiary) mineralization, the tungsten conceivably was remobilized from the earlier formed (Cretaceous) veins. The paragenetic data that show significant deposition of scheelite during a second hydrothermal stage, possibly derived by remobilization of huebnerite, indicate the availability of tungsten during hydrothermal activity

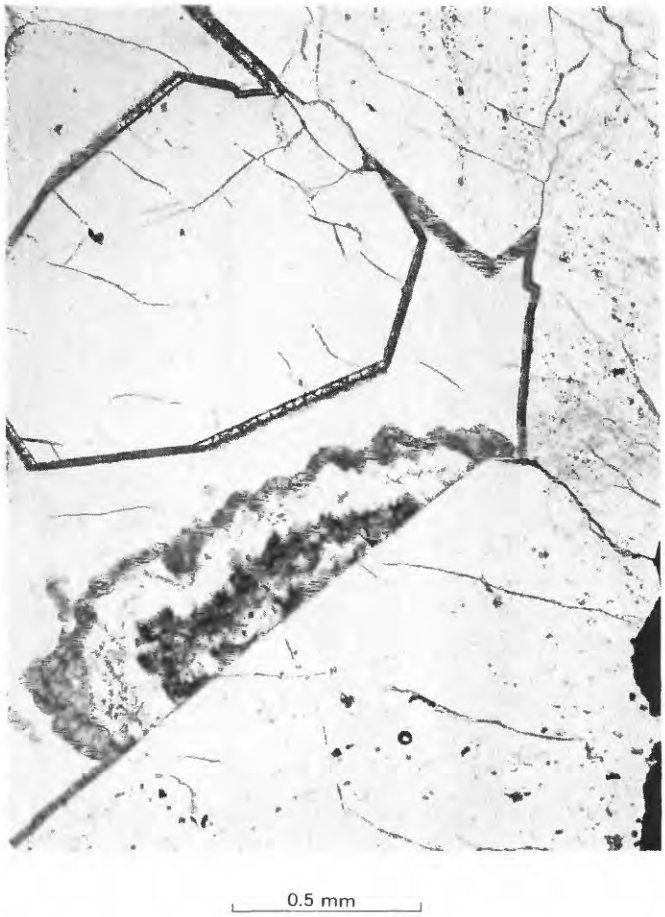

FIGURE 32.—Vug in vein quartz (white with numerous trains of fluid inclusions—black specks) lined with chrysocolla (gray) and filled with chalcedony (white, faintly layered), plane-polarized light, polished thin section of sample DRS–78–2B. Alternating layers of chrysocolla and chalcedony form a colloform mass on quartz prism face (below center). Stibiconite (black, lower right) is a selvage on tetrahedrite-tennantite (outside field of view).

FIGURE 33.—Late veinlet of secondary minerals cutting quartz (white) and huebnerite (dark gray), plane-polarized light, thin section of sample DRS–78–2A. Principal veinlet, extending across view, is filled with chrysocolla (light gray) that within the huebnerite crystal is partly replaced or filled with chalcedony (white). Thinner veinlets of chrysocolla follow cracks in huebnerite and along huebnerite-quartz contact. A thin, late veinlet of chalcedony follows the right margin of the principal chrysocolla veinlet; in the huebnerite crystal the chalcedony veinlet locally merges with chalcedony that replaced or filled chrysocolla. Outside the field of view the chalcedony veinlet is seen to transgress the chrysocolla veinlet to its left margin, indicating that it postdates the chrysocolla veinlet. Tiny grains of iron oxide (limonite) or sulfate (jarosite)—dark specks—are present within the late chalcedony veinlet.

that took place at some time following initial vein formation.

GEOCHEMISTRY OF THE HUEBNERITE VEINS

Semiquantitative spectrographic and other analyses of five samples of tungsten-bearing quartz vein material, given in tables 7 and 8, provide information on variations in mineralization of the veins that are indicated by the varied distributions of minerals described previously. The samples are part of a group of several hundred collected throughout the area of figure 2 for the purpose of determining patterns of metal distribution (Shawe, 1977b). Those samples were collected with an effort to obtain the most intensely mineralized material within a local area, and consisted of visibly mineralized rocks such as strongly iron-stained rocks, quartz and iron oxide-coated fracture surfaces, thin quartz and iron oxide veinlets, and quartz vein material containing sulfide and other ore minerals. Three of the samples listed in tables 7 and 8 (DRS–74–194, DRS–74–221, and DRS–74–252A) were collected within zones of base- and precious-metal mineralization as determined by the geochemical survey, and two samples (DRS–74–64 and DRS–74–200) were collected outside of those zones.

Highest amounts of a number of metals, including mercury, gold, silver, arsenic, bismuth, copper, molyb-

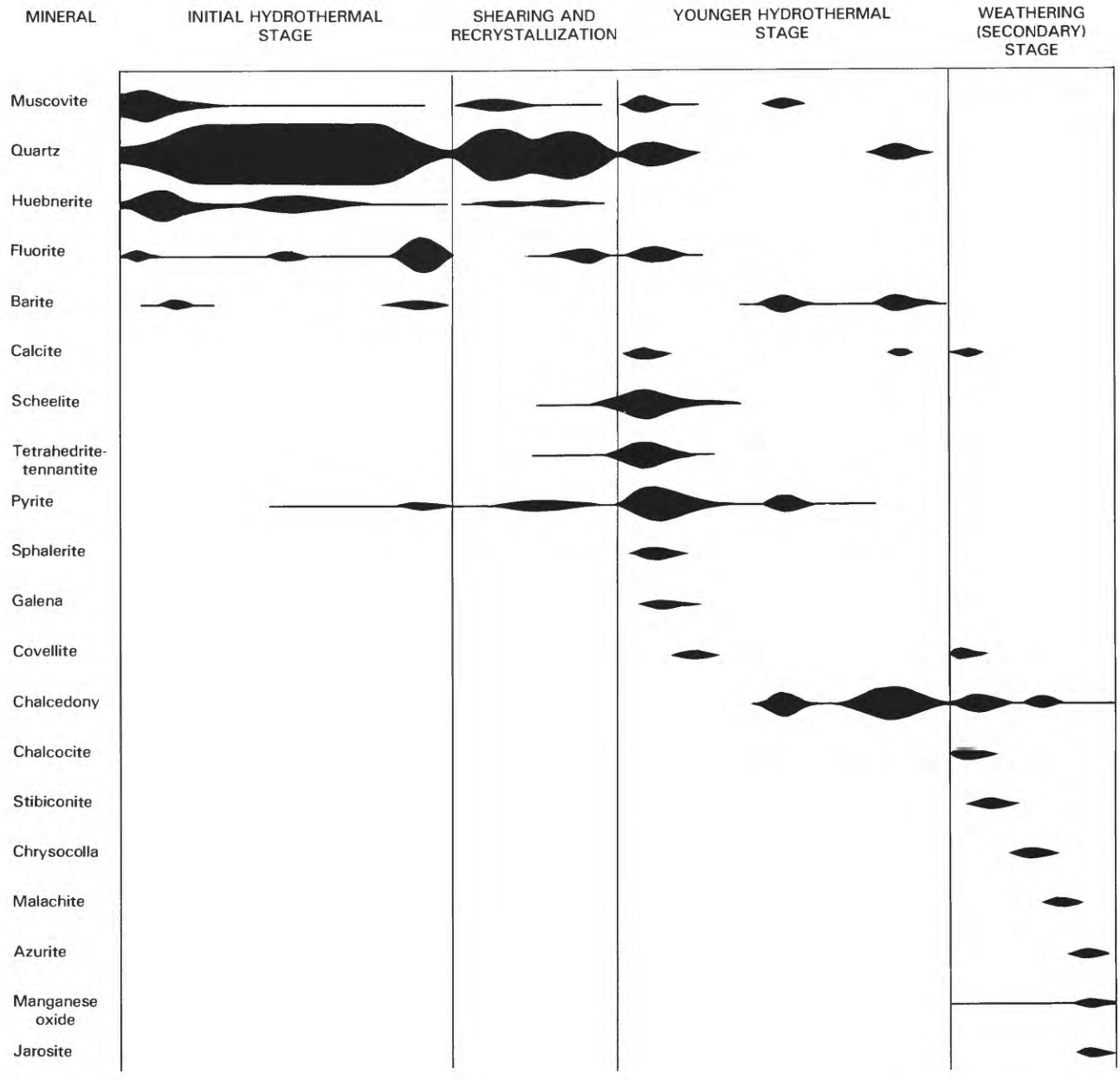

FIGURE 34.—Paragenesis of huebnerite veins. Thicknesses of bars suggest relative abundance of minerals in each stage of mineralization.

denum, lead, antimony, and zinc, were detected in the three samples collected within zones of base- and precious-metal mineralization. On the other hand, tungsten and a few elements such as manganese, iron, barium, fluorine, and niobium appear to be randomly concentrated through all five samples. Two elements, germanium and selenium, are more abundant in veins outside the zones of base- and precious-metal mineralization than within them.

DISCUSSION

Huebnerite has been reported from a large number of occurrences worldwide, but nearly end-member huebnerite, as in Japan (Lee, 1955, p. 49), Egypt (Takla, 1976; Takla and others, 1977), Mexico (Ramdohr, 1966, p. 1068), and western Transbaikal (Shnuraeva, 1972), is uncommon. In the United States substantial amounts of huebnerite have been mined

TABLE 5.—*Electron microprobe analyses, in weight percent, of 19 samples of huebnerite from quartz-vein samples collected east and south of Round Mountain (localities shown on fig. 2)*

[Analyses by E. E. Foord; variation in total and some of the variation in component values resulted from variation in conditions of the microprobe analyses. Leaders (--), not applicable]

Sample No. DRS-	FeO	Min FeO	Max FeO	MnO	WO_3	Total	No. of analyses	Structural formulas (basis of 4 oxygens)
67-30	1.6	1.23	1.97	21.8	77.6	101.0	6	$(Mn_{.92}Fe_{.07})_{0.99}W_{1.00}O_4$
67-33	1.9	1.38	2.41	21.7	77.8	101.4	4	$(Mn_{.91}Fe_{.08})_{0.99}W_{1.00}O_4$
73-17	.5	.22	.94	22.9	76.6	100.0	5	$(Mn_{.98}Fe_{.02})_{1.00}W_{1.00}O_4$
73-19	1.4	1.05	1.57	21.9	77.2	100.5	5	$(Mn_{.93}Fe_{.06})_{0.99}W_{1.00}O_4$
73-21	1.5	.84	2.07	21.8	77.0	100.3	5	$(Mn_{.93}Fe_{.06})_{0.99}W_{1.00}O_4$
73-27	1.0	.22	1.80	22.9	78.9	102.8	7	$(Mn_{.95}Fe_{.04})_{0.99}W_{1.00}O_4$
74-66	.4	.00	1.08	23.0	75.9	99.3	5	$(Mn_{.99}Fe_{.02})_{1.01}W_{1.00}O_4$
74-70	.6	.04	.92	22.5	77.5	100.6	5	$(Mn_{.96}Fe_{.03})_{0.99}W_{1.01}O_4$
74-72	.4	.00	.87	22.7	78.4	101.5	4	$(Mn_{.96}Fe_{.02})_{0.98}W_{1.01}O_4$
74-76	2.1	.84	3.57	21.1	76.3	99.5	9	$(Mn_{.91}Fe_{.09})_{1.00}W_{1.00}O_4$
74-105	2.9	.17	5.94	21.6	76.7	101.2	6	$(Mn_{.92}Fe_{.12})_{1.04}W_{0.99}O_4$
74-193	.5	.00	.48	23.3	77.7	101.5	3	$(Mn_{.98}Fe_{.02})_{1.00}W_{1.00}O_4$
74-200	.4	.32	.39	22.6	78.2	101.2	2	$(Mn_{.95}Fe_{.02})_{0.97}W_{1.01}O_4$
74-218	.2	.19	.29	22.9	76.9	100.0	3	$(Mn_{.98}Fe_{.01})_{0.99}W_{1.00}O_4$
74-221	.3	.00	.43	22.9	76.7	99.9	6	$(Mn_{.98}Fe_{.01})_{0.99}W_{1.00}O_4$
78-1	.1	--	--	23.0	77.2	100.3	1	$(Mn_{.98}Fe_{.004})_{0.98}W_{1.00}O_4$
78-2	.1	.10	.12	23.1	76.7	99.9	2	$(Mn_{.99}Fe_{.004})_{0.99}W_{1.00}O_4$
79-67	.3	.30	.35	23.0	76.9	100.2	2	$(Mn_{.98}Fe_{.01})_{0.99}W_{1.00}O_4$
79-68	.3	.24	.30	23.3	77.4	101.0	3	$(Mn_{.98}Fe_{.01})_{0.99}W_{1.00}O_4$

from veins at the Hamme (Tungsten Queen) Mine, N.C. (White, 1945; Bird and Gair, 1976), and small amounts have been mined from or recognized in veins at Butte, Mont., in the San Juan Mountains, in Boulder, Chaffee, Gunnison, Park, and Summit Counties, at Leadville, and at Cripple Creek, Colo. (Eckel, 1961), in Lincoln County, N. Mex., in Valley County (Leonard and others, 1968) and in Lemhi County, Idaho, and near Round Mountain, and from pegmatites in the Black Hills, S. Dak. (see, for example, Palache and others, 1951, p. 1064, 1068–1070). Elsewhere in Nevada huebnerite occurs near Austin (first reported occurrence of the mineral, in 1865) and near Osceola (Palache and others, 1951, p. 1064, 1070) in quartz veins similar to those near Round Mountain. Huebnerite also was found in quartz gangue of epithermal veins of the Tonopah district, associated with sulfides and sulfosalts (Melhase, 1935). Despite the description of the Tonopah veins as epithermal, they were probably deposited at temperatures (350°C–200°C; Bonham and Garside, 1979, p. 107) similar to those of the Round Mountain huebnerite veins. Of the deposits in the United States, only those at the Hamme Mine and near Round Mountain are reported to contain end-member huebnerite ($\lesssim$1 weight percent FeO) (Bird and Gair, 1976; Shawe and others, this report).

The huebnerite veins near Round Mountain are similar to those at the Hamme Mine in their mineralogy, rock associations, and conditions of formation. At the Hamme deposit quartz veins that contain huebnerite, fluorite, sulfides, and tetrahedrite occur in a north-northeast-trending linear belt nearly 6 km long, mostly

TABLE 6.—*Semiquantitative spectrographic analyses, in weight percent, of 23 samples of huebnerite from quartz-vein samples collected east and south of Round Mountain (localities shown on fig. 2)*

[Analyses by Nancy M. Conklin. N, not detected at limit of detection or at value shown; L, detected, but below limit of determination or below value shown; G, greater than 10 percent. Also looked for but not found: Na, K, P, As, B, Pd, Pt, Sn, Te, U, V, Zr, Ga, Ge, Hf, In, Li, Re, Ta, Th, Tl. (--), not looked for. Approximate lower limits (in percent) of determination for elements analyzed by six-step spectrographic method as shown in table 4, except for Ag (0.0002), Ba (0.0003), Be (0.0002), Cd (0.005), Co (0.0005), Cr (0.00015), Dy (0.003), La (0.005), Mo (0.0005), Nb (0.02), Ni (0.0002), Sr (0.001), Y (0.002), Yb (0.0005), Zn (0.03)]

Sample No.---	DRS-67-30	DRS-67-33	DRS-73-17	DRS-73-19	DRS-73-21	DRS-73-27	DRS-73-168	DRS-74-66	DRS-74-70	DRS-74-72	DRS-74-76A	DRS-74-76B
Si	0.03	0.7	0.7	0.07	0.15	0.05	0.1	0.07	0.15	0.03	0.05	0.15
Al	N .015	N .015	N .015	N .015	N .015	N .015	N .015	N .015	N .015	N .015	N .015	N .015
Fe	1	2	.7	1.5	1.5	1.5	.7	.7	1	.7	1.5	1.5
Mg	.03	.015	.003	.007	.015	.007	.007	.015	.015	.015	.015	.03
Ca	.015	.015	.03	.03	.07	.01	.03	.015	.03	.02	.015	--
Ti	.0015	.007	.007	.0015	.005	.0015	.003	.001	.0015	L .001	.003	.0015
Mn	G	G	G	G	G	G	G	G	G	G	G	G
Ag	N	.002	N	N	N	N	N	N	N	N	.0007	.0007
Ba	.015	.015	.05	.07	.1	.015	N .0003	.005	.007	.0015	.005	.0015
Be	N	.0003	N	N	N	N	N	N	N	N	N	N
Bi	.007	.003	N	N	N	N	N	N	N	N	N	N
Cd	N	N	N	N	N	N	N	N	N	N	N	N
Ce	N	.015	N	N	N	N	N	N	N	N	N	N
Co	N	N	N	N	.002	N	N	N	N	N	N	N
Cr	N .0005	N .0005	N .0005	N .0005	N .0005	.0007	N .0003	.0015	.0003	.00015	.0005	N .0003
Cu	.007	.015	.015	.015	.02	.001	.0015	.0015	.0007	.0002	.007	.007
Dy	.01	.005	.005	.003	.005	.003	.007	N .003	N .003	N .003	N .003	.003
La	N	.007	N	N	N	N	N	N	N	N	N	N
Mo	N	.001	N	N	N	N	N	N	N	N	N	N
Nb	.02	.02	.03	N .02	N .02	N .02	.03	.03	N .02	N .02	N .02	N .02
Nd	N	.007	N	N	N	N	N	N	N	N	N	N
Ni	N	N	N	N	N	N	N	N	N	N	N	N
Pb	.03	.07	.15	N .01	.15	N .01	N	.01	.015	N	.02	N
Sb	N	N	N	N	N	N	N	N	N	N	N	N
Sc	.003	.0015	.0007	.0015	.003	.0015	.0015	.003	.0015	.002	.0015	.003
Sr	N	N	.002	.002	.0015	N	N	N	N	N	N	N
W	G	G	G	G	G	G	G	G	G	G	G	G
Y	.02	.007	.007	.007	.007	.003	.007	.003	.003	.003	.003	.007
Yb	.01	.005	.005	.003	.007	.002	.007	.002	.003	.003	.003	.005
Zn	N	N	N	N	N	N	N	N	N	N	N	N

in a granitic (granodioritic-tonalitic) pluton but extending a short distance into phyllite wall rocks. The huebnerite contains about 0.2–1.2 percent FeO and shows growth zoning similar to, although coarser than, that of the Round Mountain huebnerites. Microprobe analyses of the zoned huebnerites showed that dark-colored growth layers commonly contain 0.1–0.4 percent more FeO than do the light-colored growth zones. Depositional temperatures of the Hamme deposit probably were less than 350°C (summarized from Bird and Gair, 1976).

The significance of variations in manganese and iron contents of wolframites, commonly stated as the huebnerite-ferberite molecular ratio (H:F), as an indication of conditions of deposition is controversial. Early work in western Europe and Africa by Oelsner (1944, 1952, 1954), Leutwein (1952), Bolduan (1954), Varlamoff (1958), and de Magnée and Aderca (1960) indicated that huebnerite has been deposited at higher temperatures than ferberite. More recently, in the Soviet Union and elsewhere, Churikov (1959), Ganeev and Sechina (1960), and Taylor and Hosking (1970) presented data to suggest that the opposite has been true. Clark's (1970) data on Cornwall deposits indicated that wolframite in pegmatitic veins contained more iron than that in associated "normal" (presumably lower temperature) lodes. Nevertheless, Hollister (1970) pointed out that Bolivian tin districts and Peruvian and North American molybdenum porphyry districts are zoned outward from huebnerite-rich cores to ferberite-rich peripheral zones. Landis and Rye (1974) noted zonation outward from wolframite to ferberite in the Pasto Bueno tungsten-base metal district, Peru. Other studies in Tasmania, Europe, and the United States by Edwards and Lyon (1957), Baumann and Starke (1964), Bird and Gair (1976), Amossé (1978a), and Moore and Howie (1978), indicated more complex relations between H:F and environment. The studies of Groves and Baker (1972) in northern Tasmania showed that regional variations in H:F probably reflect regional compositional differences among ore fluids, these differences being much greater than variations in the ratio within local ore areas. This conclusion is supported by the experimental data of Hsu (1976). Amossé (1978b) has suggested, by thermodynamic considerations applied to wolframite from the Borralha Mine, Portugal, that H:F cannot be used as a geothermometer, but rather indicates direction toward the source of mineralization. Hsu (1976) also

TABLE 6.—Continued

Sample No.---	DRS-74-105	DRS-74-193	DRS-74-200	DRS-74-218	DRS-74-221A	DRS-74-221B	DRS-78-1	DRS-78-2	DRS-79-67A	DRS-79-67B	DRS-79-68
Si	0.05	0.07	0.15	1	0.3	0.15	0.05	3	0.2	0.07	0.15
Al	N .015	N .015	N .015	N .015	N .015	N .0015	N .015	N .015	N .015	N .015	N .015
Fe	1.5	.3	1.5	.7	7	3	.15	.3	.3	.3	.2
Mg	.007	.005	.005	.005	.0015	.002	.007	.003	.007	.002	.005
Ca	.005	.015	.05	.005	.03	--	.005	.07	.05	.01	.03
Ti	L .001	.007	.002	.005	.003	.003	N	.007	.03	.03	.007
Mn	G	G	G	G	G	G	G	G	G	G	G
Ag	N	N	N	N	.005	.0007	N .0007	.005	N	N	N
Ba	.03	.0015	.05	.0007	.03	.007	.001	.015	.01	.007	.007
Be	N	N	N	N	N	N	N	N	N	N	N
Bi	.0015	N	N	N	L	N	N	N	N	N	N
Cd	N	N	N	N	N	N	N	.015	N	N	N
Ce	N	N	N	N	N	N	N	N	N	N	N
Co	N	N	.0015	N	N	N	N	N	N	N	N
Cr	.0007	.0002	.0002	.00015	.0002	N .0003	N .0005	N .0005	.0003	.0002	.0003
Cu	.0015	.03	.02	.0007	.07	.03	.02	.3	.0007	.0015	.007
Dy	N .003	N .003	.003	N .003	N .003	N .003	N .003	N .003	N .003	N .003	N .003
La	N	N	N	N	N	N	N	N	N	N	N
Mo	N	N	N	N	N	N	N	N	N	N	N
Nb	N .02	.03	N .02	N .02	.02	.02	N .02	.05	.03	.03	.07
Nd	N	N	N	N	N	N	N	N	N	N	N
Ni	N	N	.0003	.0002	.0003	N	N	N	.0007	.0015	.002
Pb	.003	.05	.007	.03	.2	.05	N	.03	N	N	N .003
Sb	N	N	N	N	.15	N	N	N	N	N	N
Sc	.001	.003	.0005	.007	.007	.007	.005	.007	.003	.003	.0015
Sr	.002	N	.001	N	.001	N	N	.003	.001	N	.002
W	G	G	G	G	G	G	G	G	G	G	G
Y	.003	.002	.003	N .002	N .002	N .002	.002	.002	N .002	N .002	N .002
Yb	.003	.002	.003	.0007	.0007	.0007	.002	.002	.0007	.0007	.0005
Zn	N	N	N	N	.03	.07	N	N	N	N	N

concluded that H:F is of little value as a clue to temperature, pressure, and oxygen and sulfur fugacity during ore formation. Wiendl (1968, p. 265–279) showed that pH of mineralizing fluids generally is more important than temperature in determining the manganese-iron content of wolframite; a lateral increase in iron results from neutralization of ore fluids by wall rocks. Horner's (1979) theoretical and experimental data indicated that huebnerite should form at temperatures above 200°C from neutral to weakly alkaline solutions, whereas ferberite should form through a wide temperature range but from acidic solutions. Studies by Vinogradova, Barabanov, and Sorokin (1980) suggested that ferruginous wolframites precipitated at low pH were richer in scandium and niobium than crystals precipitated from more alkaline (manganiferous) media. Niobium was not detected in less ferruginous wolframites formed in a less acid medium. Moore and Howie (1978) indicated that the uneven distribution of manganese and iron may be controlled not only by the concentration of these elements in ore fluids but by rapid changes in the composition of ore fluids, by competing mineral phases (for example, sulfides) if present, and by subsequent remobilization of manganese and iron. Voyevodin (1981) emphasized the influence of varied complex factors on composition of wolframites.

Oscillatory zoning of iron and manganese in wolframite crystals may be controlled by local concentration gradients at the crystal-liquid interface, or by periodic supercooling of the liquid, or by "constitutional" supercooling as proposed for oscillatory zoning in plagioclase feldspars by Sibley and others (1976), or to the thermodynamic changes proposed by Amossé (1980). Major compositional changes in broad growth zones may be due to changes in external conditions.

Lawrence (1961) attempted to correlate the habit of wolframite with temperature of crystallization. He concluded that stout prismatic crystals grew at higher temperatures, whereas platy crystals grew at lower temperatures; iron-composition differences (0.5 weight percent between the two types) were slight, however. Landis and Rye (1974) showed at Pasto Bueno, Peru, that early-stage wolframite (75 weight percent $MnWO_4$) formed stubby bladed crystals and was deposited at a temperature of about 235°C and late-stage ferberite (<5 weight percent $MnWO_4$) formed elongate crystals and was deposited at a temperature of about 180°C. We note in the huebnerite veins near Round Mountain a tendency for stubby crystals to form where wall rock is schist, which also is at the lowest altitude of vein exposure and where huebnerite contains only about 0.2 weight percent FeO. In granite and at higher altitudes, huebnerite may occur more commonly as tapered tabular crystals, and the mineral in this part of the vein system contains 0.7–3.0 weight percent FeO. We do

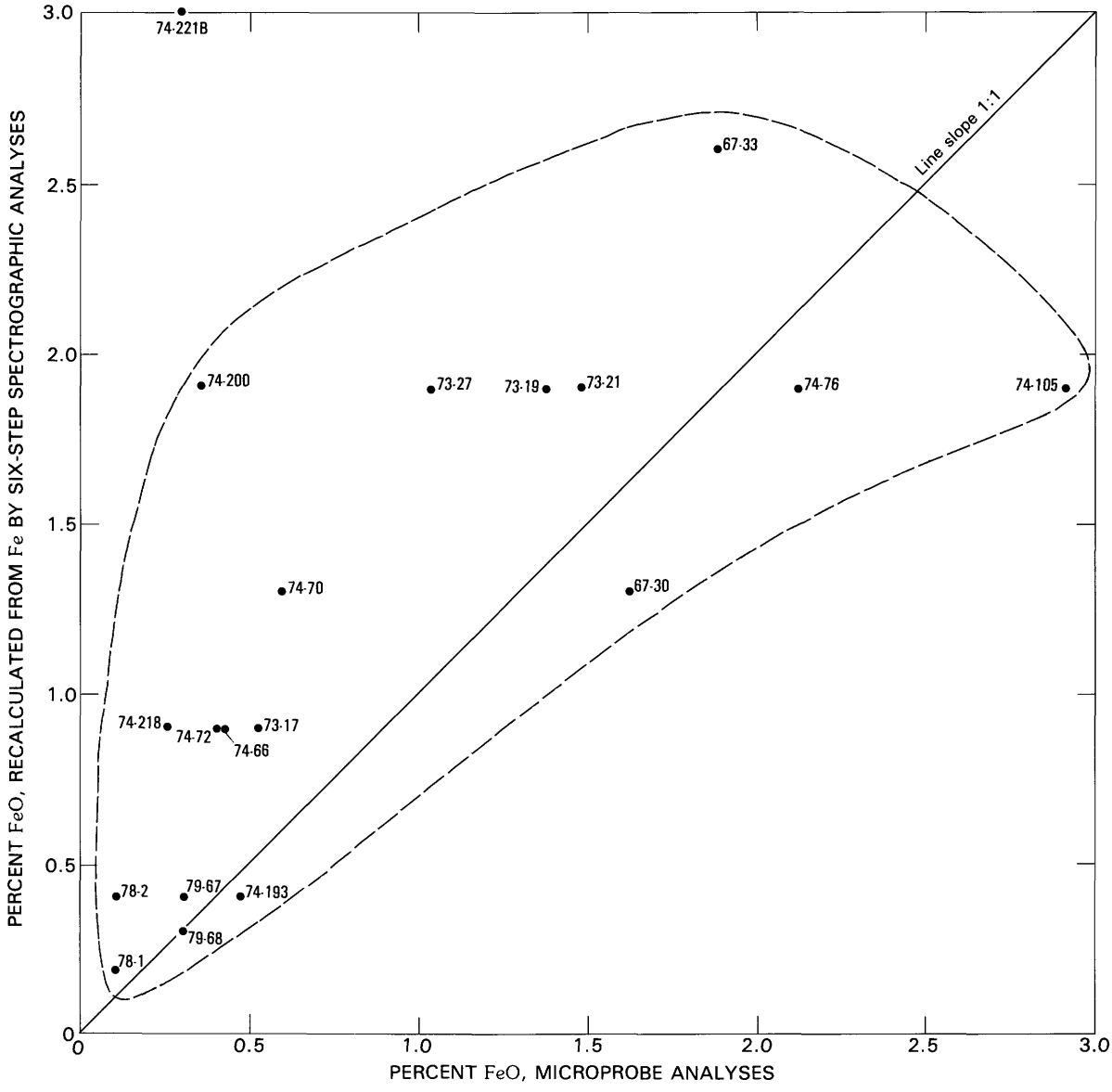

FIGURE 35.—Comparison of iron (recalculated as FeO) in huebnerite samples determined by six-step spectrographic analyses, and by microprobe analyses. Numbers are sample numbers.

not have adequate data to indicate whether or not there was a temperature difference between deposition of the two forms of huebnerite.

An assessment of the geologic setting of the huebnerite veins near Round Mountain permits an estimate of depth of burial of the veins at the time of their formation and an estimate of some of the parameters of the hydrothermal fluids that deposited the veins. A reconstruction of the domed granite, based on attitudes of granite contacts and of foliation within the granite, suggests that the apex of the pluton was about 1.5–2 km above the present erosional level. Perhaps another 1.5 km of Paleozoic sedimentary rocks lay above the dome at the time of its formation, interpreted to be the time of tungsten mineralization. Erosional stripping of some or all of the Paleozoic rocks during doming cannot be evaluated easily, and we discount it in this assessment. Thus the depth of formation of the present huebnerite veins was likely about 3–3.5 km beneath the surface. Fluid pressure at the time of vein formation is difficult to assess. Hydrostatic rather than lithostatic pressure may have prevailed, because of the evidence of some brittle deformation at the time of vein formation, and because locally much open space in the veins implies through-going solution flow. However, at times during the course of vein deposition, deformation took place under high confining pressure. Such deformation is evidenced by the recrystallization of prismatic quartz

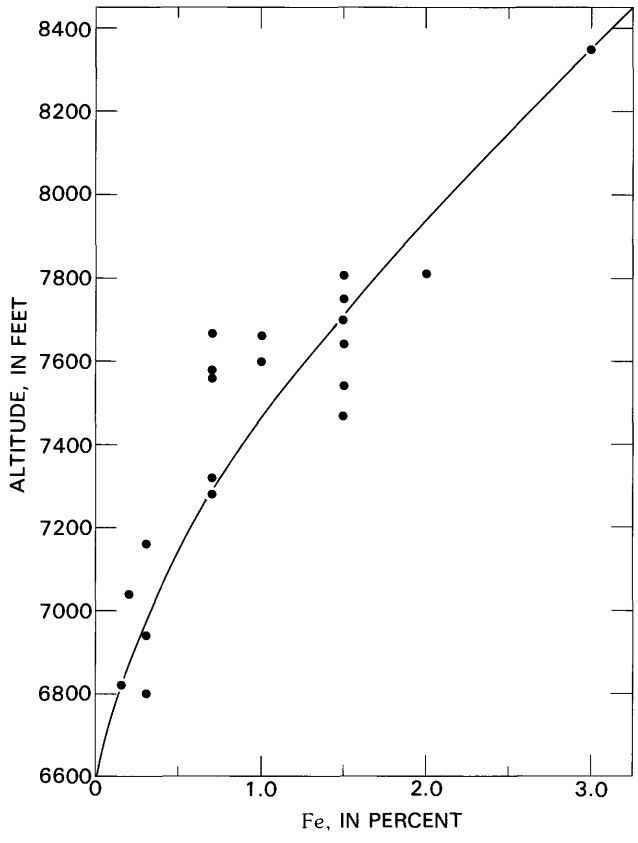

FIGURE 36.—Positive correlation between spectrographically determined iron composition of huebnerite samples and altitude in the vein system.

crystals to form massive mosaic vein quartz that contains carbon dioxide-bearing fluid inclusions, and by the fact that along some vein walls partial replacement of wall rocks rather than open-space filling took place. Uncertainties as to the amount of carbon dioxide present in vein fluids, the temperature of the vein fluids at the level of and above the present huebnerite veins, and the height of the column of fluids in the vein system above the present veins also make an evaluation of fluid density uncertain. We use the assumptions that hydrostatic pressure prevailed and that the column of fluids extended upward to the surface. Like Landis and Rye (1974, p. 1043), we have arbitrarily selected an average density of 0.8 g/cm^3 (80 bars/km) as possible and reasonable. Maximum fluid pressures at depths of 3–3.5 km thus would have been about 240–280 bars. If lithostatic pressure is assumed (granite density ≅2.65 g/cm^3), maximum pressure would have been about 640–740 bars.

We believe that clear quartz crystals that penetrate vugs, on which J. T. Nash (written commun., March 1980) determined filling temperatures of about 190°C and which contain no liquid carbon dioxide, were formed near the end of the initial episode of mineralization during which huebnerite was deposited. Temperatures at the beginning of this stage may have been much higher. Following this stage of vein formation, the veins were deformed, quartz was recrystallized except where quartz prisms penetrated vugs, and fluid inclusions, some bearing carbon dioxide, were formed in the recrystallized quartz. Nash determined filling temperatures of 250°–270°C for these fluid inclusions. Fluorite that fills vugs penetrated by clear quartz crystals contains fluid inclusions that have filling temperatures of 230°–260°C, according to Nash, and he indicated that some of the fluid inclusions with filling temperature of 260°C contain carbon dioxide dissolved in the aqueous phase. Younger fluorite contains fluid inclusions that have filling temperatures of about 190°C, and these inclusions contain no liquid carbon dioxide. These temperatures, corrected for estimated maximum pressures at about 5 weight percent equivalent NaCl (Lemmlein and Klevtsov, 1961, fig. 4), are about 210°C for early quartz and late fluorite, 270°–290°C for recrystallized quartz, and 250°–280°C for early fluorite, at pressures of about 240–280 bars. At pressures of about 640–740 bars, they are about 245°C for early quartz and late fluorite, 310°–330°C for recrystallized quartz, and 290°–320°C for early fluorite.

A fluid under pressure of 240–280 bars (hydrostatic conditions) and with about 5 weight percent NaCl should boil at about 380°–480°C, and a fluid under pressure of 640–740 bars (lithostatic conditions, considered improbable) should boil at about 515°–545°C (Takenouchi and Kennedy, 1965, fig. 5). Perhaps the uneven distribution of carbon dioxide in fluid inclusions in recrystallized vein quartz suggests the possibility of boiling during the formation of these secondary inclusions. However, the pressure-salinity data that indicate boiling in the range 380°–480°C, well above the estimated temperature of formation (270°–290°C) of the carbon dioxide-bearing fluid inclusions in recrystallized quartz, argue against boiling. The variation in carbon dioxide contents of these secondary fluid inclusions suggests instead a variation with time in carbon dioxide contents of the depositing fluids through the period of quartz recrystallization.

J. T. Nash's estimate (written commun., March 1980) of 2–10 mol percent (5–20 weight percent) CO_2 in fluids that were trapped in inclusions in the recrystallized (milky) quartz seems reasonable. According to Takenouchi and Kennedy (1965, fig. 2), in the temperature range of 270°–290°C and pressure range of 240–280 bars, at which the recrystallized quartz formed, 6 weight percent NaCl solution could contain a maximum of 6–7 weight percent CO_2. At 210°C and the same pressures and salinity, the maximum carbon dioxide content

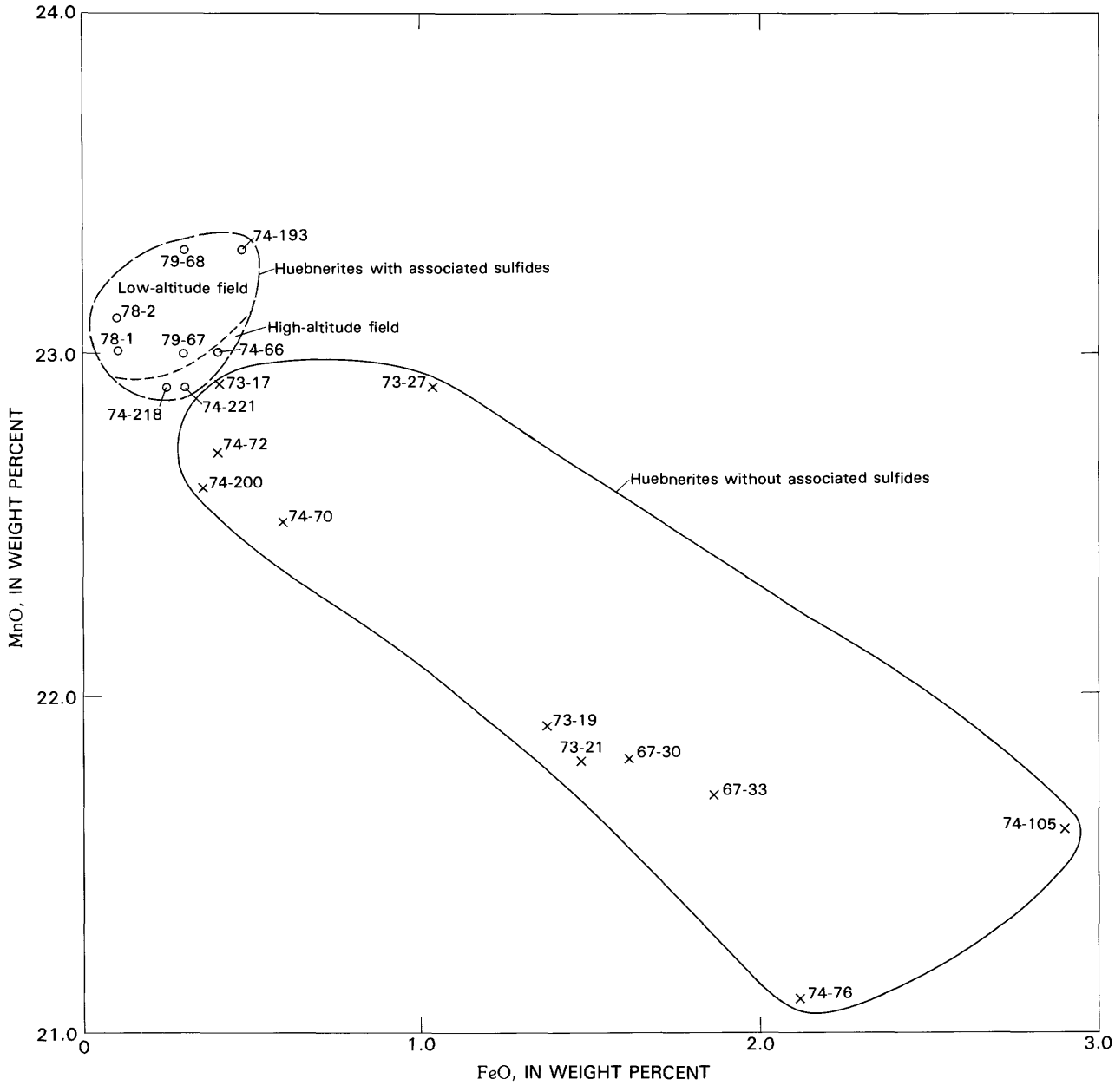

FIGURE 37.—Comparison of FeO and MnO in huebnerites analyzed by microprobe. Numbers are sample numbers.

would be 5 weight percent; Nash detected no carbon dioxide in quartz and fluorite that were deposited at 210°C.

The huebnerite veins near Round Mountain probably represent the lower part of a mineralized system, the bulk of which has been eroded away. Wolframite-bearing vein systems that are spatially associated with granitic rocks commonly appear to have maximum development—that is, show the greatest concentration of rich and large veins—at and near the crests of cupolas. Examples are Panasqueira, Portugal (Kelly and Rye, 1979), Borralha, Portugal (Amossé, 1978b); several localities in Thailand (Shawe, personal observations, 1974); Pasto Bueno, Peru (Landis and Rye, 1974); Las Guijas, Arizona (Sheikh, 1970); several localities in Tasmania (Groves and Baker, 1972); and Cligga Head, Cornwall, England (Moore and Jackson, 1977). If the Round Mountain vein system had reached as high as cupolas near the apex of the granitic pluton, it would have had a vertical extent of 1.5–2 km. However, G. P. Landis (written commun., 1980) suggested to us that a chemically integrated continuum of wolframite deposition possibly could not be maintained through such a vertical extent. The fact that nearly end-member huebnerite was deposited in the Round Mountain veins also suggests that they are near the base of a tungsten

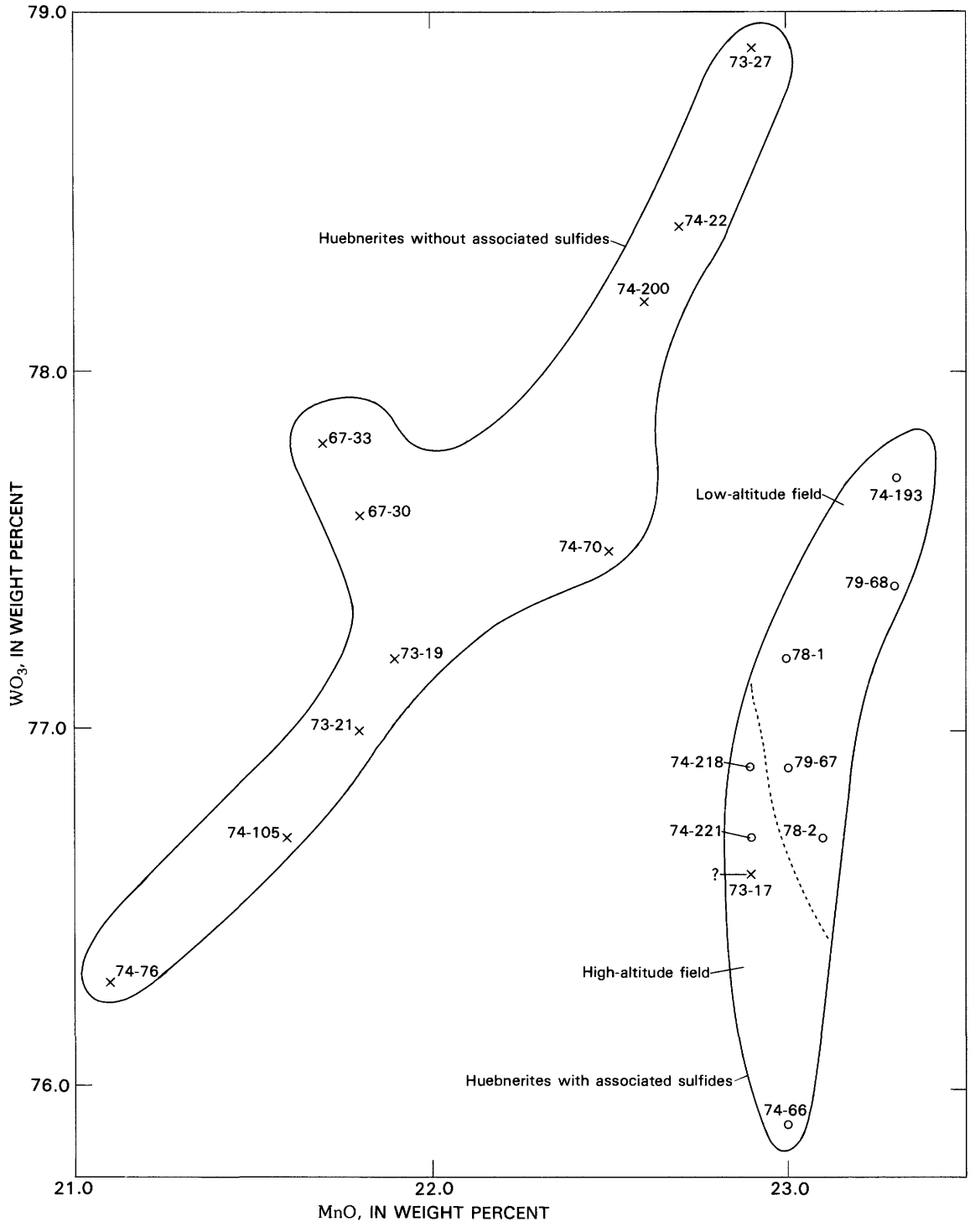

FIGURE 38.—Comparison of MnO and WO_3 in huebnerites analyzed by microprobe. Numbers are sample numbers; query indicates that the position of sample DRS–73–17 in the field of huebnerites with associated sulfides is anomalous.

vein system. Once huebnerite started to precipitate, as hydrothermal fluids rose through fractures, solution compositions changed so that huebnerites deposited higher in the system were more iron rich. Thus, where end-member huebnerite is present in a vein system that shows systematic increase upward in the iron content of the huebnerites, we interpret that the end-member huebnerite indicates the lowest part of the vein system.

Assuming that huebnerite compositions changed toward that of ferberite with increasing altitude in the vein system, the diagram of iron versus altitude of the Round Mountain veins (fig. 36) suggests that at a level

TABLE 7.—*Semiquantitative spectrographic analyses, in weight percent, of five samples of tungsten-bearing quartz vein material (sample localities shown on fig. 2)*

[Analyses by Harriet G. Neiman. N, not detected at limit of detection. G, greater than 10 percent. Also looked for but not found: Au, B, Co, La, Ni, Pd, Pt, Sc, Sn, Te, U, Y, P, Ce, Ge, Hf, In, Li, Re, Ta, Th, Tl, Eu]

Sample No.---	DRS-74-64	DRS-74-194	DRS-74-200	DRS-74-221	DRS-74-252A
SiO_2	86	100	100	88	98
Al_2O_3	4.3	1.8	.65	<.5	<.5
Fe_2O_3	.88	.54	.47	.53	.66
CaO	<.1	.13	.25	.56	<.1
K_2O	1.4	.42	.23	.24	.20
TiO_2	.10	<.05	<.05	<.05	<.05
P_2O_5	<1	<1	<1	<1	<1
MnO	.66	<.05	.13	.44	<.05
S	<.08	<.08	<.08	.42	.13
Cl	<.2	<.2	<.2	<.2	<.2
F	.08	.06	.07	.05	<.04
Hg	.000023	.00015	.000009	.01	.002
Au	<.000005	.000011	<.000005	.000117	<.000005
Ag	<.002	.0094	<.002	.175	.0105
Sn	<.00001	<.00001	<.00001	.00007	<.00001
Sb	<.00001	.0142	.0011	.0432	.0168
Ge	.0021	.00044	.00085	.00021	.00018
As	<.00001	.0038	.00008	.0111	.0035
Se	.00044	.00009	.00013	<.00001	.00001

TABLE 8.—*Analyses, in weight percent, for several components of five samples of tungsten-bearing quartz vein material (sample localities shown on fig. 2)*

[SiO_2, Al_2O_3, Fe_2O_3, CaO, K_2O, TiO_2, P_2O_5, MnO, S, and Cl by X-ray fluorescence method by J. S. Wahlberg and J. W. Baker; F. by specific ion electrode method by Johnnie Gardner and Patricia Guest; Hg by wet oxidation plus atomic absorption method by J. A. Thomas; Au by fire assay plus atomic absorption method, and Ag by difference, by A. W. Haubert, L. B. Riley, and J. G. Crock; Sn, Sb, Ge, As, and Se by X-ray fluorescence by J. S. Wahlberg, J. O. Johnson, and J. W. Baker]

Sample No.---	DRS-74-64	DRS-74-194	DRS-74-200	DRS-74-221	DRS-74-252A
Si	G	G	G	G	G
Al	1.5	0.3	0.2	0.2	0.15
Fe	.2	.1	.07	.1	.15
Mg	.03	.02	.015	.015	.005
Ca	.05	.03	.2	.3	.002
Na	.5	N	N	N	N
K	1	N	N	N	N
Ti	.03	.005	.001	.001	.0005
Mn	.5	.05	.15	.2	.0015
Ag	.0002	.005	N	.1	.01
As	N	N	N	.07	N
Ba	.15	.01	.01	.02	.005
Be	.00015	N	N	N	N
Bi	.0007	.002	N	.003	.002
Cd	N	N	N	.003	N
Cr	N	N	N	.0001	N
Cu	.0007	.07	.0015	.15	.15
Ga	.0005	N	N	N	N
Mo	N	.0015	N	.0007	.003
Nb	.003	.001	.002	.005	N
Pb	.005	.007	N	.3	.03
Sb	N	.07	N	1	.1
Sr	.005	N	N	.0015	N
V		.0005	N	N	NN
W	1	.07	.1	1	.007
Yb	.0001	N	N	N	N
Zn	N	.05	N	.02	.1
Zr	.003	N	N	N	N

1.5–2 km higher in the system—that is, the interpreted level of cupola formation at the apex of the granite pluton—the composition of the tungstate mineral would be about 18 percent Fe, or virtually end-member ferberite. The uncertainty of the slope of the curve as controlled by the data points of figure 36, as well as the uncertainty of slope above the segment of the vein system represented in the diagram, make that value of iron content rather uncertain. Nevertheless, the extrapolation suggests that the wolframite would contain substantially more iron than that present in the huebnerites of the Round Mountain veins, and the composition of wolframite would be closer to compositions of wolframites in the cited cupola environments elsewhere in the world.

Trace element components of wolframites have been reported by a number of authors (Lee, 1955; Churikov, 1959; Ganeev and Sechina, 1960; Zuyev and others, 1966; Mineev, 1968; Takla and others, 1977; Vinogradova and Barabanov, 1978; Moore and Howie, 1978; Vinogradova, Barabanov, and Sorokin, 1980). With the exception of Lee (1955, p. 5) and Ganeev and Sechina (1960) none of these workers presented details on methods or effectiveness of purification of the analyzed minerals. Takla and others (1977) and Zuyev and others (1966) reported inclusions of other minerals in the wolframites they analyzed for trace elements. We believe that the presence of small amounts of other minerals enclosed in the analyzed wolframites was likely in many of the reported studies of trace elements in wolframites, and in some cases therefore speculations on the residence and absolute amounts of trace elements in the wolframite structure are not valid. The association with wolframite of minor amounts of minerals of certain compositions, however, as suggested by the analytical data, undoubtedly has geochemical significance. Noting, then, the uncertainty of residence of many of the trace elements associated with the Round Mountain huebnerites, we can point out some perhaps meaningful associations. Yttrium-group rare-earth elements dominate over cerium-group rare-earth elements, a relation also described for wolframites from the Soviet Union (Mineev, 1968; Vinogradova and Barabanov, 1978). We detected yttrium and ytterbium values as high as 0.007 percent each in Round Mountain huebnerites, whereas Ganeev and Sechina (1960) reported as much as 0.08 percent Y and Vinogradova and Barabanov (1978) reported as much as 0.036 percent Y in wolframites of the Soviet Union. Scandium was found in Round Mountain huebnerites in amounts as high as 0.07 percent,

whereas Ganeev and Sechina (1960) found as much as 0.032 percent Sc and Vinogradova and Barabanov (1978) found as much as 0.11 percent Sc in wolframites from the Soviet Union. A microprobe study of five zoned wolframite crystals from vein-type deposits (Vinogradova, Barabanov, and Sorokin, 1980) showed a range of 0.17 to 1.04 percent Sc_2O_3. Beddoe-Stephens and Fortey (1981) detected as much as 0.03 percent Sc_2O_3 in wolframite from the Carrock Fell tungsten deposit in the English Lake district. Ganeev and Sechina (1960) suggested close correlations between scandium and iron and between yttrium and manganese in the Soviet Union wolframites, but we see no such correlations in the Round Mountain huebnerites, possibly owing to their narrow iron-compositional range. Niobium was undetected above 0.02 percent in most Round Mountain huebnerites, but it ranges as high as 0.07 percent in those in which it was found. Takla and others (1977) reported 0–0.05 percent Nb in Egyptian huebnerites, Ganeev and Sechina (1960) reported 0–0.1 percent Nb in Soviet Union wolframites, and Moore and Howie (1978) reported as much as 0.5 percent Nb in Cornwall wolframites. Vinogradova, Barabanov, and Sorokin (1980) reported as much as 0.56 weight percent Nb_2O_5 in zoned wolframites from the U.S.S.R. Zuyev and others (1966) showed by means of selective chemical extraction and electron microprobe studies that practically 100 percent of the tantalum and niobium in epithermal wolframite from quartz veins is due to the isomorphous entry of these elements into the mineral. Examination of hypothermal wolframite (from albitized and greisenized granite) showed that only part of the tantalum and niobium is an isomorphous admixture, the remainder occurring in inclusions of columbite and microlite. An average of 0.19 percent Ta_2O_5 was found to enter isomorphously into the wolframite structure. Beddoe-Stephens and Fortey (1981) detected (by electron microprobe) as much as 0.98 percent Nb_2O_5 in wolframite from quartz veins in the Carrock Fell tungsten deposit in the English Lake district; minute amounts of columbite are associated with the wolframite. Where other minerals have replaced the Carrock Fell wolframite, no concentration of niobium at mineral contacts was detected, suggesting that the niobium content of the wolframite was primary. Moreover, microprobe analyses showed that niobium enrichment occurred in zones in wolframite close to primary crystal faces, suggesting original growth zoning. A niobium-rich wolframite (20.25 weight percent Nb_2O_5) was reported by Saari, von Knorring, and Sahama (1968) from the Nuaparra pegmatite, Zambezia, Mozambique. The wolframite also contained 5.35 percent Ta_2O_5, 2.68 percent TiO_2, 1.52 percent SnO_2 plus Sb_2O_3, and significantly, 8.43 percent Fe_2O_3 compared to 7.43 percent FeO.

We have interpreted that much of the calcium detected in analyses of Round Mountain huebnerites is actually resident in scheelite or calcite impurities. Phase equilibria studies by Chang (1967) have shown only a limited solid solution between $CaWO_4$ and $MnWO_4$ and even less between $CaWO_4$ and $FeWO_4$. Zinc was detected in huebnerite from only one locality (DRS–74–221), where the huebnerite-bearing quartz vein also contains appreciable sphalerite. Although a complete series of solid solutions forms in the system $ZnWO_4$–$MnWO_4$ above 840°C (Chang, 1968), it seems unlikely that a phase of this system is present in the Round Mountain material.

The magmatic-metamorphic episode that was accompanied by tungsten mineralization near Round Mountain about 80 m.y. ago may have been widespread in the region. For example, we interpret that the Jurassic Snake Creek pluton in the southern Snake Range in eastern Nevada was metamorphosed and invaded by aplites and pegmatites and mineralized by tungsten-bearing quartz veins at various times following emplacement; one such episode took place about 71–78 m.y. ago (data from Lee and Van Loenen, 1971; Lee and others, 1970). At Tungsten, site of an important scheelite-producing district in northwestern Nevada, granitic rocks were metamorphosed about 74–79 m.y. ago and tungsten mineralization took place about 72–76 m.y. ago (Tingley, 1975). Near the site of large production of scheelite ores at Pine Creek, Calif., about 200 km southwest of Round Mountain, plutonic rocks yielded K-Ar (biotite) ages of 70–80 m.y. in contrast to surrounding plutonic rocks that yielded K-Ar (hornblende) ages of 80–100 m.y. (Evernden and Kistler, 1970). Possibly these relations indicate metamorphism of the plutonic rocks in the vicinity of Pine Creek at the time of tungsten mineralization. At the Old Woman Mountains in southeastern California, tungsten mineralization took place in granitic rocks that yield a Rb-Sr (whole rock) age of 80 m.y. (Miller, 1977).

SUMMARY AND CONCLUSIONS

Huebnerite-bearing quartz veins were deposited about 80 m.y. ago near Round Mountain, mostly in Cretaceous granite (emplaced about 95 m.y. ago), when the granite was invaded by pegmatite and aplite dikes, was domed, and was metamorphosed. Depth of burial at the time of vein formation was probably about 3–3.5 km, based on geologic reconstruction. Through the initial stage of vein deposition, pressures were probably about 240–280 bars or only slightly higher, and salinity of the fluids persisted at about 5 weight percent NaCl. Muscovite, quartz, and huebnerite were the principal minerals of early-stage deposition in the veins. Quartz crystals

deposited near the end of this initial phase were precipitated from solutions at a temperature of about 210°C and contained little if any carbon dioxide. Following the precipitation of quartz, fluorite was deposited at temperatures of about 250°–280°C, from solutions that contained small amounts of carbon dioxide (about 5 weight percent?). Also, after initial precipitation of vein quartz, the veins were deformed, and the quartz was recrystallized and permeated by solutions at a temperature of about 270°–290°C that contained carbon dioxide (5–20 weight percent?). Probably following this deformation, additional fluorite was deposited at a temperature of about 210°C from solutions that contained little or no carbon dioxide. Foose, Slack, and Casadevall (1980) documented post-mineralization deformation at the Tungsten Queen (Hamme) deposit, North Carolina. Casadevall and Rye (1980) presented evidence that metamorphic temperatures exceeded earlier primary-mineralization temperatures at the Tungsten Queen deposit.

During the initial stage of vein deposition at Round Mountain, some pyrite was deposited along with the other vein minerals. Possibly other sulfides and sulfosalts were deposited in the veins or in altered rocks adjacent to the veins at that time, but the amounts were likely quite small.

After the initial hydrothermal stage of vein deposition, the veins were sheared and reopened, possibly at the time of widespread recrystallization of vein quartz, but more likely at a later time. A second stage of hydrothermal mineralization then took place, involving minor deposition of muscovite, quartz, and fluorite, but characterized mainly by deposition of sulfides, tetrahedrite-tennantite, scheelite (altered from initial-stage huebnerite), and near the end of the stage, barite and chalcedony. Although we have no direct evidence of the age of this mineralization, its dominant spatial association with 35-m.y.-old intrusive rocks (southwest end of rhyolite dike swarm and vicinity of granodiorite stock) leads us to believe that the younger hydrothermal stage of mineralization was related to a geologic episode that saw emplacement of those igneous rocks. Moreover, sulfide and minor tungsten mineralization took place in 35-m.y.-old rocks in the vicinity of the granodiorite stock. The mineralization of Tertiary rocks and the presence of chalcedony in late phases of the younger hydrothermal stage suggest that the younger hydrothermal stage took place at a shallower level at lower temperatures and pressures than did the initial hydrothermal stage.

We note that Leonard, Mead, and Conklin (1968, p. C19–C20) interpreted the New Snowbird, Idaho, tungsten-bearing quartz lode, somewhat similar to the Round Mountain huebnerite veins, to be the product of a single (although complex) episode of mineralization, even though they admitted that it might consist of two principal stages: early higher temperature tungsten mineralization and late lower temperature sulfide mineralization, as Schneider-Scherbina (1962) had interpreted for so-called telescoped mineralization of the Bolivian tin-silver deposits.

Following uplift and erosion of the Round Mountain huebnerite vein system in late Tertiary and Quaternary times the veins were weathered, with the development of numerous secondary minerals derived from the breakdown of primary vein minerals.

Possibly the huebnerite veins near Round Mountain represent the lower part of a vein system that when formed extended to a much higher level and resulted in mineralization of cupolas at the apex of the granite pluton. By analogy with wolframite deposits known elsewhere in the world that are associated with granite cupolas, the richest part of the Round Mountain vein system may have formed at that level, and thus was destroyed by erosion long ago. If the zonation of the iron content of the huebnerites in the Round Mountain vein system, increasing with altitude, is valid, we are led to believe that any such eroded deposits in cupolas must have contained wolframites with iron compositions much higher than those in the Round Mountain veins. Cupolas of granite plutons in the Basin and Range province in Nevada and adjacent States that have had deformation and metamorphic histories similar to the granite near Round Mountain, and that have not been unroofed by erosion, seem to be likely sites for undiscovered wolframite vein deposits, perhaps of large size. Such postulated deposits, as well as known ones, may have formed dominantly during a major regional event of tungsten mineralization about 80 m.y. ago.

REFERENCES CITED

Amossé, Jean, 1978a, Variation in wolframite composition according to temperature, at Borralha, Portugal, and Enguyales, France: Economic Geology, v. 73, no. 6, p. 1170–1175.

———1978b, Physicochemical study of the huebnerite-ferberite ($MnWO_4$-$FeWO_4$) zonal distribution in wolframite ($Mn_xFe_{(1-x)}WO_4$) deposits; Application to the Borralha Mine (Portugal): Physics and Chemistry of Minerals, v. 3, p. 331–341.

———1980, Physicochemical interpretation of the mechanism of the oscillatory zoning in wolframite crystals: International Mineralogical Association, Collected abstracts, 12th General Meeting, Orleans, France (July 4–6, 1980), p. 29.

Banerjee, K. S., 1969, Origin of weak ferromagnetism and remanence in natural cassiterite crystals: Journal of Geophysical Research, v. 74, p. 3789–3795.

Banerjee, K. S., Johnson, C. E., and Krs, M., 1970, Mossbauer study to find the origin of weak ferromagnetism in cassiterite: Nature, v. 225, p. 173–175.

Baumann, L., and Starke, R., 1964, Beitrag zur verteilung der H/F-koeffizienten innerhalb der wolframitlagerstatte Pechtelsgrun auf grund neuer rontgenographischer untersuchungen: Bergakademie 16, p. 79–82.

Beddoe-Stephens, B., and Fortey, N. J., 1981, Columbite from the Carrock Fell tungsten deposit: Mineralogical Magazine, v. 44, p. 217–223.

Bird, M. L., and Gair, J. E., 1976, Compositional variations in wolframite from the Hamme (Tungsten Queen) Mine, North Carolina: U.S. Geological Survey Journal of Research, v. 4, no. 5, p. 583–588.

Bolduan, Helmut, 1954, Genetische untersuchung der wolframitlagerstätte Pechtelgrün (Vogtland) und besonderer berucksichtigung der verteilung des H/F-koeffizienten und der spurenelemente niob und tantal in wolframit: Freiberger Forschungshefte, ser. C, no. 10, p. 46–61.

Bonham, H. F., Jr., and Garside, L. J., 1979, Geology of the Tonopah, Lone Mountain, Klondike, and northern Mud Lake quadrangles, Nevada: Nevada Bureau of Mines and Geology Bulletin 92, 142 p.

Brown, G. C., 1911, Round Mountain tungsten mine: The Salt Lake Mining Review, August 15, 1911, p. 16.

Casadevall, Tom, and Rye, R. O., 1980, The Tungsten Queen deposit, Hamme district, Vance County, North Carolina—A stable isotope study of a metamorphosed quartz-huebnerite vein: Economic Geology, v. 75, no. 4, p. 523–537.

Chang, L. L. Y., 1967, Solid solutions of scheelite with other $R^{II}WO_4$-type tungstates: American Mineralogist, v. 52, nos. 3–4, p. 427–435.

———1968, Subsolidus phase relations in the system $ZnWO_4$-$ZnMoO_4$-$MnWO_4$-$MnMoO_4$: Mineralogical Magazine, v. 36, p. 992–996.

Churikov, V. S., 1959, Certain features of the chemical composition of wolframites—Materials relating to the geology, petrography, mineralogy and geochemistry of ore deposits: Academy of Sciences of the U.S.S.R., p. 235–250. [In Russian.]

Clark, A. H., 1970, Manganese-iron ratios in wolframite, South Crofty Mine, Cornwall—A discussion: Economic Geology, v. 65, p. 889–892.

de Magnée, I., and Aderca, B., 1960, Contribution à la connaissance du tungsten belt Ruandais (aspects géologiques, géochemique, metallogenique): Academie Royale Sciences Outre-Mer, c. 1, Sci. Nat. Mem., In. 8°, n.s.t., 11, f. 7, 56 p.

Eckel, E. B., 1961, Minerals of Colorado, a 100-year record: U.S. Geological Survey Bulletin 1114, 399 p.

Edwards, A. B., and Lyon, P. J., 1957, Mineralization at Aberfoyle tin mine, Rossarden, Tasmania: Proceedings of the Australian Institute of Mining and Metallurgy, v. 181, p. 93–145.

Evernden, J. F., and Kistler, R. W., 1970, Chronology of emplacement of Mesozoic batholithic complexes in California and western Nevada: U.S. Geological Survey Professional Paper 623, 42 p.

Ferguson, H. G., 1921, The Round Mountain district, Nevada: U.S. Geological Survey Bulletin 725–I, p. 383–406.

Foose, M. P., Slack, J. F., and Casadevall, Tom, 1980, Textural and structural evidence for predeformation hydrothermal origin of the Tungsten Queen deposit, Hamme district, North Carolina: Economic Geology, v. 75, no. 4, p. 515–522.

Ganeev, I. G., and Sechina, N. P., 1960, The geochemical peculiarities of wolframites: Geochemistry, v. 6, p. 617–623.

Glass, J. J., 1935, The pegmatite minerals from near Amelia, Virginia: American Mineralogist, v. 20, p. 754–756.

Groves, D. I., and Baker, W. E., 1972, The regional variation in compositions of wolframites from Tasmania: Economic Geology, v. 67, p. 362–368.

Grubb, P. L. C., 1967, Solid solution relationships between wolframite and scheelite: American Mineralogist, v. 52, p. 418–426.

Hogarth, D. D., and Chao, G. Y., 1979, Jixianite, *in* New mineral names: American Mineralogist, v. 64, p. 1330.

Hollister, V. F., 1970, Manganese-iron ratios in wolframite, South Crofty Mine, Cornwall—a discussion: Economic Geology, v. 65, no. 5, p. 592.

Horner, C., 1979, Solubility and hydrolysis of $FeWO_4$ and $MnWO_4$ in the 25°–300°C range, and the zonation of wolframite: Chemical Geology, v. 27, p. 85–97.

Hsu, L. C., 1976, The stability relations of the wolframite series: American Mineralogist, v. 61, p. 944–955.

Jianchang, Liu, 1979, Jixianite, $Pb(W,Fe^{+3})_2(O,OH)_7$—a new tungsten mineral: Acta Geologica Sinica, v. 53, p. 46–49.

Kelly, W. C., and Rye, R. O., 1979, Geologic, fluid inclusion, and stable isotope studies of the tin-tungsten deposits of Panasqueira, Portugal: Economic Geology, v. 74, no. 8, p. 1721–1822.

Koschmann, A. H., and Bergendahl, M. H., 1968, Principal gold-producing districts of the United States: U.S. Geological Survey Professional Paper 610, 283 p.

Kral, V. E., 1951, Mineral resources of Nye County, Nevada: Nevada University Bulletin, v. 45, no. 3, Geology and Mining Series 50, 223 p.

Landis, G. P., and Rye, R. O., 1974, Geologic, fluid inclusion, and stable isotope studies of the Pasto Bueno tungsten-base metal ore deposit, northern Peru: Economic Geology, v. 69, no. 7, p. 1025–1059.

Lawrence, L. J., 1961, Crystal habit of wolframite as an indication of relative temperature of formation: Neues Jahrbuch fur Mineralogie. Monatshefte, p. 241–247.

Lee, D. E., 1955, Mineralogy of some Japanese manganese ores: Stanford University Publications, University Series, Geological Sciences, v. 5, 64 p.

Lee, D. E., and Van Loenen, R. E., 1971, Hybrid granitoid rocks of the southern Snake Range, Nevada: U.S. Geological Survey Professional Paper 668, 48 p.

Lee, D. E., Marvin, R. F., Stern, T. W., and Peterman, Z. E., 1970, Modification of potassium-argon ages by Tertiary thrusting in the Snake Range, White Pine County, Nevada, *in* Geological Survey research 1970: U.S. Geological Survey Professional Paper 700–D, p. D92–D102.

Lemmlein, G. G., and Klevtsov, P. V., 1961, Relations among the principal thermodynamic parameters in a part of the system H_2O–NaCl: Geokhimiya, 1961, no. 2, p. 133–142 (in Russian); translated in Geochemistry, no. 2, p. 148–158, 1961.

Leonard, B. F., Mead, C. W., and Conklin, Nancy, 1968, Silver-rich disseminated sulfides from a tungsten-bearing quartz lode, Big Creek district, central Idaho: U.S. Geological Survey Professional Paper 594–C, p. C1–C24.

Leutwein, F., 1952, Die chemische zusammensetzung des wolframit und ihre lagerstättenkundliche bedeutung: Acta Geologica Akademiae Scientiarum Hungaricae, v. 1, p. 133–141.

Machin, M. P., and Süsse, P., 1975, On the crystal structure of ferritungstite, $(W,Fe^{+3})_2O_4(OH)_2$–$\frac{1}{2}H_2O$: Fortschritte der Mineralogie, v. 53, p. 50 [abs.].

Marvin, R. F., and Dobson, S. W., 1979, Radiometric ages— Compilation B, U.S. Geological Survey: Isochron/West, no. 26, p. 3–32.

Melhase, John, 1935, Nevada, the mineral collector's Mecca: Mineralogist, v. 3, no. 4, p. 9–10, 37–38.

Miller, C. F., 1977, Muscovite granite with high initial Sr^{87}/Sr^{86}, Old Woman Mountains, California; a product of upper crustal anatexis?: Geological Society of America Abstracts with Programs, v. 9, no. 4, p. 466.

Mineev, D. A., 1968, Average composition of lanthanoids in minerals: Geochemistry, no. 7, p. 825–835. [In Russian, English abs.]

Moore, F., and Howie, R. A., 1978, On the application of the huebnerite:ferberite ratio as a geothermometer: Mineralium Deposita, v. 13, p. 391–397.

———1979, Geochemistry of some Cornubian cassiterites: Mineralium Deposita, v. 14, p. 103–107.

Moore, J. M., and Jackson, N., 1977, Structure and mineralization in the Cligga granite stock, Cornwall: Journal Geological Society of London, v. 133, p. 467–480.

Myers, A. T., Havens, R. G., and Dunton, P. J., 1961, A spectrochemical method for the semiquantitative analysis of rocks and ores: U.S. Geological Survey Bulletin 1081–I, p. 207–229.

Oelsner, Oscar, 1944, Über Erzgebirgische wolframit: Freiberger Geologischen Gesellschaft Bergbau, v. 20, p. 44–49.

———1952, Die pegmatitisch-pneumatolytischen lagerstätten des Erzgebirges mit ausnahme der kontakt-lagerstätten: Freiberger Forschungshefte, ser. C, no. 4, 80 p.

———1954, Bemerkungen über die anwendbarkeit des H/F-koeffizienten zur deutung der genese von wolframiten: Freiberger Forschungshefte, ser. C, no. 10, p. 62–67.

Palache, Charles, Berman, Harry, and Frondel, Clifford, 1951, The system of mineralogy, 7th ed., vol. II: New York, John Wiley, 1124 p.

Ramdohr, Paul, 1966, The ore minerals and their intergrowths, English translation of 3d ed.: Oxford, Pergamon Press.

Saari, E., von Knorring, O., and Sahama, Th. G., 1968, Niobian wolframite from the Nuaparra pegmatite, Zambezia, Mozambique: Lithos, v. 1, no. 2, p. 164–168.

Schilling, J. H., 1963, Tungsten mines in Nevada: Nevada Bureau of Mines Map 18.

Schneider-Scherbina, Alexander, 1962, Uber metallogenetische epochen Boliviens und den hybriden charakter der sogenannten Zinn-Silber-Formation: Geologische Jahrbuch, v. 81, p. 157–170 [1964].

Shawe, D. R., 1977a, Preliminary generalized geologic map of the Round Mountain quadrangle, Nye County, Nevada (with text): U.S. Geological Survey Miscellaneous Field Studies Map MF–833.

———1977b, Geochemical and generalized geologic maps showing distribution of iron, copper, lead, zinc, molybdenum, silver, antimony, arsenic, tungsten, barium, potassium, and boron in the Round Mountain quadrangle, Nye County, Nevada (12 separate maps): U.S. Geological Survey Miscellaneous Field Studies Maps MF–835A–I.

Sheikh, A. M., 1970, Geology and ore deposits of Las Guijas tungsten district, Pima County, Arizona: Economic Geology, v. 65, no. 7, p. 875–882.

Shnuraeva, L. Ya., 1972, The typomorphism of heubnerite of the Bom-Gorkonsk tungsten deposit (western Transbaikal): Zapiski Vsesoyuznevo Mineralogichestvo Obshchestvo 101, p. 118–122. [In Russian.]

Sibley, D. F., Vogel, T. A., Walker, B. M., and Byerly, G., 1976, The origin of oscillatory zoning in plagioclase—A diffusion and growth controlled model: American Journal of Science, v. 276, p. 275–284.

Takenouchi, Sukune, and Kennedy, G. C., 1965, The solubility of carbon dioxide in NaCl solutions at high temperatures and pressures: American Journal of Science, v. 263, p. 445–454.

Takla, M. A., 1976, Electron microprobe of zoned wolframite from Elba, Egypt: Neues Jahrbuch für Mineralogie Monatshefte, v. 11, p. 477–483.

Takla, M. A., Sharkawi, M. A., and Fawzi, E., 1977, The geochemistry of Egyptian wolframites: Chemie der Erde, v. 36, p. 10–19.

Taylor, R. G., and Hosking, K. F. G., 1970, Manganese-iron ratios in wolframite, South Crofty Mine, Cornwall: Economic Geology, v. 65, p. 47–53.

Tingley, J. V., 1975, K-Ar dates on granodiorite and related scheelite-bearing quartz veins at Tungsten, Pershing County, Nevada: Isochron/West, no. 12, p. 3–4.

Varlamoff, N., 1958, Les gisements de tungestene au congo belge au Ruanda-Urundi, matériaux pour l'étude de leur géologie et de leur classification: Académie Royale Sciences, Colon. Brussels, nov. ser., 8, fasc. 2.

Vinogradova, L. G., and Barabanov, V. F., 1978, On the question about the chemistry of wolframite: Zapiski Vsesoyuznevo Mineralogichestvo Obshchestvo 107, no. 5, p. 585–590. [In Russian.]

Vinogradova, L. G., Barabanov, V. F., and Sorokin, N. D., 1980, On the distribution of iron, manganese, niobium, and scandium in wolframites: Zapiski Vesesoyuznovo Mineralogischestvo Obshchestvo, v. 109, p. 351–358. [In Russian.]

Voyevodin, V. N., 1981, The relation between chemical composition of wolframites and the geological conditions of their formation: International Geology Review, v. 23, no. 5, p. 561–570.

White, W. A., 1945, Tungsten deposit near Townsville, North Carolina: American Mineralogist, v. 30, p. 97–110.

Wiendl, Ulrich, 1968, Zur geochemie und lagerstätten kunde des wolframs: Technischen Universität Clausthal, Disertation zur erlangung des grades eines Doktor-Ingenieurs, 295 p. (Genehmigt von der Fakultat fur Bergbau. Hüttenwesen und Maschinenwesen).

Zuyuv, V. N., Zubkov, L. B., Zubynina, K. B., Utkina, T. F., and Chistov, L. B., 1966, New data on the modes of occurrence of tantalum and niobium in wolframite: Doklady of the Academy of Sciences of the U.S.S.R., v. 166, no. 106, p. 105–107.

☆ U.S. GOVERNMENT PRINTING OFFICE: 1984—776-041/4030 REGION NO. 8